



## APPENDICES

ลิขสิทธิ์มหาวิทยาลัยเชียงใหม่

Copyright© by Chiang Mai University  
All rights reserved

## APPENDIX A

### Calculations Examples

#### A.1 Stoichiometric Ratio

Calculation SR of mimosa from equation 4.4 as follow

$$SR = \left( \frac{C\%}{12} + \frac{H\%}{4} - \frac{O\%}{32} \right) \left( 1 + \frac{79}{21} \right) \left( 1 - \frac{Ash\%}{100} \right) \frac{28.84}{100}$$

$$SR = \left( \frac{43.9}{12} + \frac{6.0}{4} - \frac{48.7}{32} \right) \left( 1 + \frac{79}{21} \right) \left( 1 - \frac{3.7}{100} \right) \frac{28.84}{100} = 4.81$$

Calculation SR of bamboo from equation 4.4 as follow

$$SR = \left( \frac{C\%}{12} + \frac{H\%}{4} - \frac{O\%}{32} \right) \left( 1 + \frac{79}{21} \right) \left( 1 - \frac{Ash\%}{100} \right) \frac{28.84}{100}$$

$$SR = \left( \frac{45.6}{12} + \frac{4.3}{4} - \frac{49.7}{32} \right) \left( 1 + \frac{79}{21} \right) \left( 1 - \frac{5.6}{100} \right) \frac{28.84}{100} = 4.31$$

#### A.2 Equivalent Ratio

Calculation SR of mimosa from equation A.1 as follow

$$ER = \frac{\text{Gasification ratio}(GR)}{\text{stoichiometric ratio}(SR)} = \frac{(A/F)_{actual}}{(A/F)_{stoichiometry}} \quad (A.1)$$

$$0.25 = \frac{(A/F)_{actual}}{4.81}$$

$$(A/F)_{actual} = 1.21$$

Calculation SR of bamboo from equation A.1 as follow

$$ER = \frac{\text{Gasification ratio}(GR)}{\text{stoichiometric ratio}(SR)} = \frac{(A/F)_{\text{actual}}}{(A/F)_{\text{stoichiometry}}} \quad (\text{A.1})$$

$$0.25 = \frac{(A/F)_{\text{actual}}}{4.31}$$

$$(A/F)_{\text{actual}} = 1.08$$

Mimosa was used 10 g, its required air 12.1 g

Biomass	A/F <sub>actual</sub>	Feed (g)	Air(g)	Air(Litre)
Mimosa	1.21	10	12.1	10.25
Bamboo	1.08	10	10.8	9.15

### A.3 Product Gas Analysis and Conversion

Gas mixture standard was analyzed by GC and collected the chromatogram area for the mixture gases. The area was the average value from five experiments.

$$\text{conversion ratio} = \frac{\text{Gas standard (\%mol)}}{\text{GC area}} \quad (\text{A.2})$$

Table 4.3 Gas standard composition and conversion

	Gas Standard ( %mol)	GC area	Conversion ratio	Read area	Calculated mol%	Correction mol%
H <sub>2</sub>	4	246	0.0162602	41	0.664	1.020
O <sub>2</sub>	5	11818	0.0004231	6175	2.612	4.014
N <sub>2</sub>	4.99	14594	0.0003419	126346	43.2	66.376
CO	5.03	15047	0.0003343	9102	3.043	4.675
CO <sub>2</sub>	4	9253	0.0004323	1686	0.729	1.120
CH <sub>4</sub>	5	10213	0.0004896	30302	14.836	22.795
He	71.98	-	-	-	-	-
Total	100	-	-	-	65.084	100

#### A.4 Carbon Conversion Efficiency

Carbon elements in any materials were measured by CHNO analysis.

$$\eta_c = \frac{V_{gas} \times \frac{[CH_4\% + CO\% + CO_2\%]}{100} \times 12/22.4 \times 100\%}{W \left(1 - \frac{ash\%}{100}\right) \times \frac{C\%}{100}} \quad (A.3)$$

$$\eta_c = \frac{13.6 \times \frac{[1.120\% + 4.675\% + 22.795\%]}{100} \times (12/22.4) \times 100\%}{10 \left(1 - \frac{3.7\%}{100}\right) \times \frac{43.9\%}{100}}$$

$$\eta_c = 49.27\%$$



### A.5 Gas Low Heating Value

The low heating value of gas product is calorific value of gas from dry biomass

$$LHV = \frac{(30 \times CO\% + 25.7 \times H_2\% + 85.4 \times CH_4\%)}{100} \times 4.2 \text{ (kJ/Nm}^3\text{)} \quad (\text{A.4})$$

$$LHV = \frac{(30 \times 4.675\% + 25.7 \times 1.020\% + 85.4 \times 1.120\%)}{100} \times 4.2$$

$$LHV = 1,101 \text{ kJ/Nm}^3$$

## APPENDIX B

### Experimental Data

#### B.1 Fixed Bed Gasification

##### B.1.1 Biomass without catalyst

Table B.1 Results of effect of temperature on gas yields of bamboo and mimosa  
fixed bed gasification

Biomass	Temperature (°C)	H <sub>2</sub> (mol %)	CO (mol %)	CH <sub>4</sub> (mol %)	CO <sub>2</sub> (mol %)	O <sub>2</sub> (mol %)	N <sub>2</sub> (mol %)	Total (mol %)
Bamboo	600.00	0.42	4.99	1.21	17.79	8.84	66.76	100.00
	700.00	0.47	4.85	1.21	16.09	8.35	69.03	100.00
	800.00	0.53	4.85	1.05	16.16	8.21	69.20	100.00
	900.00	0.82	4.88	1.00	15.62	9.28	68.40	100.00
Mimosa	600.00	0.50	3.44	1.02	17.21	7.36	70.47	100.00
	700.00	1.00	4.49	1.46	19.50	9.20	64.36	100.00
	800.00	1.02	4.39	1.45	23.88	5.95	63.31	100.00
	900.00	1.26	4.68	1.12	22.79	4.01	66.14	100.00
Mimosa*	600.00	4.60	10.50	3.88	17.50	5.12	58.40	100.00
	700.00	5.80	12.60	5.04	18.30	4.32	53.94	100.00
	800.00	7.43	12.00	4.88	20.16	2.18	53.35	100.00
	900.00	10.80	17.90	5.10	24.50	1.20	40.50	100.00

Table B.2 Results of effect of temperature on fixed bed gasification product gas ratio

<b>Biomass</b>	<b>Temperature (°C)</b>	<b>H<sub>2</sub>/CO (mol/mol)</b>	<b>CO/CO<sub>2</sub> (mol/mol)</b>
Bamboo	600.00	0.08	0.28
	700.00	0.10	0.30
	800.00	0.11	0.30
	900.00	0.17	0.31
Mimosa	600.00	0.14	0.20
	700.00	0.22	0.23
	800.00	0.23	0.18
	900.00	0.27	0.21
Mimosa*	600.00	0.44	0.60
	700.00	0.46	0.69
	800.00	0.62	0.60
	900.00	0.60	0.73

Table B.3 Results of gas low heating value of bamboo and mimosa fixed bed  
gasification

Biomass	Temperature (°C)	LHV (kJ/Nm <sup>3</sup> )	Carbon Conversion Efficiency (%)	Gas Yield (Nm <sup>3</sup> / kg Biomass)
Bamboo	600.00	1105.40	39.10	1.31
	700.00	1095.97	36.39	1.32
	800.00	1043.61	36.51	1.33
	900.00	1062.75	36.38	1.36
Mimosa	600.00	852.23	35.98	1.31
	700.00	1195.96	42.56	1.32
	800.00	1183.76	50.09	1.33
	900.00	1126.79	49.27	1.36
Mimosa*	600.00	3211.52	54.94	1.36
	700.00	4021.40	66.49	1.46
	800.00	4064.35	72.28	1.54
	900.00	5250.42	98.71	1.64

Table B.4 Results of effect of temperature on product yields of bamboo and mimosa  
fixed bed gasification

Biomass	Temperature (°C)	Char (w/w)	Tar (w/w)	Gas (w/w)
Bamboo	600.00	26.00	13.60	60.40
	700.00	25.20	13.00	61.80
	800.00	24.00	12.50	63.50
	900.00	22.20	11.60	66.20
Mimosa	600.00	25.20	24.80	50.00
	700.00	24.00	23.40	52.60
	800.00	23.00	22.50	54.50
	900.00	22.00	21.20	56.80
Mimosa*	600.00	20.00	20.50	59.50
	700.00	16.50	15.50	68.00
	800.00	12.00	14.00	74.00
	900.00	7.00	11.90	81.10

## B.1.2 Biomass with catalyze

Table B.5 Results of effect of temperature on gas yields of bamboo and mimosa  
fixed bed gasification with catalyst

<b>Biomass &amp; Catalyze</b>	<b>Catalyst : Biomass</b>	<b>H<sub>2</sub></b>	<b>CO</b>	<b>CH<sub>4</sub></b>	<b>CO<sub>2</sub></b>	<b>O<sub>2</sub></b>	<b>N<sub>2</sub></b>	<b>Total</b>
	(w/w)	(mol %)	(mol %)	(mol %)	(mol %)	(mol %)	(mol %)	(mol %)
Bamboo &Dolomite	0.00	0.82	4.88	1.00	15.62	9.28	68.40	100.00
	0.25	1.63	5.08	1.01	17.03	7.13	68.13	100.00
	0.50	1.68	6.14	1.20	15.96	8.00	67.03	100.00
	1.00	1.99	7.73	1.00	17.42	7.52	64.35	100.00
Mimosa &Dolomite	0.00	1.26	4.68	1.12	22.79	4.01	66.14	100.00
	0.50	2.67	6.57	1.39	13.67	8.83	66.88	100.00
	1.00	3.17	8.26	1.14	15.05	7.93	64.45	100.00
Mimosa* &Dolomite	0.00	10.80	17.90	5.10	24.50	1.20	40.50	100.00
	0.50	11.50	21.00	3.80	23.00	1.10	39.60	100.00
	1.00	13.30	23.00	2.00	15.00	1.40	45.30	100.00
	1.50	12.00	16.00	2.80	23.00	1.50	44.70	100.00
	2.00	11.50	14.00	3.30	24.00	1.50	45.70	100.00

Table B.6 Results of effect of temperature on fixed bed gasification with catalyst

product gas ratio

<b>Biomass &amp; Catalyze</b>	<b>Catalyst : Biomass (w/w)</b>	<b>H<sub>2</sub>/CO (mol/mol)</b>	<b>CO/CO<sub>2</sub> (mol/mol)</b>
Bamboo &Dolomite	0.00	0.17	0.31
	0.25	0.32	0.30
	0.50	0.27	0.38
	1.00	0.26	0.44
Mimosa &Dolomite	0.00	0.27	0.21
	0.50	0.41	0.48
	1.00	0.38	0.55
Mimosa* &Dolomite	0.00	0.60	0.73
	0.50	0.55	0.91
	1.00	0.58	1.53
	1.50	0.75	0.70
	2.00	0.82	0.58

Table B.7 Results of gas low heating value of bamboo and mimosa fixed bed  
gasification with catalyst

<b>Biomass &amp; Catalyze</b>	<b>Catalyst : Biomass (w/w)</b>	<b>LHV (kJ/Nm<sup>3</sup>)</b>	<b>Carbon Conversion Efficiency (%)</b>	<b>Gas Yield (Nm<sup>3</sup>/ kg Biomass)</b>
Bamboo &Dolomite	0.00	1062.74	36.38	1.36
	0.25	1176.42	39.70	1.38
	0.50	1383.67	40.01	1.38
	1.00	1545.34	48.80	1.50
Mimosa &Dolomite	0.00	1126.79	49.27	1.36
	0.50	1613.13	41.11	1.50
	1.00	1791.90	45.54	1.47
Mimosa* &Dolomite	0.00	5250.42	98.71	1.64
	0.50	3785.67	86.88	1.66
	1.00	5337.91	86.17	1.70
	1.50	4784.14	88.99	1.68
	2.00	3903.27	85.83	1.64



Table B.8 Results of effect of temperature on product yields of bamboo and mimosa  
fixed bed gasification with catalyst

<b>Biomass &amp; Catalyze</b>	<b>Catalyst : Biomass (w/w)</b>	<b>Char (w/w)</b>	<b>Tar (w/w)</b>	<b>Gas (w/w)</b>
Bamboo &Dolomite	0.00	22.20	11.60	66.20
	0.25	22.00	11.00	67.00
	0.50	21.20	10.00	68.80
	1.00	21.00	10.00	69.00
Mimosa &Dolomite	0.00	22.00	21.20	56.80
	0.50	18.00	20.00	62.00
	1.00	17.60	19.00	63.40
Mimosa* &Dolomite	0.00	7.00	11.90	81.10
	0.50	7.10	10.00	82.90
	1.00	7.20	8.00	84.80
	1.50	7.30	9.50	83.20
	2.00	7.20	10.00	82.80

## B.2 Fluidized Bed Gasification

### B.2.1 Biomass without catalyst

Table B.9 Results of effect of temperature on gas yields of bamboo and mimosa  
fluidized bed gasification

Biomass	Temperature	H <sub>2</sub>	CO	CH <sub>4</sub>	CO <sub>2</sub>	O <sub>2</sub>	N <sub>2</sub>	Total
	(°C)	(mol %)	(mol %)	(mol %)	(mol %)	(mol %)	(mol %)	(mol %)
Bamboo	400.00	2.33	8.70	1.29	16.16	4.97	66.55	100.00
	500.00	2.12	8.27	1.58	17.94	4.40	65.69	100.00
	600.00	1.96	6.98	1.54	19.15	3.79	66.57	100.00
	700.00	0.77	5.96	1.30	19.41	4.64	67.91	100.00
Mimosa	400.00	3.13	9.84	1.72	14.65	5.31	65.35	100.00
	500.00	4.44	9.70	1.37	13.21	8.78	62.51	100.00
	600.00	1.96	8.27	1.54	19.15	3.79	65.28	100.00
	700.00	0.77	6.98	1.30	19.41	4.64	66.88	100.00

Table B.10 Results of effect of temperature on fluidized bed gasification product gas

ratio			
Biomass	Temperature (°C)	H <sub>2</sub> /CO (mol/mol)	CO/CO <sub>2</sub> (mol/mol)
Bamboo	400.00	0.27	0.54
	500.00	0.26	0.46
	600.00	0.28	0.36
	700.00	0.13	0.31
Mimosa	400.00	0.32	0.67
	500.00	0.46	0.73
	600.00	0.24	0.43
	700.00	0.11	0.36

Table B.11 Results of gas low heating value of bamboo and mimosa fixed bed  
gasification

Biomass	Temperature (°C)	LHV (kJ/Nm <sup>3</sup> )	Carbon Conversion Efficiency (%)	Gas Yield (Nm <sup>3</sup> / kg Biomass)
Bamboo	400.00	1810.41	63.62	1.96
	500.00	1837.47	67.42	1.95
	600.00	1643.33	65.52	1.90
	700.00	1301.87	62.77	1.89
Mimosa	400.00	2195.81	76.95	2.32
	500.00	2192.07	70.87	2.30
	600.00	1805.66	82.46	2.25
	700.00	1431.00	78.10	2.23

Table B.12 Results of effect of temperature on product yields of bamboo and mimosa fluidized bed gasification without catalyst

Biomass	Temperature (°C)	Char (w/w)	Tar (w/w)	Gas (w/w)
Bamboo	400.00	14.50	31.80	53.70
	500.00	12.90	34.10	53.00
	600.00	12.20	40.30	47.50
	700.00	11.20	42.70	46.10
Mimosa	400.00	13.50	31.60	54.90
	500.00	12.50	34.50	53.00
	600.00	12.00	40.00	48.00
	700.00	11.80	42.50	45.70

## B.2.2 Biomass with catalyst

Table B.13 Results of effect of temperature on gas yields of bamboo and mimosa fluidized bed gasification with catalyst

Biomass & Catalyze	Catalyst : Biomass (w/w)	H <sub>2</sub> (mol %)	CO (mol %)	CH <sub>4</sub> (mol %)	CO <sub>2</sub> (mol %)	O <sub>2</sub> (mol %)	N <sub>2</sub> (mol %)	Total (mol %)
Bamboo & Dolomite	0.00	0.77	5.96	1.30	19.41	4.64	67.91	100.00
	1.00	2.80	10.00	1.20	16.00	5.00	65.0	100.00
Mimosa & Dolomite	0.00	0.77	6.98	1.30	19.41	4.64	66.88	100.00
	1.00	5.00	10.00	1.20	12.00	6.00	65.80	100.00

Table B.13 Results of effect of temperature on fluidized bed gasification with catalyst product gas ratio

Biomass & Catalyze	Catalyst : Biomass (w/w)	H <sub>2</sub> /CO (mol/mol)	CO/CO <sub>2</sub> (mol/mol)
Bamboo & Dolomite	0.00	0.13	0.31
	1.00	0.28	0.63
Mimosa & Dolomite	0.00	0.11	0.36
	1.00	0.50	0.83

Table B.14 Results of gas low heating value of bamboo and mimosa fixed bed  
gasification with catalyst

<b>Biomass</b>	<b>Catalyst : Biomass (w/w)</b>	<b>LHV (kJ/Nm<sup>3</sup>)</b>	<b>Carbon Conversion Efficiency (%)</b>	<b>Gas Yield (Nm<sup>3</sup>/ kg Biomass)</b>
Bamboo	0.00	1301.87	62.77	1.89
	1.00	1992.65	68.82	2.03
Mimosa	0.00	1431.00	78.10	2.23
	1.00	2230.12	70.56	2.40

Table B.15 Results of effect of temperature on product yields of bamboo and  
mimosa fluidized bed gasification without catalyst

<b>Biomass</b>	<b>Catalyst : Biomass (w/w)</b>	<b>Char (w/w)</b>	<b>Tar (w/w)</b>	<b>Gas (w/w)</b>
Bamboo	0.00	11.20	42.70	46.10
	1.00	9.60	27.50	62.90
Mimosa	0.00	11.80	42.50	45.70
	1.00	9.50	26.00	64.50

## APPENDIX C

### Gas Production Modeling

#### C.1 Model Calculation

Table C.1  $\bar{h}_f^\circ$  and the coefficient of empirical equation for  $\Delta \bar{g}_{f,T}^\circ$  (unit:  $\frac{kJ}{mol}$ )

Compound	$CO$	$CO_2$	$H_2O$	$CH_4$
$\bar{h}_f^\circ$	-110.5	-393.5	-241.8	-74.8
$a'$	$5.619 \times 10^{-3}$	$-1.949 \times 10^{-2}$	$-8.950 \times 10^{-3}$	$-4.620 \times 10^{-2}$
$b'$	$-1.190 \times 10^{-5}$	$3.122 \times 10^{-5}$	$-3.672 \times 10^{-6}$	$1.130 \times 10^{-5}$
$c'$	$6.383 \times 10^{-9}$	$-2.448 \times 10^{-8}$	$5.209 \times 10^{-9}$	$1.319 \times 10^{-8}$
$d'$	$-1.846 \times 10^{-12}$	$6.946 \times 10^{-12}$	$-1.478 \times 10^{-12}$	$-6.647 \times 10^{-12}$
$e'$	$-4.891 \times 10^2$	$-4.891 \times 10^2$	0.00	$-4.891 \times 10^2$
$f'$	$8.684 \times 10^{-1}$	5.270	2.868	$1.411 \times 10^1$
$g'$	$-6.131 \times 10^{-2}$	$-1.207 \times 10^{-1}$	$-1.722 \times 10^{-2}$	$-2.234 \times 10^{-1}$

Source: S. Jarungthammachote and A. Dutta (2006)



Table C.2 Specific heat coefficient of empirical equation

Gas species	$a$	$b$	$c$	$d$	Temperature (K)
$H_2$	29.11	- $0.1916 \times 10^{-2}$	$0.4003 \times 10^{-5}$	- $0.8704 \times 10^{-9}$	273 - 1800
$CO$	28.16	$0.1675 \times 10^{-2}$	$0.5372 \times 10^{-5}$	$-2.222 \times 10^{-9}$	273 - 1800
$CO_2$	22.26	$5.981 \times 10^{-2}$	$-3.501 \times 10^{-5}$	$-7.469 \times 10^{-9}$	273 - 1800
$H_2O$	32.24	$0.1923 \times 10^{-2}$	$1.055 \times 10^{-5}$	$-3.595 \times 10^{-9}$	273 - 1800
$CH_4$	19.89	$5.204 \times 10^{-2}$	$1.269 \times 10^{-5}$	$-11.01 \times 10^{-9}$	273 - 1800
$N_2$	28.90	- $0.1571 \times 10^{-2}$	$0.8081 \times 10^{-5}$	$-2.873 \times 10^{-9}$	273 - 1800

Source: S. Jarungthammachote and A. Dutta (2006)

## C.1.1 Formula and model calculation

**Given :**  $n_{CO} = x_1$ ,  $n_{CO_2} = x_2$ ,  $n_{CH_4} = x_3$ ,  $n_{H_2} = x_4$ ,  $n_{H_2O} = x_5$

**Mass Balance :**

- Carbon mass balance:  $f_1 = 0 = x_1 + x_2 + x_3 - 1$
- Hydrogen mass balance:  $f_2 = 0 = 2x_4 + 2x_5 + 4x_3 - nH - 2w$
- Oxygen mass balance:  $f_3 = 0 = x_1 + 2x_2 + x_5 - w - 2m - nO$

**Equilibrium Thermodynamics :**

- Equilibrium constant of methane reaction:

$$f_4 = 0 = K_1(x_1)(x_5) - (x_2)(x_4)$$

- Equilibrium constant of water-gas shift reaction:

$$f_5 = 0 = K_2(x_4)^2 - (x_3)(x_{total})$$

A Standard Gibbs function of formation of  $CO, CO_2, CH_4, H_2, N_2$  at any temperature can be calculated using the following equation:

$$\Delta \bar{g}_{f,T,i}^\circ = \bar{h}_f^\circ - a'T \ln(T) - b'T^2 - \left(\frac{c'}{2}\right)T^3 - \left(\frac{d'}{3}\right)T^4 + \left(\frac{e'}{2T}\right) + f' + g'T$$

where  $\bar{h}_f^\circ, a', b', c', d', e', f', g'$  refer to Table A.1.

A Standard Gibbs Function of gases involving methane and water gas shift reaction can be calculated using the following equation:

$$\Delta G_T^\circ = \sum_i \nu_i \Delta \bar{g}_{f,T,i}^\circ$$

Methane reaction:  $C + 2H_2 \rightarrow CH_4$

Water-gas shift reaction:  $CO + H_2O \rightarrow CO_2 + H_2$

where  $\nu$  is stoichiometric number of gases involving reaction. Sign convention for stoichiometric number is always a plus sign (+) for product. For reactants, the value of the term will be negative (-).

Equilibrium constants of methane and water gas shift reaction can be calculated using the following equation:

$$\ln K = -\frac{\Delta G_T^\circ}{RT}$$

where  $\bar{R}$  is gas constant,  $8.314 \text{ kJ/kmol.K}$

Substituting  $K_1, K_2$  which solved by above calculation in  $f_4, f_5$  then using Newton Rapshon Method to solve  $n_{CO}, n_{CO_2}, n_{CH_4}, n_{H_2}, n_{H_2O}$  or  $x_1, x_2, x_3, x_4, x_5$ .

Using amount of production gas  $n_{CO}, n_{CO_2}, n_{CH_4}, n_{H_2}, n_{H_2O}$  to calculate temperature during gasification process ( $T_{new}$ )

$$\sum_{j=react} \bar{h}_{f,j}^\circ = \sum_{i=prodt} n_i \bar{h}_{f,i}^\circ + \left[ \left( \sum_i n_i a_i \right) T + \left( \sum_i n_i b_i \right) T^2 + \left( \sum_i n_i c_i \right) T^3 + \left( \sum_i n_i d_i \right) T^4 + \sum_i n_i k_i \right]$$

Where  $\sum_{i=prodt} n_i \bar{h}_{f,i}^\circ$  = summarization of multiply between  $\bar{h}_f^\circ$  and production gas mole

( $CO, CO_2, CH_4, H_2, N_2$ ) and  $\sum_{i=prodt} n_i \bar{h}_{f,i}^\circ$  = summarization of multiply between integral

( $\int_{29815}^T \bar{C}_p(T) dT = aT + bT^2 + cT^3 + dT^4 + k$ ) and production gas mole. According to

above equation, it results temperature during gasification process ( $T_{new}$ )

Testing condition to check amount of production gas by using  $|T_{new} - T| < 0.1$ . If condition is fault, program will process it to second process. During second process,

$T_{-}$  will substitute in Standard Gibbs function of formation ( $T = T_{new}$ ) till condition comes true.

### C.1.2 Calculation Sample

**Input data as following;**  $T = 298.15$  K,  $x_0 = [0.5; 0.3; 0.001; 0.1; 0.1]$ ,  $m_c = 0$ ,  $C = 43.9$ ,  $H = 6.0$ ,  $O = 48.7$ ,  $N = 1.4$ ,  $S = 0$  and,  $m = 0.44$

Calculation mole of fuel per number of carbon.

**Given :**  $n_C = 1$

$$n_H = (H/1.00794)/(C/12.0107) = 1.6286 \text{ mole/ mole carbon}$$

$$n_O = (O/15.9994)/(C/12.0107) = 0.8328 \text{ mole/ mole carbon}$$

$$n_N = (N/14.0074)/(C/12.0107) = 0.0273 \text{ mole/ mole carbon}$$

$$n_S = (S/32.066)/(C/12.0107) = 0 \text{ mole/ mole carbon}$$

$$\begin{aligned} \text{Hence, } M &= (12.0107 * n_C) + (1.00794 * n_H) + (15.9994 * n_O) \\ &= 26.9762 \text{ mole/ mole carbon} \end{aligned}$$

Testing condition error  $> 0.1$ . If condition is true, program will proceed gibb function to calculate  $\overline{g}_f^0$ .

Gas type	Calculate ( $\text{kJ}/\text{kmol}$ )	Table ( $\text{kJ}/\text{kmol}$ )
gibb_CH4	- 50,847	-50,790
gibb_CO	- 137,330	-137,150
gibb_CO2	- 394,420	-394,360
gibb_H2O	- 228,620	-228,590

Source: Dow Chemical Co., 1971

When get  $\text{gibb\_CH}_4$ ,  $\text{gibb\_CO}$ ,  $\text{gibb\_CO}_2$ ,  $\text{gibb\_H}_2\text{O}$ , program will automate run  $\text{G\_K}$  function to find the answer.

$$\text{G\_K1} = -28,468 \text{ kJ/kmol}$$

$$\text{G\_K2} = -50,847 \text{ kJ/kmol}$$

Substituting  $\text{G\_K1}$ ,  $\text{G\_K2}$  in  $\text{K}$  equation. The answer show below.

$$\text{K1} = 97,198$$

$$\text{K2} = 8.1 \times 10^8$$

Substituting  $\text{K}$  in  $\text{f}$  and  $\text{jacobain}$  function.

Program will run Raphson function to solve 5 unknown equation then result amount of production gas ( $x$ ) as below then substituting in  $\text{Hwood}$  function and enthalpy balance result polynomial of degree 4 then using these equations to solve  $\text{T\_new}$  through  $\text{h}$  function.

Given  $\text{T\_new} = \text{T}$ ,  $\text{error} = |\text{T}_{\text{new}} - \text{T}|$  then using error to test the condition. The result show following.

## C.2 Model Code

### C.2.1 Gas Production Modeling

#### C.2.1.1 main\_gas.m function

```
% Finding temeprature
T = input('enter -> T = ');
x0 = input('enter -> x0 = ');
mc = input('enter -> mc = '); %input moisture/100
C = input('enter -> C = '); %input carbon (wt%)
H = input('enter -> H = '); %input hydrogen (wt%)
O = input('enter -> O = '); %input oxygen (wt%)
N = input('enter -> N = '); %input nitrogen (wt%)
S = input('enter -> S = '); %input sulfur (wt%)
nC = 1 ;
nH = (H/1.00794)/(C/12.0107);
nO = (O/15.9994)/(C/12.0107);
nN = (N/14.0074)/(C/12.0107);
nS = (S/32.066)/(C/12.0107);
M = (12.0107*nC)+(1.00794*nH)+(15.9994*nO);
w=(M*mc)/(18.015*(1-mc));
m = input('enter -> m = '); % m =(air*M*0.21)/(22.4*1.187)or input kmol of
oxygen per kmol
save ('main_gas.mat','nC','nH','nO','nN','nS','w','x0','mc','C','H','O','N','S','M','m');

N = 1;
error = 0.2;
while error > 0.1

    % Gibbs function of reaction
    eval('[gibb_CH4, gibb_CO,gibb_CO2,gibb_H2O] = gibb(T)') ;

    % The standard gibbs function of reaction
    eval('[G_K1,G_K2] = G_K ( gibb_CO2,gibb_H2O,gibb_CO,gibb_CH4)');

    % The standard gibbs function of reaction
    eval('[K1,K2] = K (G_K1,G_K2,T)') ;

    % modified from example in Numercial Methods in Chemical Engineering
    eval('[solution] = Raphson(@f,@jacobain,x0)');

    % enthalpy
    eval('[enthalpy] = enrhalpy(nN,w,m,solution,Hwood)')

    %solve T_new
```

```

eval(['T_new] = h(enthalpy)')
error = abs(T_new-T);
N = N+1;
T=T_new;
x0 = solution ;
clear glibb_CH4 glibb_H2O glibb_CO glibb_CO2 G_K1 G_K2 K1 K2 enthalpy
solution
end

total = x0(1,1)+x0(2,1)+x0(3,1)+x0(4,1)+ x0(5,1)+(nN/2+(3.76*m));
disp(['total = ' num2str(total)])
CO_persen = (x0(1,1)*100)/total ;
CO2_persen = (x0(2,1)*100)/total ;
CH4_persen = (x0(3,1)*100)/total ;
H2_persen = (x0(4,1)*100)/total ;
H2O_persen = (x0(5,1)*100)/total ;
N2_persen = ((nN/2+(3.76*m))*100)/total ;
disp(['H2_persen = ' num2str(H2_persen)])
disp(['CO_persen = ' num2str(CO_persen)])
disp(['CO2_persen = ' num2str(CO2_persen)])
disp(['CH4_persen = ' num2str(CH4_persen)])
disp(['N2_persen = ' num2str(N2_persen)])
disp(['H2O_persen = ' num2str(H2O_persen)])
save
('main_gas.mat','CO_persen','CO2_persen','CH4_persen','H2_persen','N2_perse
n');

```

### C.2.1.2 main\_gas\_temp.m function

This function was fixed temperature for calculation mol of gas product.

```

T = input('enter -> T = '); %input temperature in kelvin.
x0 = input('enter -> x0 = ');
mc = input('enter -> mc = '); %input moisture/100
C = input('enter -> C = '); %input carbon (wt%)
H = input('enter -> H = '); %input hydrogen (wt%)
O = input('enter -> O = '); %input oxygen (wt%)
N = input('enter -> N = '); %input nitrogen (wt%)
S = input('enter -> S = '); %input sulfur (wt%)
C = 50; %input carbon (wt%)
H=6; %input hydrogen (wt%)
O=44; %input oxygen (wt%)
N=0; %input nitrogen (wt%)
S=0; %input sulfur (wt%)
nC = 1 ;
nH = (H/1.00794)/(C/12.0107);
nO = (O/15.9994)/(C/12.0107);

```



```

nN = (N/14.0074)/(C/12.0107);
nS = (S/32.066)/(C/12.0107);
M = (12.0107*nC)+(1.00794*nH)+(15.9994*nO);
w=(M*mc)/(18.015*(1-mc));
m = input('enter -> m = '); % m =(air*M*0.21)/(22.4*1.187)or input kmol of
oxygen per kmol

save ('main_gas.mat','nC','nH','nO','nN','w','x0','mc','M','m');

% Gibbs function of reaction
eval('[gibb_CH4,gibb_CO,gibb_CO2,gibb_H2O] = gibb(T)') ;

% The standard gibbs function of reaction
eval('[G_K1,G_K2] = G_K ( gibb_CO2,gibb_H2O,gibb_CO,gibb_CH4)');

% The standard gibbs function of reaction
eval('[K1,K2] = K (G_K1,G_K2,T)') ;

% modified from example in Numerical Methods in Chemical Engineering
eval('[solution] = Raphson(@f,@jacobain,x0)');

% enthalpy
eval('[enthalpy] = enrhalpy(nN,w,m,solution,Hwood)')

%solve m_new
eval('[m_new] = h(enthalpy)')
error = abs(m_new-m);
N = N+1;
m=m_new;
x0 = solution ;
clear enthalpy solution
end

total = solution(1,1)+solution(2,1)+solution(3,1)+solution(4,1)+
solution(5,1)+((nN/2+(3.76*m)));
disp(['total = ' num2str(total)])
CO_persen = (solution(1,1)*100)/total ;
CO2_persen = (solution(2,1)*100)/total ;
CH4_persen = (solution(3,1)*100)/total ;
H2_persen = (solution(4,1)*100)/total ;
H2O_persen = (solution(5,1)*100)/total ;
N2_persen = ((nN/2+(3.76*m))*100)/total ;
disp(['H2_persen = ' num2str(H2_persen)])
disp(['CO_persen = ' num2str(CO_persen)])
disp(['CO2_persen = ' num2str(CO2_persen)])
disp(['CH4_persen = ' num2str(CH4_persen)])
disp(['N2_persen = ' num2str(N2_persen)])

```



```
disp(['H2O_persen = ' num2str(H2O_persen)])

save('main_gas.mat','CO_persen','CO2_persen','CH4_persen','H2_persen','N2_persen');
```

#### C.1.1.1 gibb.m function

```
function [gibb_CH4,gibb_CO,gibb_CO2,gibb_H2O] = gibb (T)
% Gibbs function of reaction
gibb_CH4 = (-74850) - (((-4620)*(10^(-2)))*T*log(T))-(((1130)*(10^(-5)))...
*(T^2))-(((1319)*(10^(-8)))/(2))*(T^3))-(((6647)*(10^(-12)))/(3))...
*(T^4))+((-4891)*(10^2))/(2*T))+((1411)*(10^1))+((-2234)*(10^(-1)))*T);

gibb_CO = (-110530) - (((5619)*(10^(-3)))*T*log(T))-(((1190)*(10^(-5)))...
*(T^2))-(((6383)*(10^(-9)))/(2))*(T^3))-(((1846)*(10^(-12)))/(3))*(T^4))...
+((-4891)*(10^2))/(2*T))+((8684)*(10^(-1)))+((-6131)*(10^(-2)))*T);

gibb_CO2 = (-393520) - (((1949)*(10^(-2)))*T*log(T))-(((3122)*(10^(-5)))...
*(T^2))-((-2448)*(10^(-8)))/(2))*(T^3))-(((6946)*(10^(-12)))/(3))...
*(T^4))+((-4891)*(10^2))/(2*T))+5270+((-1207)*(10^(-1)))*T);

gibb_H2O = (-241820) - (((8950)*(10^(-3)))*T*log(T))-(((3672)*(10^(-6)))...
*(T^2))-(((5209)*(10^(-9)))/(2))*(T^3))-(((1478)*(10^(-12)))/(3))...
*(T^4))+((0)/(2*T))+2868+((-1722)*(10^(-2)))*T);

save ('gibb.mat','gibb_CH4','gibb_CO','gibb_CO2','gibb_H2O')
```

#### C.1.1.2 G\_K.m function

```
function [G_K1,G_K2] = G_K ( gibb_CO2,gibb_H2O,gibb_CO,gibb_CH4)
% The standard gibbs function of reaction
G_K1 = gibb_CO2 - gibb_H2O - gibb_CO;
G_K2 = gibb_CH4 ;

save ('G_K.mat','G_K1','G_K2')
```

#### C.1.1.3 K.m function

```
function [K1,K2] = K (G_K1,G_K2,T)
% The equilibrium constants
K1 =(exp(-((G_K1)/(8.314*T))));
```

```
K2=(exp(-((G_K2)/(8.314*T))));
```

```
save ('K.mat','K1','K2')
```

#### C.1.1.4f.m function

```
function [f] = f(x)
load K.mat;
load ('main_gas.mat','nH','nO','nN','w');
load ('main_gas.mat','m')
%Function balancing
f1 = x(1)+x(2)+x(3)-1; % Carbon balance
f2= 2*x(4)+2*x(5)+4*x(3)-nH-2*w; % hydrogen balance
f3 = x(1)+2*x(2)+x(5)-w-2*m-nO; % oxygen balance
f4 = K1*x(1)*x(5)-x(2)*x(4); % equilibriumb constant balance 1
f5 = K2*(x(4))^2-x(3)*(x(1)+x(2)+x(3)+x(4)+x(5)+(nN/2+(3.76*m)))); %
equilibriumb constant balance 2
f = [f1;f2;f3;f4;f5];
% end function
```

#### C.1.1.5jacobain.m function

```
function [J] = jacobain (x)
load K.mat;
load main_gas.mat;
%Jacobian
J(1,1) = 1; J(1,2) = 1; J(1,3) = 1; J(1,4) = 0; J(1,5) = 0;
J(2,1) = 0; J(2,2) = 0; J(2,3) = 4; J(2,4) = 2; J(2,5) = 2;
J(3,1) = 1; J(3,2) = 2; J(3,3) = 0; J(3,4) = 0; J(3,5) = 1;
J(4,1) = K1*x(5); J(4,2) = -x(4); J(4,3) = 0; J(4,4) = -x(2); J(4,5) = K1*x(1);
J(5,1) = (-x(3)); J(5,2) = (-x(3)); J(5,3) = -2*x(3)-
(x(1)+x(2)+x(4)+x(5)+(nN/2+(3.76*m))); J(5,4) =2*K2*x(4)-x(3); J(5,5) = (-
x(3));
```

```
% end function
```

#### C.1.1.6 Raphson.m function

```
% Newton Raphson Method %
function [solution] = Raphson(f,jacobain,x0)
x=x0;
error = 2*1e-6;
iter = 0;
while error > 1e-6
```

```

P = feval(f,x);
P = double(P);
error1 = max(abs(P(:)));
J = feval(jacobain,x);
dx = J\(-P);
error2 = max(abs(P(:)));
m = 1;
while error2 >= error1 || ~isreal(P)
    xnew = x+(dx*0.5^m);
    P = feval(f,xnew);
    P = double(P);
    error2 = max(abs(P(:)));
    m = m+1;
end
x=xnew;
error = error2;
iter = iter+1;

end
solution = x ;

save ('Raphson.mat','solution')

```

#### C.1.1.7 Hwood.m function

```

function [Hwood] = Hwood(C,H,O)
load ('main_gas.mat','C','H','O','M','nH','S','mc','nN','N')
load ('Raphson.mat','solution')
LHV=4.187*(81*C+300*H-26*(O-S)-6*(9*nH+mc))*M;
Hwood = LHV+ (nH/2)*(-241820)+(-393520);
save ('Hwood.mat','Hwood')

```

#### C.1.1.8 Enthalpy.m function

```

%function for solving T_new if calculating m_now change T_new to m_new
function [enthalpy] = enthalpy (nN,w,m,solution,Hwood)
syms T_new
enthalpy =
((solution(1,1)*(110530))+(solution(2,1)*(393520))+(solution(3,1)*(-74850))
+(solution(4,1)*0)+(solution(5,1)*(241820))+((nN/2+(3.76*m))*0))+((solution(
1,1)*28.16)+(solution(2,1)*22.26)+(solution(3,1)*19.89)+(solution(4,1)*29.11)
+(solution(5,1)*32.24)+((nN/2+(3.76*m))*28.90))*T_new...
+((solution(1,1)*(0.1675*(10^(-2))))+(solution(2,1)*(5.981*(10^(-2))))
+(solution(3,1)*(5.204*(10^(-2))))+(solution(4,1)*(-0.1916*(10^(-2))))
+(solution(5,1)*(0.1923*(10^(-2))))+((nN/2+(3.76*m))*(-0.1571*(10^(-
2))))*(T_new^2)+ ((solution(1,1)*(0.5372*(10^(-5))))+(solution(2,1)*(-

```

```

3.501*(10^(-5))))+(solution(3,1)*(1.269*(10^(-
5))))+(solution(4,1)*(0.4003*(0.5372*(10^(-5))))+(solution(5,1)*(1.055*(10^(-
5))))+((nN/2+(3.76*m))*(0.8081*(10^(-5))))*(T_new^3)...
+((solution(1,1)*(-2.222*(10^(-9))))+(solution(2,1)*((-7.469)*(10^(-
9))))+(solution(3,1)*(-11.010*(10^(-9))))+(solution(4,1)*(-0.8704*(10^(-
9))))+(solution(5,1)*(-3.595*(10^(-9))))+((nN/2+(3.76*m))*(-2.873*(10^(-
9))))*(T_new^4).+(solution(1,1)*28.5539)+(solution(2,1)*30.0859)+(solution(
3,1)*27.9468)+(solution(4,1)*(28.9373))+(solution(5,1)*32.8150)+((nN/2+(3.7
6*m))*(28.8861)) - (Hwood) - w*(-285830+(2441.7*18.0153));

```

#### C.1.1.9 h.m

```

%function for solving T_new if calculating m_now change T_new to m_new
function [T_new] = h(enthalpy)
syms T_new
S = solve(enthalpy);
S = double(S);
T_new = min(abs(S(:)));
T_new = double(T_new);
save('h','T_new')

```

### C.3.2 Model Modifications

In order to make a model more accurate, main\_gas.m and K.m function have been adapted. By changing function from K function to K\_modi function line.

```

% The standard gibbs function of reaction
eval('[K1,K2] = K_modi (G_K1,G_K2,T)') ;

```

#### C.3.2.1 K\_modi.m function

```

function [K1,K2] = K_modi (G_K1,G_K2,T)
% The standard gibbs function of reaction
modified_Co1=0.954;% For experimental coefficient of K1 is 0.954 and model
coefficient
of K1 is 0.954
modified_Co2=1.52;% For experimental coefficient of K2 is 27.92 and model
coefficient of K2 is 1.52
K1 =modified_Co1*(exp(-((G_K1)/(8.314*T))));
K2 =modified_Co2*(exp(-((G_K2)/(8.314*T))));
save('K.mat','K1','K2')

```

## C.1 Flow Chart

### C.1.1 Designing and writing software

There are two main\_gas function that used for calculation gas yield with different condition: fixed temperature and finding temperature.

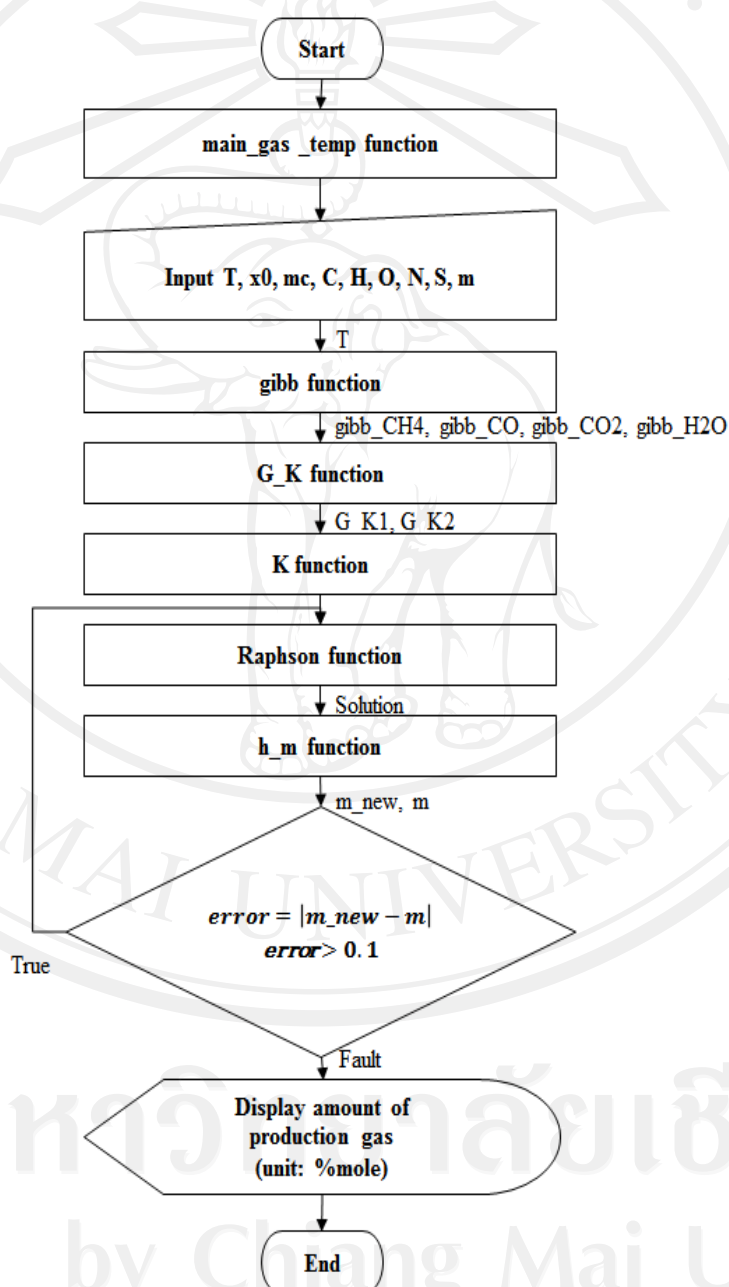


Figure C.1 Gas production model with fixed temperature

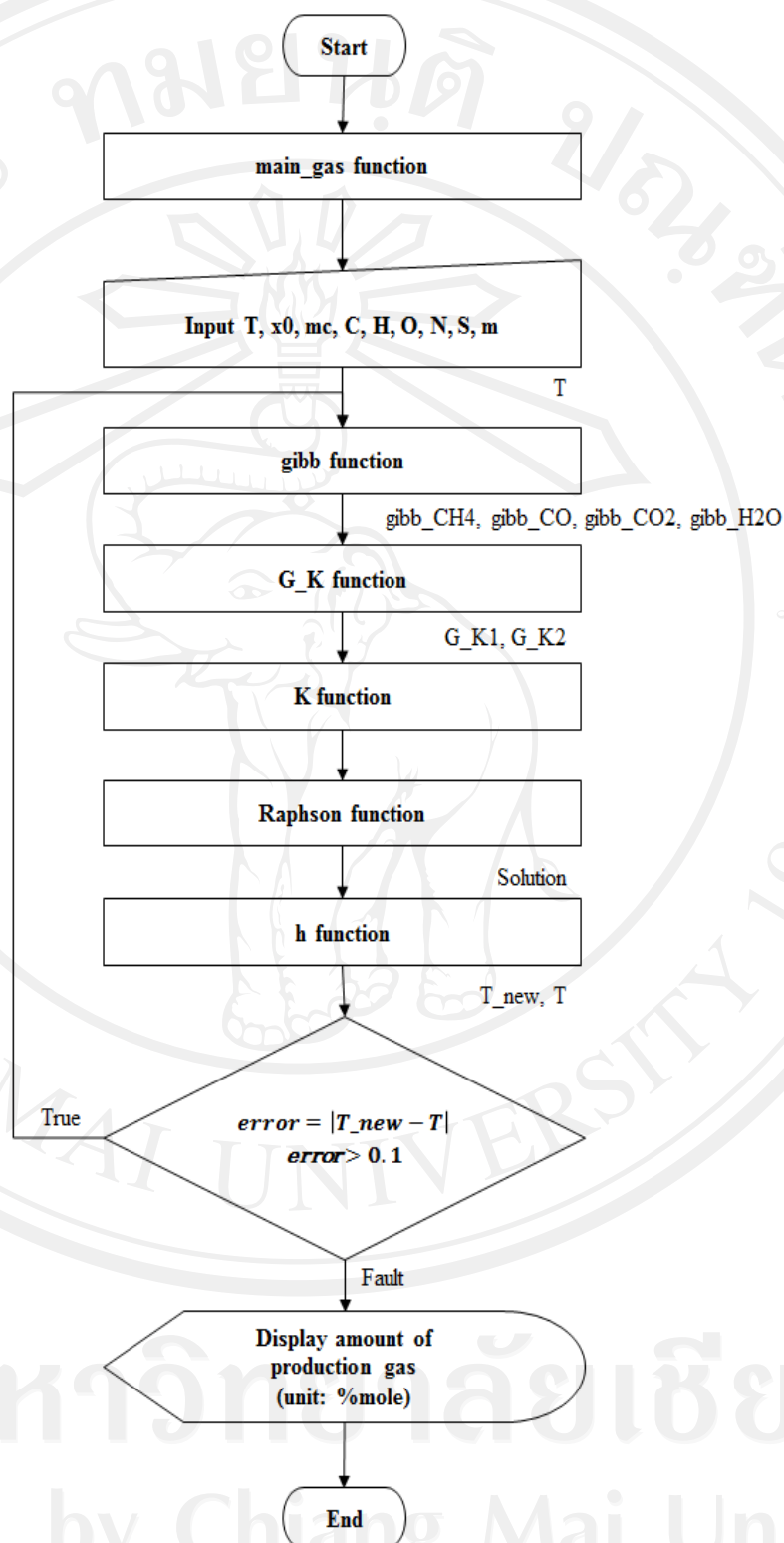


Figure C.2 Gas production model with finding temperature



## C.1.1.1 gibb function

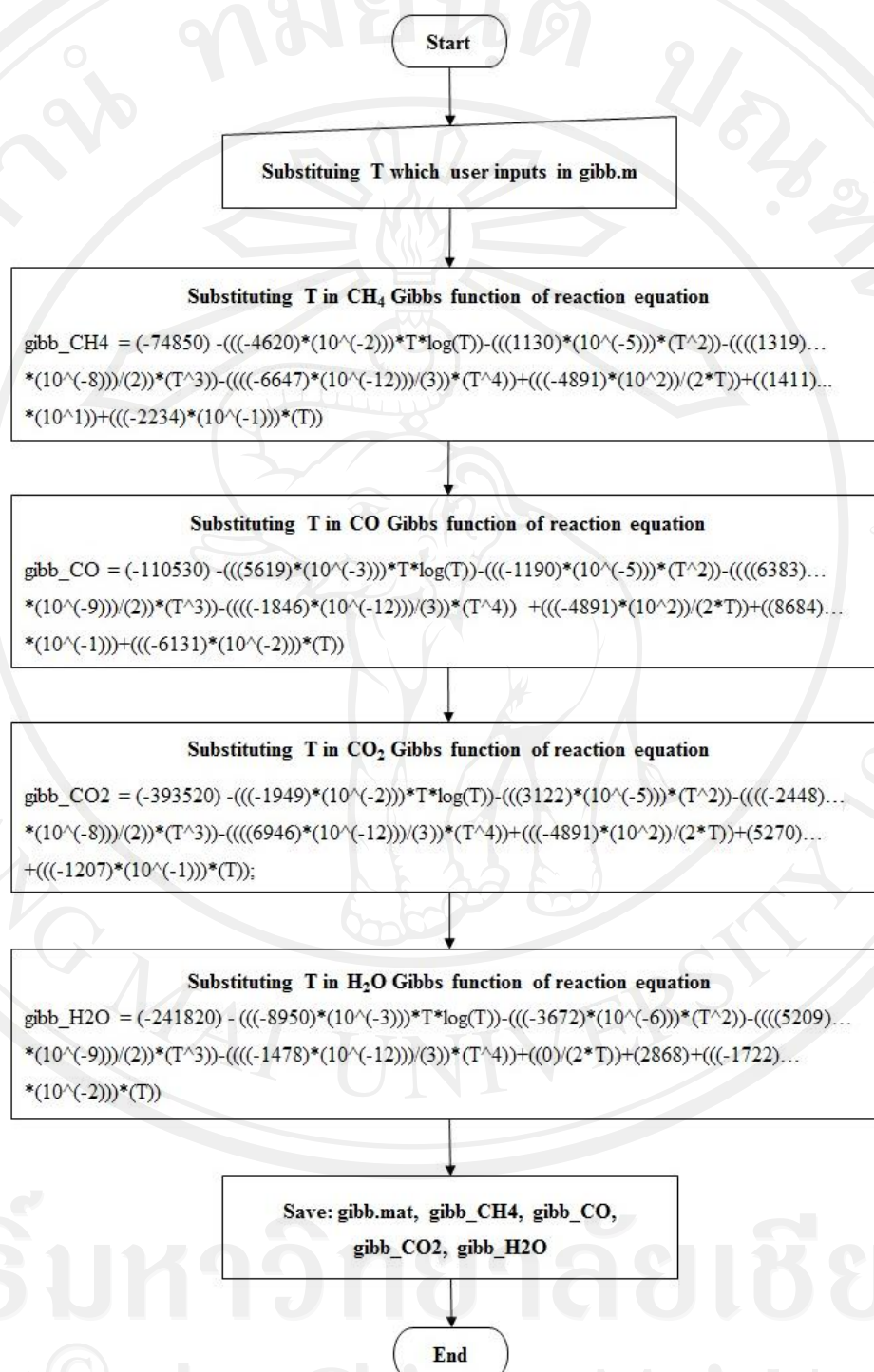


Figure C.3 Design process flow of Standard Gibbs function of formation

Gibb is function of Standard Gibbs function of formation. Even though it is not predictable how rapidly reactions proceed, with Gibbs energy it can help us to confirm whether the process is spontaneous reaction or not. In case of Standard Gibbs function of formation has negative sign convection, process is spontaneous reaction. In the other hand, positive convection, process is not spontaneous reaction. And if process has zero Standard Gibbs function of formation, reaction is reversible. For non-compound gas or stable element such as  $N_2$ , Standard Gibbs function of formation is 0.

Refer to figure C.2, once user input T, program will substitute T into equation which is derived from Standard Gibbs function of formation equation and record gibb\_CH4, gibb\_CO, gibb\_CO2, gibb\_H2O for further action.

$$\Delta \bar{g}^{\circ}_{f,T,i} = \bar{h}_f^{\circ} - a'T \ln(T) - b'T^2 - \left(\frac{c'}{2}\right)T^3 - \left(\frac{d'}{3}\right)T^4 + \left(\frac{e'}{2T}\right) + f' + g'T$$



## C.1.1.2G\_K function

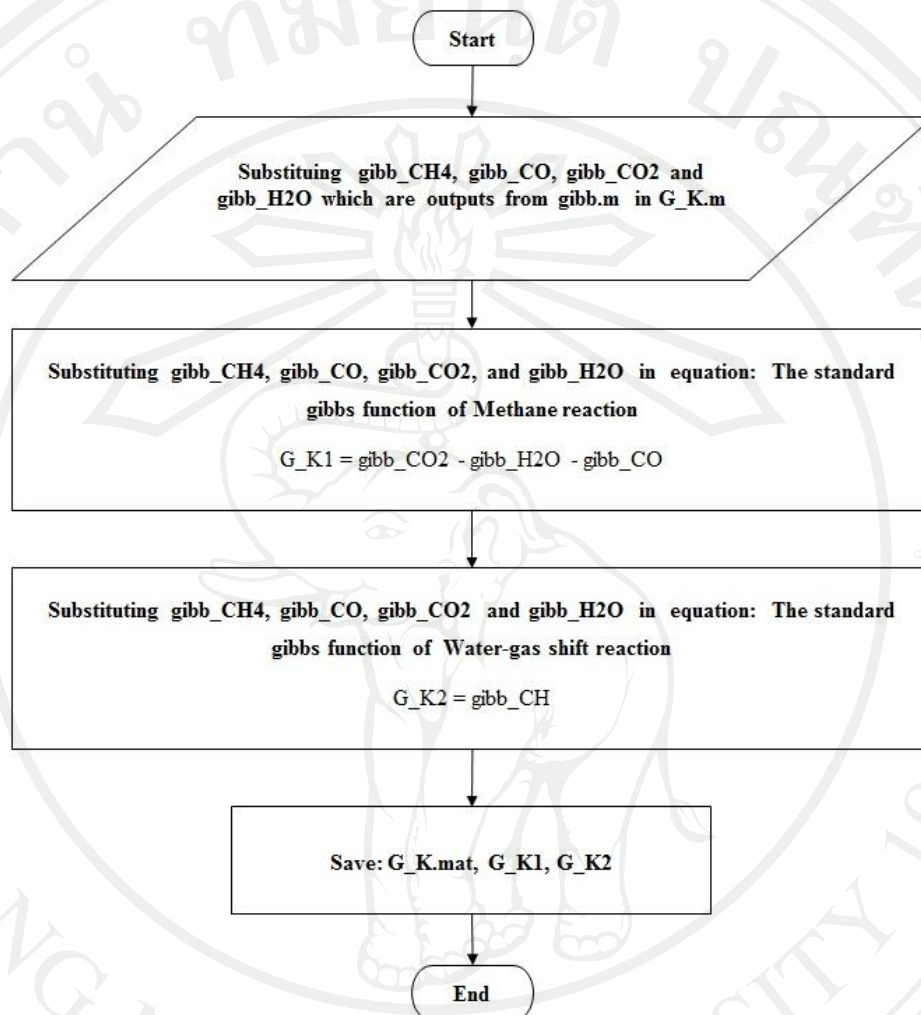
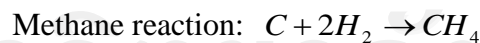


Figure C.4 Design process flow of Standard Gibbs function

G\_K is function of Standard Gibbs function which used to calculate Gibbs energy of gases involving methane and water gas shift reaction.



According to figure C.3, once get gibb\_CH4, gibb\_CO, gibb\_CO2, gibb\_H2O from gibb.m, program will substitute these values into Standard Gibbs function (

$\Delta G_T^\circ = \sum_i v_i \Delta \bar{g}_{f,T,i}^\circ$ ). Per aforesaid, for non-compound gas or stable element such as  $N_2$ ,

Standard Gibbs function of formation is 0. Hence, equation will be reduced form as figure C1.3. Program will record results which are G\_K1, G\_K2 for further action.

### C.1.1.3K function

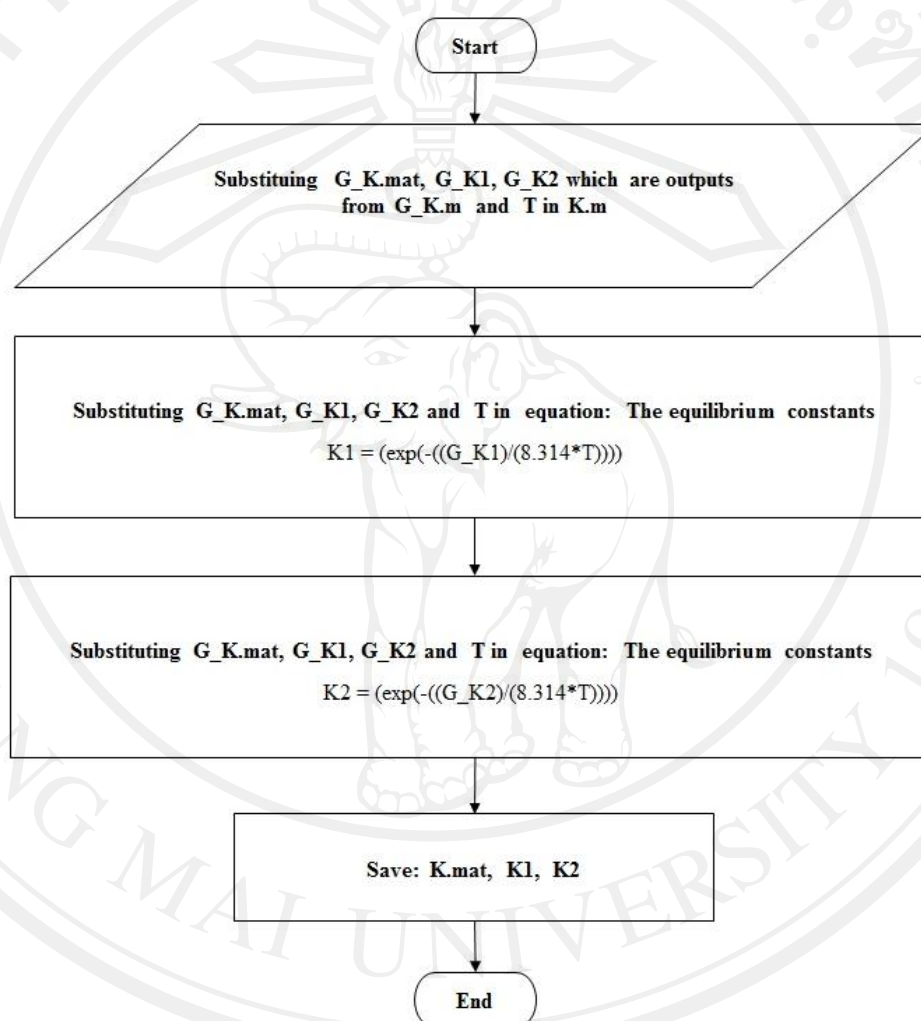


Figure C.5 Design process flow of K function

K is function of Equilibrium constants function which used to calculate Equilibrium constants of methane and water gas shift reaction. Equilibrium constants can be find by solving equation:  $\ln K = -\frac{\Delta G_r^\circ}{RT}$  (where  $\bar{R}$  is gas constant, 8.314 kJ/kmol.K). Program will substitute G\_K1, G\_K2 from G\_K.m and T in this equation and record G\_K1, G\_K2 for further action.

## C.1.1.4f function

f is function which used to derive 5 equations since having 5 unknown values.

Given:  $n_{CO} = x_1$ ,  $n_{CO_2} = x_2$ ,  $n_{CH_4} = x_3$ ,  $n_{H_2} = x_4$ ,  $n_{H_2O} = x_5$

Hence, following equations can be made from mass balancing and equilibrium thermodynamics.

Carbon balance:  $f_1 = x(1)+x(2)+x(3)-1$

Hydrogen balance:  $f_2 = 2*x(4)+2*x(5)+4*x(3)-nH-2*w$

Oxygen balance:  $f_3 = x(1)+2*x(2)+x(5)-w-2*m-nO$

Equilibrium constant balance 1:  $f_4 = K_1*x(1)*x(5)-x(2)*x(4)$

Equilibrium constant balance 2:  $f_5 = K_2*(x(4))^2-x(3)*(x(1)+x(2)+x(3)+x(4)+x(5)+(nN/2+(3.76*m)))$

Then, forming these functions into matrix as following;

$$f = \begin{bmatrix} f_1 \\ f_2 \\ f_3 \\ f_4 \\ f_5 \end{bmatrix}$$

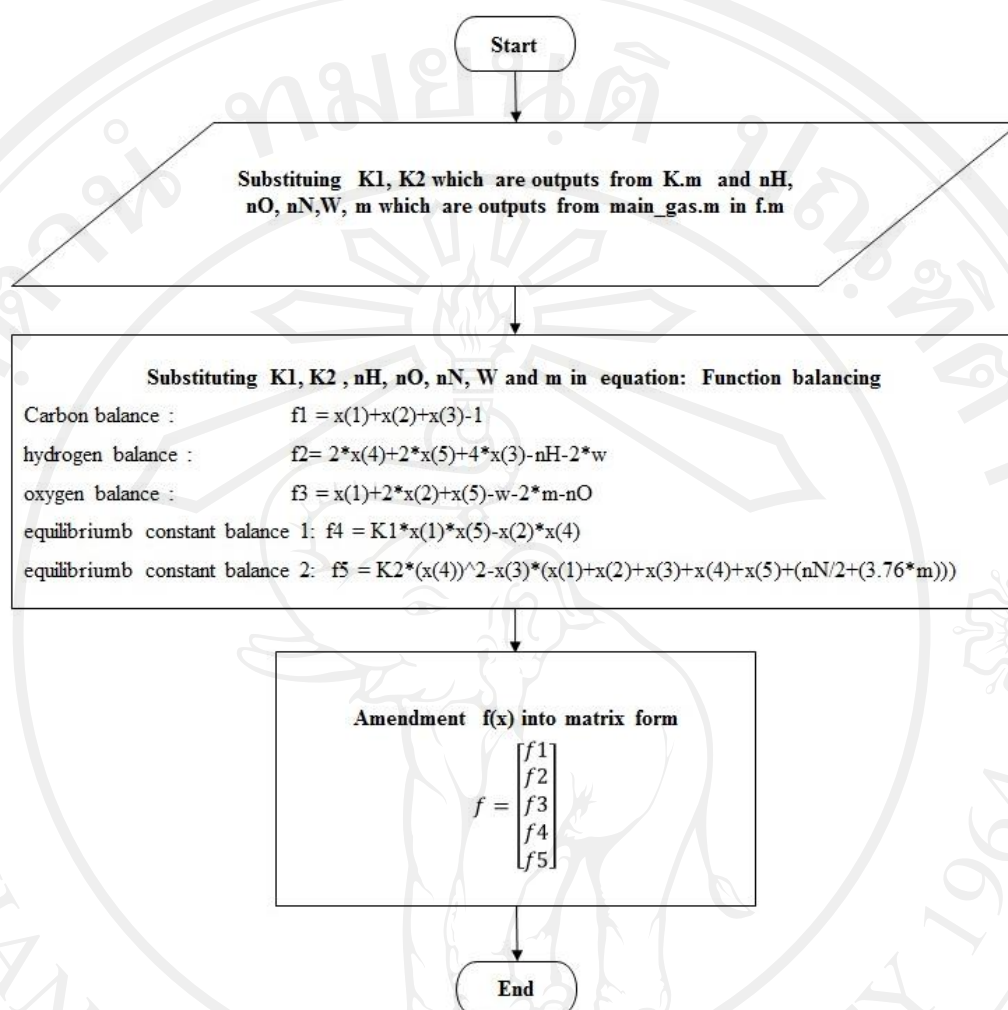


Figure C.6 Design process flow of f function

## C.1.1.5 jacobain function

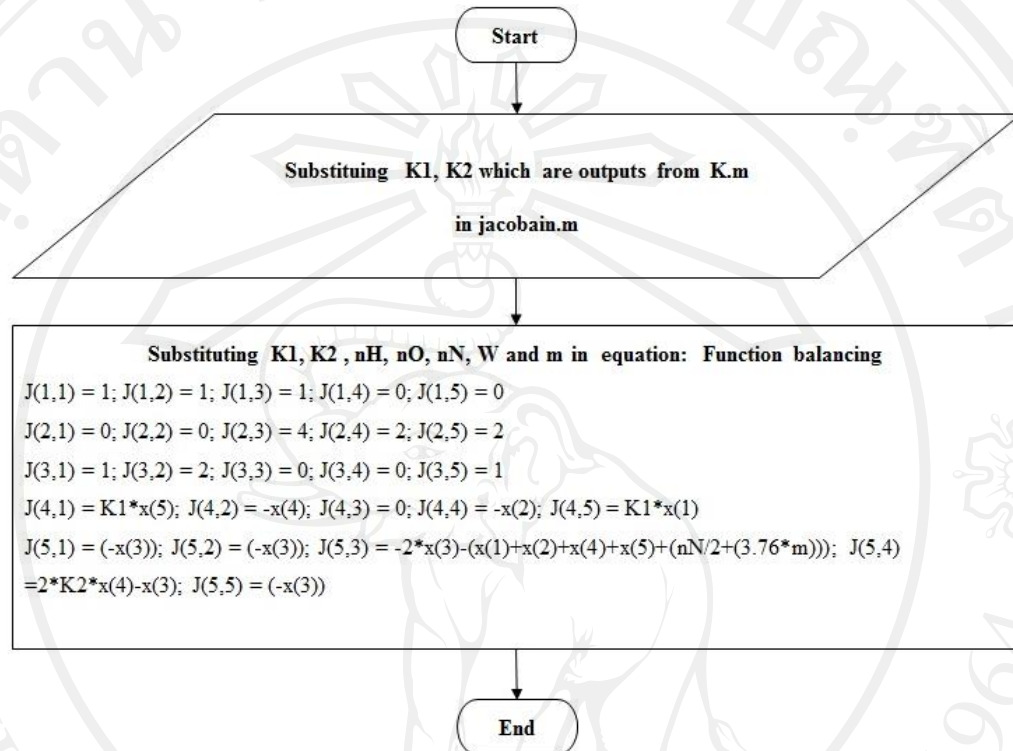


Figure C.7 Design process flow of jacobain function

## C.1.1.6 Raphson function

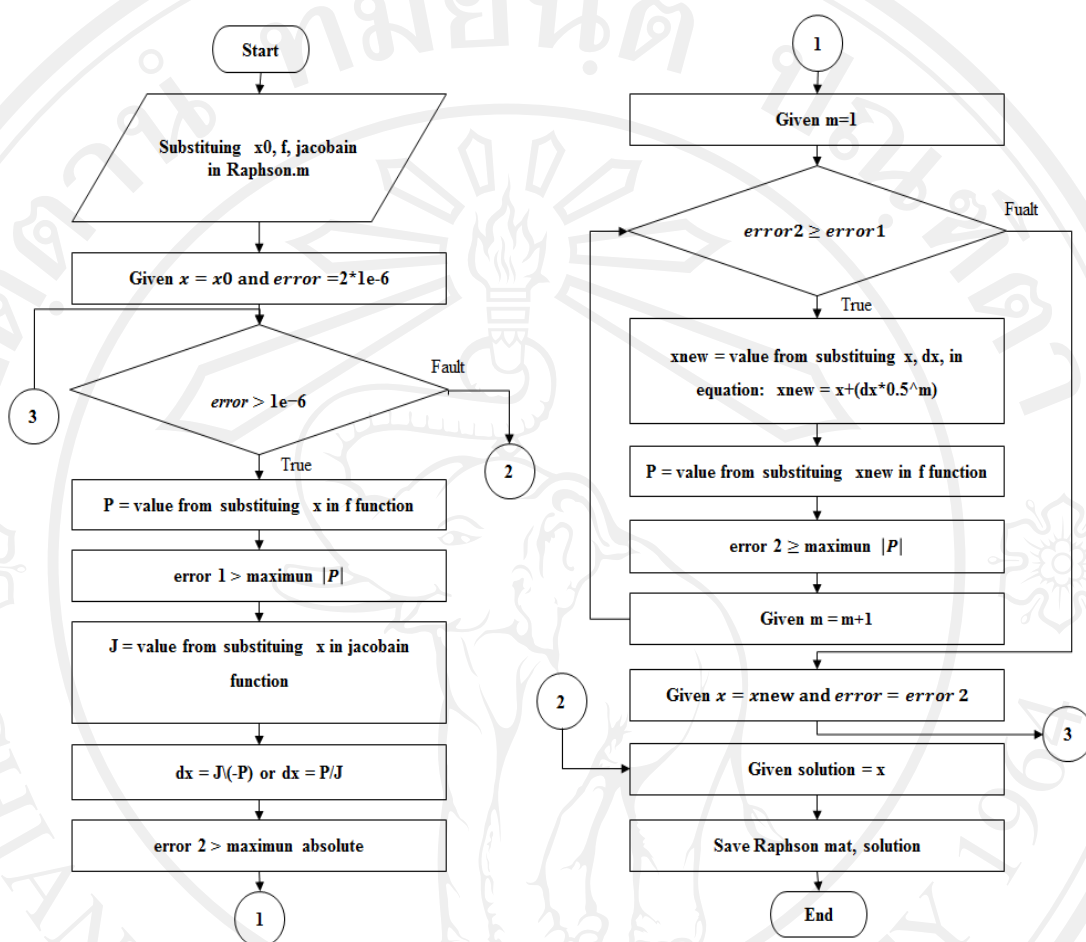


Figure C.8 Design process flow of Raphson function

Raphson function is mathematical methodology which used to predict amount of production gas in gasification process. Main purpose of this function is to check the condition.

## C.1.1.7 Hwood function

Hwood is function to find fuel's enthalpy which is used in process. This function will start from finding LHL in  $kJ/kmol$  unit, substituting LHL in equation to solve Hwood then record Hwood for further action.

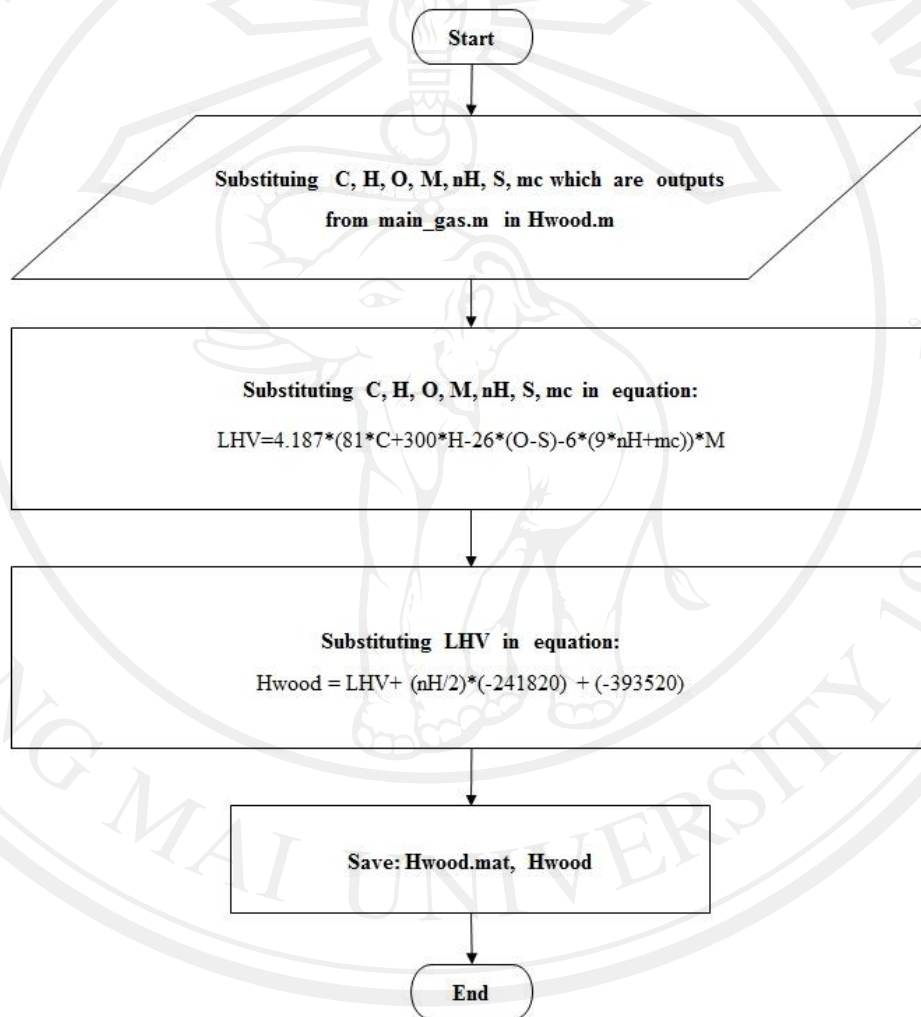


Figure C.9 Design process flow of Hwood function



## C.1.1.8 enthalpy function

Enthalpy is function to create equations from energy balance in order to find temperature during gasification process.

$$\sum_{j=react} \bar{h}_{f,j}^{\circ} = \sum_{i=prod} \bar{h}_{f,i}^{\circ} + \left[ \left( \sum_i n_i a_i \right) T + \left( \sum_i n_i b_i \right) T^2 + \left( \sum_i n_i c_i \right) T^3 + \left( \sum_i n_i d_i \right) T^4 + \sum_i n_i k_i \right]$$

When substituting constant values in equation, it results equation which has one variable unknown (T\_new). Program will solve polynomial of degree 4 and record enthalpy for further action.

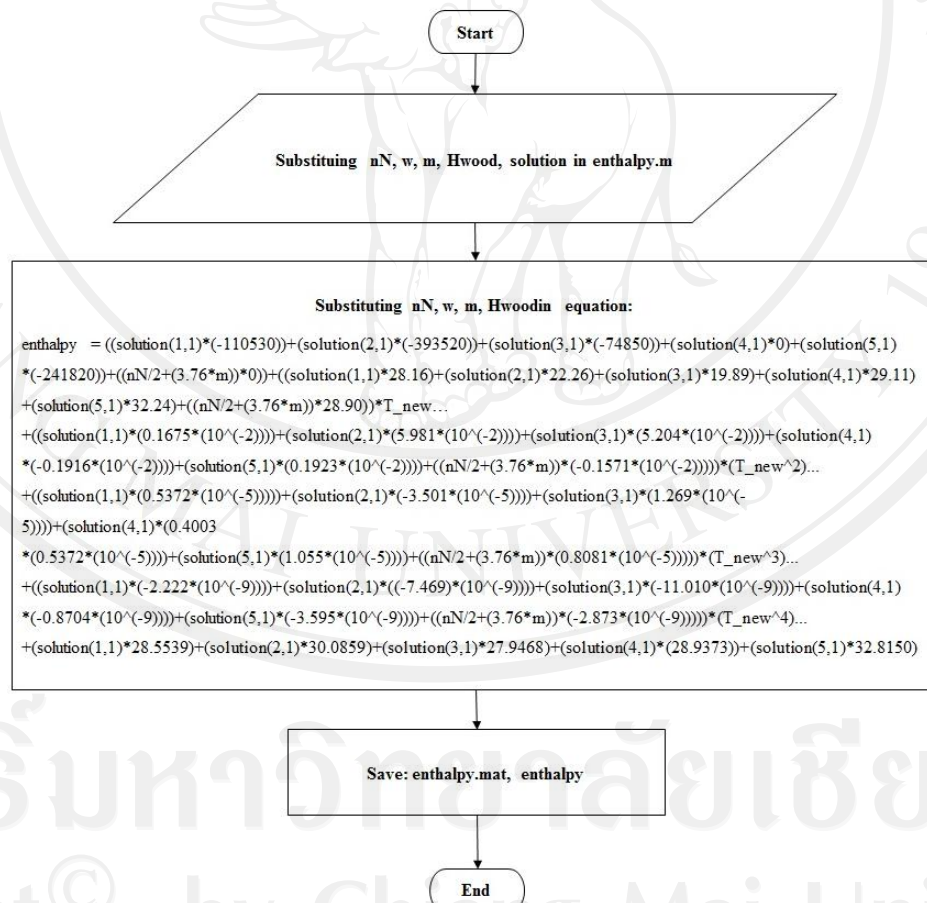


Figure C.10 Design process flow of enthalpy function



## C.1.1.9 h function

h is function to solve polynomial of degree 4 for finding  $T_{\text{new}}$  or finding  $m_{\text{new}}$  in gasification process.

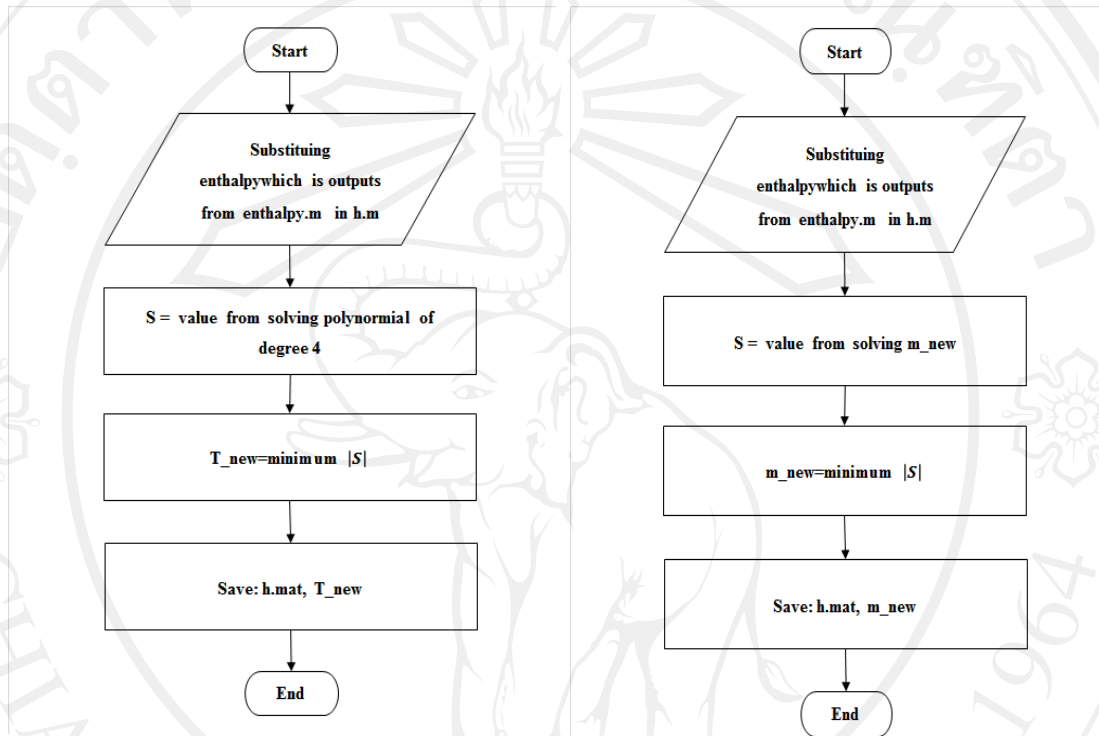


Figure C.11 Design process flow of h function

## APPENDIX D

### Model Validation

#### D.1 Model Validation

##### D.1.1 Fixed Bed Gasification

##### D.1.1.1 RMSE Calculation for Present Model

Table D.1 Results of RMSE calculation for experimental results and present models for fixed gasification

Biomass	Temperature	H <sub>2</sub>	CO	CH <sub>4</sub>	CO <sub>2</sub>	O <sub>2</sub>	N <sub>2</sub>	Total
	(°C)	(mol %)	(mol %)	(mol %)	(mol %)	(mol %)	(mol %)	(mol %)
Bamboo	600.00	0.42	4.99	1.21	17.79	0.00	66.76	100.00
	700.00	0.47	4.85	1.21	16.09	0.00	69.03	100.00
	800.00	0.53	4.85	1.05	16.16	0.00	69.20	100.00
	900.00	0.82	4.88	1.00	15.62	0.00	68.40	100.00
	RMSE	4.36	2.15	1.07	3.93	0.00	1.09	
	AVG. RMSE							2.52
Mimosa	600.00	0.50	3.44	1.02	17.21	0.00	70.47	100.00
	700.00	1.00	4.49	1.46	19.50	0.00	64.36	100.00
	800.00	1.02	4.39	1.45	23.88	0.00	63.07	100.00
	900.00	1.26	4.68	1.12	22.79	0.00	66.38	100.00
	RMSE	6.20	3.30	1.20	4.61	0.00	3.45	
	AVG. RMSE							3.75

## D.1.1.2 RMSE Calculation for Modified Model

Table D.2 Results of RMSE calculation for experimental results and modified models for fixed bed gasification

Biomass	Temperature	H <sub>2</sub>	CO	CH <sub>4</sub>	CO <sub>2</sub>	O <sub>2</sub>	N <sub>2</sub>	Total
	(°C)	(mol %)	(mol %)	(mol %)	(mol %)	(mol %)	(mol %)	(mol %)
Bamboo	600.00	0.42	4.99	1.21	17.79	0.00	66.76	100.00
	700.00	0.47	4.85	1.21	16.09	0.00	69.03	100.00
	800.00	0.53	4.85	1.05	16.16	0.00	69.20	100.00
	900.00	0.82	4.88	1.00	15.62	0.00	68.40	100.00
	RMSE	3.73	1.74	0.69	5.30	0.00	1.35	
	AVG. RMSE							2.56
Mimosa	600.00	0.50	3.44	1.02	17.21	0.00	70.47	100.00
	700.00	1.00	4.49	1.46	19.50	0.00	64.36	100.00
	800.00	1.02	4.39	1.45	23.88	0.00	63.07	100.00
	900.00	1.26	4.68	1.12	22.79	0.00	66.38	100.00
	RMSE	5.80	1.72	0.91	4.15	0.00	2.84	
	AVG. RMSE							3.08

## D.1.2 Fluidized Bed Gasification

## D.1.2.1 RMSE Calculation for Present Model

Table D.3 Results of RMSE calculation for experimental results and present models for fluidized bed gasification

Biomass	Temperature	H <sub>2</sub>	CO	CH <sub>4</sub>	CO <sub>2</sub>	O <sub>2</sub>	N <sub>2</sub>	Total
	(°C)	(mol %)	(mol %)	(mol %)	(mol %)	(mol %)	(mol %)	(mol %)
Bamboo	400.00	2.33	8.70	1.29	16.16	4.97	66.55	100.00
	500.00	2.12	8.27	1.58	17.94	4.40	65.69	100.00
	600.00	1.96	6.98	1.54	19.15	3.79	66.57	100.00
	700.00	0.77	5.96	1.30	19.41	4.64	67.91	100.00
	RMSE	3.53	4.61	1.09	5.32	0.00	1.15	
	AVG. RMSE							3.14
Mimosa	400.00	3.13	9.84	1.72	14.65	5.31	65.35	100.00
	500.00	4.44	9.70	1.37	13.21	8.78	62.51	100.00
	600.00	1.96	8.27	1.54	19.15	3.79	65.28	100.00
	700.00	0.77	6.98	1.30	19.41	4.64	66.88	100.00
	RMSE	4.81	5.84	0.99	5.84	0.00	3.26	
	AVG. RMSE							4.15

## D.1.2.2 RMSE Calculation for Modified Model

Table D.4 Results of RMSE calculation for experimental results and modified models for fluidized bed gasification.

Biomass	Temperature	H <sub>2</sub>	CO	CH <sub>4</sub>	CO <sub>2</sub>	O <sub>2</sub>	N <sub>2</sub>	Total
	(°C)	(mol %)	(mol %)	(mol %)	(mol %)	(mol %)	(mol %)	(mol %)
Bamboo	400.00	2.33	8.70	1.29	16.16	4.97	66.55	100.00
	500.00	2.12	8.27	1.58	17.94	4.40	65.69	100.00
	600.00	1.96	6.98	1.54	19.15	3.79	66.57	100.00
	700.00	0.77	5.96	1.30	19.41	4.64	67.91	100.00
	RMSE	2.47	4.56	1.08	5.01	0.00	1.71	
	AVG. RMSE							2.97
Mimosa	400.00	3.13	9.84	1.72	14.65	5.31	65.35	100.00
	500.00	4.44	9.70	1.37	13.21	8.78	62.51	100.00
	600.00	1.96	8.27	1.54	19.15	3.79	65.28	100.00
	700.00	0.77	6.98	1.30	19.41	4.64	66.88	100.00
	RMSE	3.77	7.35	1.22	6.68	0.00	5.22	
	AVG. RMSE							4.85

## D.2 Model Validation and Modification

### D.2.1 Sharma (2008a)

Table D.5 Biomass components using in Sharma (2008a) model.

C	56.2%
H	5.9 %
O	36.7 %
N	0.22 %
S	0.03 %

Source: Sharma (2008a)

Remark: Relative humidity is 30% while Amount of oxygen is 0.4 at any temperature.

Table D.6 Product gas at various temperatures of present model using biomass components used in Sharma (2008a)

Temperature (K)	H <sub>2</sub>	CO	CO <sub>2</sub>	CH <sub>4</sub>	N <sub>2</sub>
1100	21.47	19.77	11.42	0.153	47.19
1150	21.09	20.58	10.82	0.095	47.42
1200	20.72	21.29	10.29	0.062	47.64
1250	20.36	21.92	9.82	0.041	47.86
1300	20.03	22.48	9.41	0.028	48.06
1350	19.72	22.99	9.04	0.020	48.24
RMSE	5.99	3.95	2.18	1.57	6.66
AVG.RMSE					4.07

Table D.7 Product gas at various temperatures from the modified model by the biomass components used in Sharma (2008a)

Temperature (K)	H <sub>2</sub>	CO	CO <sub>2</sub>	CH <sub>4</sub>	N <sub>2</sub>
1100	21.19	19.91	11.32	0.226	47.36
1150	20.86	20.75	10.70	0.141	47.56
1200	20.52	21.48	10.16	0.091	47.76
1250	20.18	22.12	9.68	0.061	47.97
1300	19.86	22.68	9.26	0.042	48.16
1350	19.56	23.19	8.88	0.029	48.34
RMSE	5.51	4.29	2.42	1.48	6.37
AVG.RMSE					4.02

#### D.2.2 Sharma (2008b)

Table D.8 Biomass components of. Sharma (2008b) Modeling.

nC	1
nH	1.4
nO	0.6

Source: Sharma (2008b)

Remark: Relative humidity is 11% while Amount of oxygen is 0.41 at any temperature.



Table D.9 Product gas at various temperatures of present model using biomass components used in Sharma (2008b)

Temperature (K)	H <sub>2</sub>	CO	CO <sub>2</sub>	CH <sub>4</sub>
850	8.76	7.46	14.73	1.987
870	11.01	10.03	14.00	1.570
890	17.34	12.99	13.37	1.235
910	18.85	16.18	12.83	0.970
932	18.99	18.82	12.30	0.745
RMSE	2.10	0.92	2.34	2.01
AVG.RMSE				1.47

Table D.10 Product gas at various temperatures from the modified model by the biomass components used in Sharma (2008b)

Temperature (K)	H <sub>2</sub>	CO	CO <sub>2</sub>	CH <sub>4</sub>
850	8.12	7.89	15.27	2.615
870	10.76	10.21	14.45	2.110
890	17.11	13.18	13.72	1.692
910	18.07	16.31	13.35	1.351
932	18.33	19.17	12.49	1.052
RMSE	1.02	0.45	1.68	3.04
AVG.RMSE				1.24

## D.2.3 Gautam Modeling

Table D.11 Biomass components of Gautam (2010) modeling.

C	50 %
H	6 %
O	44 %
N	0 %

Source: Gautam (2010)

Remark: Relative humidity is 0%

Table D.12 Product gas at various temperatures of present model using biomass components used in Gautam (2010) model

Temperature (K)	H <sub>2</sub>	CO	CO <sub>2</sub>	CH <sub>4</sub>	N <sub>2</sub>
923.00	19.00	24.07	9.71	0.854	46.36
1033.00	18.31	22.49	10.21	0.223	48.77
1143.00	16.11	22.17	9.92	0.062	51.74
1253.00	13.86	21.53	9.88	0.019	54.71
RMSE	0.37	0.39	0.24	0.01	0.54
AVG.RMSE					0.31

Table D.13 Product gas at various temperatures from the modified model by the biomass components used in Gautam (2010) model

Temperature (K)	H <sub>2</sub>	CO	CO <sub>2</sub>	CH <sub>4</sub>	N <sub>2</sub>
923.00	18.31	23.76	9.96	1.204	46.76
1033.00	17.22	23.81	9.24	0.303	49.42
1143.00	15.25	23.34	9.06	0.085	52.27
1253.00	13.12	22.54	9.13	0.027	55.18
RMSE	0.47	0.32	0.29	0.12	0.42
AVG.RMSE					0.32



# Non-isothermal pyrolysis characteristics of giant sensitive plants using thermogravimetric analysis

Thanasit Wongsiriamnuay, Nakorn Tippayawong \*

Department of Mechanical Engineering, Chiang Mai University, Chiang Mai 50200, Thailand

## ARTICLE INFO

### Article history:

Received 23 December 2009

Received in revised form 5 February 2010

Accepted 8 February 2010

Available online 1 March 2010

### Keywords:

Biomass

Mimosa

Pyrolysis

Renewable energy

Thermal decomposition

## ABSTRACT

A giant sensitive plant (*Mimosa pigra* L.) or Mimosa is a fast growing woody weed that poses a major environmental problem in agricultural and wet land areas. It may have potential to be used as a renewable energy source. In this work, thermal behaviour of dried Mimosa was investigated under inert atmosphere in a thermogravimetric analyzer at the heating rates of 10, 30, and 50 °C/min from room temperature to 1000 °C. Pyrolysis kinetic parameters in terms of apparent activation energy and pre-exponential factor were determined. Two stages of major mass loss occurred during the thermal decomposition process, corresponding to degradation of cellulose and hemicellulose between 200–375 °C and decomposition of lignin around 375–700 °C. The weed mainly devolatilized around 200–400 °C, with total volatile yield of about 60%. The char in final residue was about 20%. Mass loss and mass loss rates were strongly affected by heating rate. It was found that an increase in heating rate resulted in a shift of thermograms to higher temperatures. As the heating rates increased, average devolatilization rates were observed to increase while the activation energy decreased.

© 2010 Elsevier Ltd. All rights reserved.

## 1. Introduction

Future contribution of renewable energy is vital as energy becomes increasingly scarce and expensive. Use of diverse biomass resources is projected to contribute to a major fraction of future energy demands. Nonetheless, competition between biomass supply for fuel or for food applications has been intensified in the recent years. This concern has resulted in growing interests in alternative, non-edible biomass resources such as perennial rhizomatous grasses; miscanthus (*Miscanthus*), switchgrass (*Panicum virgatum*), reed canary grass (*Phalaris arundinacea*), giant reed (*Arundo donax*) and bamboo because of their high yield potential, appropriate biomass characteristics, low input demand and positive environmental impact (Lewandowski et al., 2003; Basso et al., 2005; Scurlock et al., 2000). In Thailand, non-plantation biomass resources have been assessed for their energy potential and found to be promising (Sujjakulnukit et al., 2005). Weeds such as giant sensitive plants are viewed to have potential as a useful bio-energy source. Giant sensitive plant is woody member of the genus *Mimosa*, in the family Fabaceae comprising about 400–450 species. It is a woody invasive shrub that originates from tropical America. Now, it can be found in tropical and subtropical areas over many countries especially Australia, Thailand, Vietnam, South American, and African countries. It forms dense, thorny impenetrable

thickets, particularly in wet areas. It is one of the worst environmental weeds. Owing to its strong, dense and woody stems, some small fraction of *Mimosa* is utilised as firewood, bean-poles, and as temporary fences. So far, there have been relatively few literatures reporting on utilisation of *Mimosa* as feedstock for bioenergy (Presnell, 2004; Wongsiriamnuay et al., 2008).

Thermal conversion technology is an attractive route to produce fuel gases from natural resources. When the thermal process is carried out in a reactor, the raw material undergoes pyrolysis, gasification and combustion. They are complicated processes consisting of several main chemical reactions and large number of intermediate reactions. Many alternative paths are available to the reacting compounds, depending on the process conditions. Physico-chemical compositions of the fuel are also important and decisive factors for the characteristics of the thermal conversion. Thermogravimetric analysis (TGA) can be an useful tool to study the thermal behaviour of materials. The rate of mass loss as a function of temperature and time is measured and provides a means to estimate the kinetic parameters in the thermal decomposition reaction. These data are crucial for efficient modeling, design and operation of pyrolysis process and related thermochemical conversion systems. To determine the effect of temperature and heating rate on their pyrolysis characteristics, the samples are pyrolyzed under non-isothermal conditions in a thermogravimetric analyzer. Many TGA studies have been carried out for pyrolysis of various non-edible biomass sources (Jeguirim and Trouve, 2009; Park et al., 2009; Kumar et al., 2008; Maiti et al., 2007; Erlich et al., 2006; Collura et al.,

\* Corresponding author. Tel.: +66 5394 5146; fax: +66 5394 4145.

E-mail address: [n.tippayawong@yahoo.com](mailto:n.tippayawong@yahoo.com) (N. Tippayawong).

2005; Cao et al., 2004; Meszaros et al., 2004; Fisher et al., 2003; Müller-Hagedorn et al., 2003; Gronli et al., 2002; Karaosmanoglu et al., 2001). To the authors' knowledge, there has not yet been a report on pyrolysis characteristics of giant sensitive plants. The objectives of this investigation are therefore to study pyrolysis characteristics and to analyze change of kinetic behaviour with conversion for the giant sensitive plant. Comparisons are made against other biomass sources.

## 2. Methods

### 2.1. Samples

The samples of Mimosa collected in agricultural zone in Chiang Mai, Thailand were used. The collected stalks were cleaned and air dried naturally in a dry store room at ambient condition. The dried samples were crushed and grounded in a high speed rotary mill, and sieved to provide a feed sample in the size range of about 0.5 mm. Preparation of samples prior to analyses was conducted in accordance with TAPPI T 257 and T 264 standards. Contents of the major biopolymer constituents of the weed, holocellulose, lignin and solvent extractive components were evaluated using TAPPI standard methods. The solubilities of extractives in ethanol and benzene mixture as well as quantity of soluble substances in sodium hydroxide and in water were established. ASTM standard methods were followed to carry out proximate analysis for the samples. The carbon, hydrogen and nitrogen contents were determined using a CHN elemental analyzer. The oxygen content was calculated by difference. The heating value of the dried Mimosa stalk was determined in compliance with ASTM standard using a Parr bomb calorimeter. It was reported as a gross heat of combustion at constant volume. Analysis results of the dried Mimosa samples are shown in Table 1.

### 2.2. Thermogravimetric apparatus

Thermal decomposition of the biomass materials were analyzed using a TGA/SDTA 851e thermogravimetric analyzer (sensitive microbalance, 1 µg resolution, 1300 °C maximum temperature at atmospheric pressure, 50 bar maximum at 1000 °C, and 30 °C/min maximum heating rate). This high performance TG analyzer has high sensitivity, vibration resistance and structure that permit rapid replacement of samples. Large number of samples can be analyzed in a short time and in succession. The system was logged to a personal computer for data handling and analysis. Prior to TGA, temperature, weight and sample platform calibrations were carried out. Each sample was placed in the platinum pan securely

and in such a way that it was confined within the pan sides and not in contact with the sides of the oven. All handling of samples were done using brass tweezers to avoid contamination. Non-isothermal experiment runs were carried out at 10, 30, and 50 °C/min under atmospheric pressure, with an initial weight sample of 5 mg and a purge gas flow of 50 cm<sup>3</sup>/min. The purge gases used were high purity nitrogen, air or oxygen. The sample was initially preheated to and equilibrated at 40 °C in nitrogen under a flow rate of 50 cm<sup>3</sup>/min for 10 min. The sample was then heated to 1000 °C at a constant heating rate. The continuous records of weight loss and temperatures were obtained. At least three runs were performed for each condition.

## 3. Results and discussion

### 3.1. Thermal decomposition

The proximate chemical compositions of Mimosa stems were found to be similar to hard woods, but with higher ash content (Nordin, 1994). Ultimate analysis showed that raw Mimosa consisted of moderately high carbon content (43.9%) and low amounts of hydrogen (6.0%) and nitrogen (1.4%). Cellulose and hemicellulose were presented in terms of holocellulose, accounting for nearly 60% of total mass. Lignin content of Mimosa was found to be relatively high (33.9%). During pyrolysis of lignocellulosic materials, mass losses occurred due to dehydration at low temperatures, decomposition of hemicellulose, cellulose and lignin. Decompositions of these components were normally overlapped (Jeguirim and Troune, 2009).

Thermal decomposition behaviours of Mimosa pyrolysis under flowing nitrogen were obtained. The results of thermogravimetric experiments were expressed as conversion  $\alpha$ , defined as:

$$\alpha = \frac{W_i - W_t}{W_i - W_f} \quad (1)$$

where  $W_i$ ,  $W_t$  and  $W_f$  are the initial mass of the sample, the mass of pyrolyzed sample, and the final residual mass, respectively. The degree of conversion versus temperature at different heating rates of 10, 30 and 50 °C/min for the giant sensitive plant in TG analyzer are shown in Fig. 1. At the temperature lower than 150 °C, the small change of conversion in the samples was attributed to vaporisation of moisture that was attached on the surface of the samples. The giant sensitive plant samples started to decompose and release volatile matter around 200 °C. The TG curves of the giant sensitive trees showed only two major weight loss stages between 200 and 400 °C, and 400 and 700 °C. It was clear that the slope of the curve changed between the two temperature intervals. Slope between 200 and 400 °C was higher than that 400 and 700 °C. The conversions at different heating rates exhibited similar patterns. It was observed at temperatures below 400 °C that the TG curve shifted slightly to the right with increasing heating rate. At low heating rates, several distinct mass loss zones observed were associated with degradation dynamics of main constituents. Since the samples contained mainly cellulose, hemicellulose and lignin, it was known that the hemicellulose started to decompose at around 225–325 °C and the cellulose was found to decompose between 325 and 375 °C. Lignin had a broad decomposition temperature range at temperatures higher than 250–500 °C (Shafizadeh, 1985; Di Blasi and Lanzetta, 1997; Ferdous et al., 2002). As the heating rate was increased, these thermal degradation zones tended to merge. Simultaneous participation of all components cannot be avoided in measured mass loss (Di Blasi, 2008). Decomposition at 500 °C or higher progressed slowly due to the remaining lignin or char, similar to that reported by Fisher et al. (2003).

**Table 1**  
Analysis of dried Mimosa samples.

Property	Unit	Method	Quantity
<i>Proximate analysis</i>			
Moisture	(% w/w)	ASTM D 3173	1.6
Volatile	(% w/w)	ASTM D 3175	71.1
Fixed carbon	(% w/w)	ASTM D 3172	23.6
Ash	(% w/w)	ASTM D 3177	3.7
<i>Ultimate analysis</i>			
Carbon	(%)	ASTM D 3174	43.9
Hydrogen	(%)	ASTM D 3174	6.0
Nitrogen	(%)	ASTM D 3174	1.4
Oxygen	(%)	By difference	48.7
<i>Lignocellulosic content</i>			
Holocellulose	(% w/w)	Wise method	58.2
Lignin	(% w/w)	TAPPI T 222	33.9
Higher heating value	(MJ/kg)	ASTM 5865	17.5



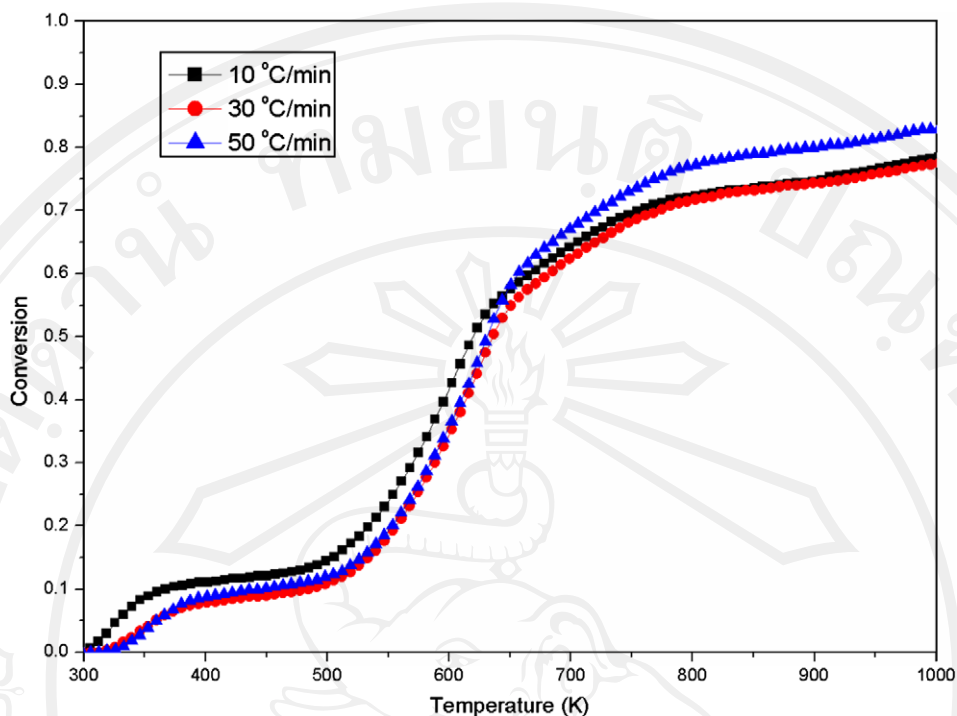


Fig. 1. Conversion as a function of temperature in the thermal treatment of Mimosa under nitrogen atmosphere at different heating rates.

The differential rates of instantaneous conversion,  $d\alpha/dt$ , were obtained from TG analysis at different heating rates, shown in Fig. 2. The differential TG curve of each heating rate has one extensive peak, occurred between 325 and 375 °C. The maximum peaks were attributed to the decomposition of cellulose and hemicellulose. Higher heating rate was found to shift the differential TG curve to a greater range of temperature. This was attributed to the fact that when the heating rate was in-

creased, the retention time was shorter and the temperature required for organic matter to decompose was greater (Ferdous et al., 2002; Senneca, 2007; Jeguirim and Trouve, 2009), causing the maximum curve rate to move rightward. These behaviours were similar to those reported by Wang et al. (2008) and Jeguirim and Trouve (2009). Increasing the heating rate also led to an increase in the maximum rate of  $d\alpha/dt$  of the TG curve (Ferdous et al., 2002; Hu et al., 2007). The maximum points of the

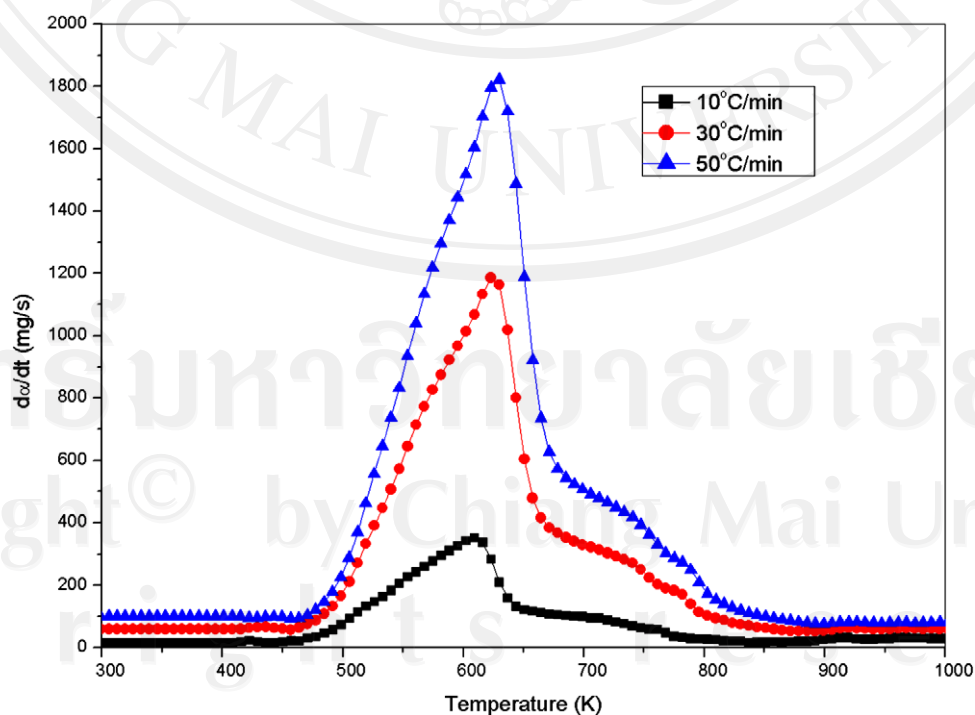
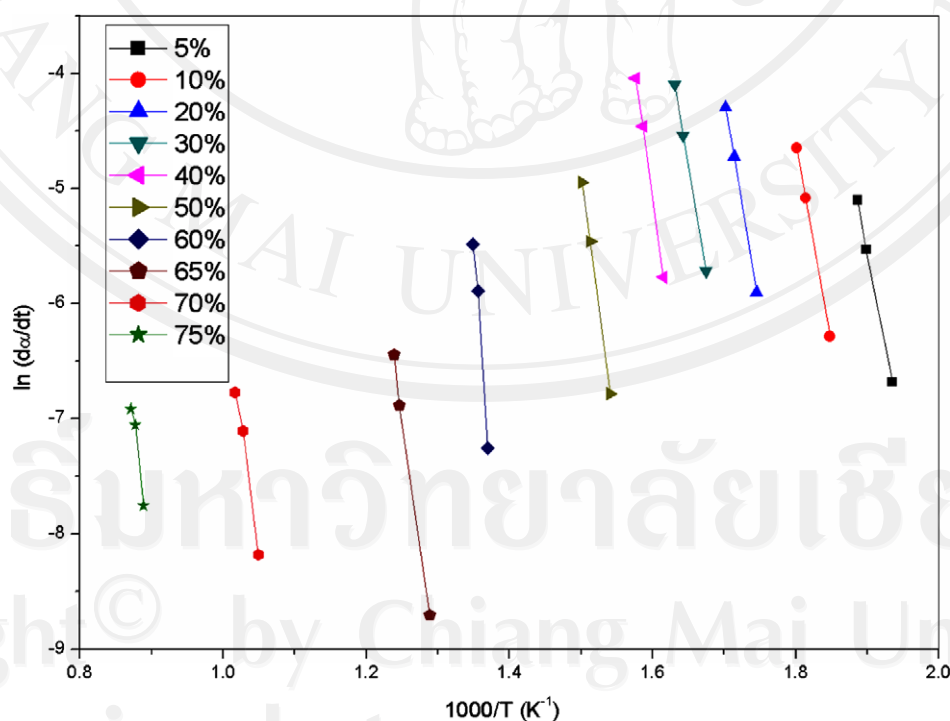


Fig. 2. DTG curves of thermal decomposition of Mimosa under nitrogen at different heating rates.

**Table 2**

Degradation characteristic of various biomass sources at low heating rates.

Reference	Biomass	$T_{\text{start}}$ (°C)	$T_{\text{peak}}$ (°C)	$dx/dt_{\text{peak}}$	$\alpha_{\text{peak}}$	$\alpha_{500^\circ\text{C}}$	Heating rate (°C/min)
This work	Mimosa	198	336	0.748	0.45	0.29	10
		191	350	2.33	0.42	0.30	30
		197	356	4.11	0.49	0.24	50
Gronli et al. (2002)	Alder	242	349	1.02	0.40	0.17	5
	Beech	248	349	0.91	0.37	0.18	5
	Birch	244	353	0.98	0.32	0.14	5
	Oak	237	338	0.89	0.45	0.23	5
	Douglas fir	243	334	0.87	0.55	0.24	5
	Pine A	238	351	0.91	0.45	0.20	5
	Pine B	209	350	0.81	0.43	0.20	5
	Redwood	235	351	0.83	0.50	0.26	5
	Spruce	249	352	0.77	0.46	0.23	5
	Hard woods	243	347	0.95	0.38	0.18	5
Kalita and Saikia (2004)	Soft woods	235	348	0.84	0.47	0.22	5
	<i>P. alba</i>	170	360	–	0.58	–	20
	<i>C. procera</i>	210	290	–	0.85	–	20
	<i>E. neerifolia</i>	180	360	–	0.76	–	20
	<i>N. indicum</i>	140	350	–	0.68	–	20
Gomez et al. (2007)	<i>M. elengi</i>	170	340	–	0.57	–	20
	Thistle	214	334	0.20	–	–	20
	Pine	254	378	0.30	–	–	20
Yao et al. (2008)	Beech	259	380	0.35	–	–	20
	Bagasse	–	299.3	–	0.53	–	2
	Bamboo	–	285.9	–	0.44	–	2
Jeguirim and Trouve (2009)	Cotton stalk	–	293.4	–	0.50	–	2
	Hemp	–	282.3	–	0.38	–	2
	Jute	–	283.1	–	0.44	–	2
	Kenaf	–	284.1	–	0.42	–	2
	Rice husk	–	297.4	–	0.37	–	2
	Rice straw	–	273.6	–	0.35	–	2
	Maple	–	308.3	–	0.58	–	2
	Pine	–	311.5	–	0.59	–	2
	Giant reed	200	308	0.826	0.58	0.29	5

**Fig. 3.** Relationships between the rate of conversion with temperature for conversions of 5–75%.

TG curves occurred at 335, 350 and 355 °C for heating rates of 10, 30 and 50 °C/min, respectively. It can be seen that the maximum rate of decomposition tended to increase at higher heat-

ing rate because it provided higher thermal energy to facilitate better heat transfer between the surrounding and inside the samples. These results were in similar trends with previous re-





ports (Park et al., 2009b; Jeguirim and Trouve, 2009; Kumar et al., 2008).

Table 2 presents comparison of degradation characteristics in terms of onset temperature from the decomposition of hemicellulose component ( $T_{\text{start}}$ ), maximum conversion ( $\alpha_{\text{peak}}$ ), maximum mass loss rate ( $dx/dt_{\text{peak}}$ ) and its corresponding temperature ( $T_{\text{peak}}$ ), and percentage char yield at 500 °C ( $\alpha_{500^\circ\text{C}}$ ) between Mimosa and other biomass sources (Jeguirim and Trouve, 2009). Decomposition of Mimosa's hemicellulose component was at similar temperature ( $\sim 200$  °C) to giant reed and latex bearing plants, but lower than wood species. It was clear that the thermal degradation of Mimosa under inert atmosphere occurred at similar temperatures to those obtained for latex plant samples at similar TGA conditions (Kalita and Saikia, 2004). The maximum mass loss rate was obtained at similar range (340–360 °C) to other wood and latex plant samples (Gronli et al., 2002; Kalita and Saikia, 2004; Gomez et al., 2007), but slightly higher than agro-residues (Yao et al., 2008). Peak mass loss rate of Mimosa at 10 °C/min heating rate was in similar magnitude to giant reed and wood samples at 5 °C/min. However, if thermal degradation of wood residues at 20 °C/min was considered (Gomez et al., 2007), the Mimosa mass loss rate at 10 and 30 °C/min was found to be higher. Mimosa appeared to exhibit similar maximum conversion to wood and agro-residues, in the range between 0.32 and 0.59.

### 3.2. Kinetic parameters

The kinetic parameters for the global pyrolysis process of Mimosa can be calculated using similar procedure adopted by Park et al. (2009b) and Maiti et al. (2007). The general non-isothermal, decomposition reaction rate is;

$$\frac{d\alpha}{dt} = k(1 - \alpha)^n \quad (2)$$

where

$$k = A \exp(-E/RT) \quad (3)$$

$T$  is the temperature,  $A$  is the pre-exponential or frequency factor,  $t$  is the time,  $E$  is the activation energy,  $R$  is the universal gas constant,  $n$  is the order of reaction. The logarithmic form for Eq. (3) is

$$\ln\left(\frac{d\alpha}{dt}\right) = \ln A + n \ln \alpha - \frac{E}{RT} \quad (4)$$

Activation energy can be determined from the relationship between  $\ln(dx/dt)$  and  $1/T$ . Fig. 3 shows the relationship between  $\ln(dx/dt)$  and  $1/T$  at various conversions from 5% to 75%. Thus, a family of parallel straight lines with a slope of  $-E/R$  is obtained. When the heating rate was of 10, 30 and 50 °C/min, for example, the 10% conversion was obtained at the temperature of 267.4, 279.3 and 282.4 °C, respectively. At these temperatures, the values of  $\ln(dx/dt)$  were  $-6.28$ ,  $-5.08$  and  $-4.65$ , respectively. From the slope of  $\ln(dx/dt)$  against  $1/T$  at the conversion of 10%, the activation energy was calculated as 293.10 kJ/mol. The intercept ( $\ln(A \cdot \alpha^n)$ ) can also be obtained from Fig. 3, at each conversion. When the apparent order of reaction is assumed to be 0th, 1st or 2nd, the pre-exponential or frequency factor can be obtained from the following equation

$$\ln(A\alpha^n) = \ln A + n \ln \alpha \quad (5)$$

The variation of activation energy as a function of the conversion level, calculated using Eq. (5) is presented in Table 3. The activation energy for the pyrolysis of Mimosa ranged from 269 to 411 kJ/mol, depending on the conversion. The activation energy was found to increase from the conversion of 5% up to 40%, and appeared to remain relatively stable at an average value of 370 kJ/mol

for the conversion between 40% and 70%. When the conversion increased from 70% to 80%, the activation energy increased sharply. This observed behaviour may be due to an influence of heat or mass transfer at high temperatures greater than 500 °C. The activation energy values obtained here were higher than those obtained from oak tree, saw dust, and woods (Park et al., 2009b; Wang et al., 2008; Müller-Hagedorn et al., 2003), except for larch and white oak at high conversion (Park et al., 2008, 2009a). Jeguirim and Trouve (2009) reported the activation energies for cellulose and hemicelluloses to be in the range of 90–140 and 110 kJ/mol while Wang et al. (2008) reported the range of 142–168 and 158–250 kJ/mol for cellulose and hemicelluloses, respectively. The increase of activation energy at higher conversion may be attributable to further devolatilization of char after the main reaction. Most of cellulose and hemicelluloses were decomposed at the pyrolytic conversion from 5% to 70% with the average activation energy of 330 kJ/mol.

Also shown in Table 3 are the calculated pre-exponential factors, assuming the reaction order as zeroth, first or second. Main decomposition occurred at the conversion from 20% to 65%, where the pre-exponential factors were in the range of  $10^{17}$ – $10^{29}$  s $^{-1}$ . When the conversion increased above 65%, the pre-exponential factors declined rapidly to  $10^7$ – $10^{16}$  s $^{-1}$ , probably attributed to greater presence of residual char. These values were much larger than those reported for main decomposition of other biomass sources. Park et al. (2008, 2009a,b) calculated the pre-exponential factors for conversion between 20% and 70% to be in the range of  $10^{13}$ – $10^{20}$  s $^{-1}$ , for larch, white oak and oak tree. Wang et al. (2008) reported even lower values for sawdust ( $10^9$ – $10^{13}$  s $^{-1}$ ).

### 4. Conclusion

Thermal degradation of Mimosa under inert environment was investigated using TGA at different heating rates. Apparent activation energy and pre-exponential factor were determined. Pyrolysis of Mimosa occurred at similar temperatures to giant reed and latex bearing plants, but at lower temperatures than wood samples, between 200 and 500 °C. Increasing heating rate was found to increase mass loss rates but delay thermal decomposition to higher temperatures. The activation energy and pre-exponential factor were 269–411 kJ/mol, and  $10^7$ – $10^{29}$  s $^{-1}$ , respectively. During pyrolysis, the kinetic parameters changed with conversion between 5% and 80%. This may be heat or mass transfer limitations at high temperatures.

### Acknowledgements

This research is financially supported by the Thailand Research Fund (Contract No. RSA5080010) and Faculty of Engineering, Chiang Mai University. The Royal Golden Jubilee PhD scholarship (PHD/0047/2550) awarded to TW is greatly appreciated. Supports from the Energy Research and Development Institute, Chiang Mai University are also acknowledged.

### References

- Basso, M.V., Cerrella, E.G., Buonomo, E.L., Bonelli, P.R., Cukierman, A.L., 2005. Thermochemical conversion of *Arundo donax* into useful solid products. *Energy Sources* 27, 1429–1438.
- Cao, Q., Xie, K.C., Bao, W.R., Shen, S.G., 2004. Pyrolysis behaviour of waste corn cob. *Bioresource Technology* 94, 83–89.
- Collura, S., Azambre, B., Weber, J.V., 2005. Thermal behaviour of *Miscanthus* grasses, an alternative biological fuel. *Environmental Chemistry Letters* 3, 95–99.
- Di Blasi, C., 2008. Modeling chemical and physical processes of wood and biomass pyrolysis. *Progress in Energy and Combustion Science* 34, 47–90.
- Di Blasi, C., Lanzetta, M., 1997. Intrinsic kinetics of isothermal xylan degradation in inert atmosphere. *Journal of Analytical and Applied Pyrolysis* 40–41, 287–303.
- Erlach, C., Bjornbom, E., Bolado, D., Giner, M., Fransson, T.H., 2006. Pyrolysis and gasification of pellets from sugar cane bagasse and wood. *Fuel* 85, 1535–1540.

- Ferdous, D., Dalai, A.K., Bej, S.K., Thring, R.W., 2002. Pyrolysis of lignins: experimental and kinetic studies. *Energy and Fuels* 16, 1405–1412.
- Fisher, T., Hajaligol, M., Waymack, B., Kellogg, D., 2003. Pyrolysis behavior and kinetics of biomass derived materials. *Journal of Analytical and Applied Pyrolysis* 62, 331–349.
- Gomez, C.J., Meszaros, E., Jakab, E., Velo, E., Puigjaner, L., 2007. Thermogravimetry/mass spectrometry study of woody residues and an herbaceous biomass crop using PCA techniques. *Journal of Analytical and Applied Pyrolysis* 80, 416–426.
- Gronli, M.G., Varhegyi, G., Di Blasi, C., 2002. Thermogravimetric analysis and devolatilization kinetics of wood. *Industrial Engineering and Chemistry Research* 41, 4201–4208.
- Hu, S., Jess, A., Xu, M., 2007. Kinetic study of Chinese biomass slow pyrolysis: comparison of different kinetic models. *Fuel* 86, 2778–2788.
- Jeguirim, M., Trouve, G., 2009. Pyrolysis characteristics and kinetics of *Arundo donax* using thermogravimetric analysis. *Bioresource Technology* 100, 4026–4031.
- Kalita, D., Saikia, C.N., 2004. Chemical constituents and energy content of some latex bearing plants. *Bioresource Technology* 92, 219–227.
- Karaosmanoglu, F., Cift, B.D., Ergudenler, A.I., 2001. Determination of reaction kinetics of straw and stalk of rapeseed using thermogravimetric analysis. *Energy Sources* 23, 767–774.
- Kumar, A., Wang, L., Dzenis, Y.A., Jones, D.D., Hanna, M.A., 2008. Thermogravimetric characterization of corn stover as gasification and pyrolysis feedstock. *Biomass and Bioenergy* 32, 460–467.
- Lewandowski, I., Scurlock, J.M.O., Lindvall, E., Christou, M., 2003. The development and current status of perennial rhizomatous grasses as energy crops in the US and Europe. *Biomass and Bioenergy* 25, 335–361.
- Maiti, S., Purakayastha, S., Ghosh, B., 2007. Thermal characterization of mustard straw and stalk in nitrogen at different heating rates. *Fuel* 86, 1513–1518.
- Meszaros, E., Varhegyi, G., Jakab, E., Marosvolgyi, B., 2004. Thermogravimetric and reaction kinetic analysis of biomass samples from an energy plantation. *Energy and Fuels* 18, 497–507.
- Müller-Hagedorn, M., Bockhorn, H., Krebs, L., Müller, U., 2003. A comparative kinetic study on the pyrolysis of three different wood species. *Journal of Analytical and Applied Pyrolysis* 68–69, 231–249.
- Nordin, A., 1994. Chemical and elemental characteristics of biomass fuels. *Biomass and Bioenergy* 6, 339–347.
- Park, H.J., Dong, J.I., Jeon, J.K., Park, Y.K., Yoo, K.S., Kim, S.S., Kim, J., Kim, S., 2008. Effects of the operating parameters on the production of bio-oil in the fast pyrolysis of Japanese larch. *Chemical Engineering Journal* 143, 124–132.
- Park, H.J., Park, Y.K., Dong, J.I., Kim, J.S., Jeon, J.K., Kim, S.S., Kim, J., Song, B., Park, J., Lee, K.J., 2009a. Pyrolysis characteristics of oriental white oak: kinetic study and fast pyrolysis in a fluidized bed with an improved reaction system. *Fuel Processing Technology* 90, 186–195.
- Park, Y.H., Kim, J., Kim, S.S., Park, Y.K., 2009b. Pyrolysis characteristics and kinetics of oak trees using thermogravimetric analyzer and micro-tubing reactor. *Bioresource Technology* 100, 400–405.
- Presnell, K., 2004. The potential use of mimosa as fuel for power generation. In: Julien, M., Flanagan, G., Heard, T., Hennecke, B., Paynter, Q., Wilson, C. (Eds.), *Research and Management of Mimosa pigra*. CSIRO Entomology, Canberra, Australia.
- Scurlock, J.M.O., Dayton, D.C., Hames, B., 2000. Bamboo: an overlooked biomass resource? *Biomass and Bioenergy* 19, 229–244.
- Senneca, O., 2007. Kinetics of pyrolysis, combustion and gasification of three biomass fuels. *Fuel Processing Technology* 88, 87–97.
- Shafizadeh, F., 1985. Pyrolytic reactions and products of biomass. In: Overend, R.P., Milne, T.A., Mudge, L.K. (Eds.), *Fundamentals of Biomass Thermochemical Conversion*. Elsevier, London, pp. 183–217.
- Sujjakulnukit, B., Yingyuad, R., Maneekhao, V., Pongnarintasut, V., Bhattacharya, S.C., Abdul Salam, P., 2005. Assessment of sustainable energy potential of non-plantation biomass resources in Thailand. *Biomass and Bioenergy* 29, 214–224.
- Wang, G., Li, W., Li, B., Chen, H., 2008. TG study on pyrolysis of biomass and its three components under syngas. *Fuel* 87, 552–558.
- Wongsiriamnuay, T., Phengpom, T., Panthong, P., Tippayawong, N., 2008. Renewable energy from thermal gasification of a giant sensitive plant (*Mimosa pigra* L.). In: 5th International Conference on Combustion, Incineration/Pyrolysis and Emission Control, December 16–19 Chiang Mai, Thailand.
- Yao, F., Wu, Q., Lei, Y., Guo, W., Xu, Y., 2008. Thermal decomposition kinetics of natural fibers: activation energy with dynamic thermogravimetric analysis. *Polymer Degradation and Stability* 93, 90–98.





# Thermogravimetric analysis of giant sensitive plants under air atmosphere

Thanasit Wongsiriamnuay, Nakorn Tippayawong\*

Department of Mechanical Engineering, Chiang Mai University, 239 Huaykaew Rd, Chiang Mai 50200, Thailand

## ARTICLE INFO

### Article history:

Received 7 May 2010

Received in revised form 23 June 2010

Accepted 25 June 2010

Available online 23 July 2010

### Keywords:

Biomass

Mimosa

Oxidation

Renewable energy

Thermal decomposition

## ABSTRACT

The aim of this work is to utilise thermal analysis to study the thermal degradation of giant sensitive plants (*Mimosa pigra* L.) or Mimosa under oxidative environment. Thermogravimetric method was used under air sweeping in dynamic conditions at the heating rates of 10, 30, and 50 °C/min, from room temperature to about 725 °C. Starting with dehydration step between 30 and 150 °C, the main thermal decomposition process under air showed two distinct degradation zones, corresponding to devolatilisation step between 200 and 375 °C and combustion step around 375–500 °C. Kinetic parameters in terms of apparent activation energy and pre-exponential factor were determined. Comparison was made against other biomass materials. Mass loss and mass loss rates were strongly affected by heating rate. It was found that an increase in heating rate resulted in a shift of thermograms to higher temperatures. As the heating rates increased, average devolatilisation and combustion rates were observed to increase while the activation energy showed slight increase.

© 2010 Elsevier Ltd. All rights reserved.

## 1. Introduction

Biomass is a source of short-cycle carbon which is of utmost importance for the future energy. Common sources of biomass include woods, agricultural crops and residues. There have been growing interests in alternative, non-edible biomass resources such as fast growing tress; birch, poplar, willow, eucalyptus, and perennial rhizomatous grasses; miscanthus, switchgrass, reed canary grass, giant reed because of their high yield potential, appropriate biomass characteristics, low input demand and positive environmental impact (Bernides et al., 2003; Lewandowski et al., 2003). Apart from these dedicated energy crops, weeds can also be utilised. In tropical and subtropical areas over many countries especially Australia, Thailand, Viet Nam, South American, and African countries, giant sensitive plants (*Mimosa pigra* L.) or Mimosa are plentiful, and may be considered to be a useful, non-plantation biomass resource (Wongsiriamnuay and Tippayawong, 2010). So far, there have been relatively few studies on utilisation of Mimosa as feed-stock for bioenergy.

Thermal conversion technology such as pyrolysis, gasification and combustion is an attractive route to produce fuel gases from natural resources. Combustion of biomass fuels occur when the volatile gaseous products from the thermal degradation ignite in the surrounding air. The heat released from combustion causes the ignition of adjacent unburned fuels. Analysis of the thermal degradation of biomass fuels is decisive in combustion and fire

research for both fundamental and practical investigation. This has motivated a number of experimental investigations, usually based on thermogravimetric analysis (TGA). TGA is useful in studying the thermal behaviour of potential fuels. The rate of mass loss as a function of temperature and time is measured and provides a means to estimate the kinetic parameters in the thermal decomposition reaction. Most reported studies on biomass thermal decomposition focused on pyrolysis. Di Blasi (2008) gave a good review about the chemical and physical process modeling of wood and biomass pyrolysis under inert atmospheres. Decomposition of biomass under inert and oxidative atmospheres are influenced by different factors. Recently, a growing amount of TGA studies on thermal degradation of various non-edible biomass sources in oxidative environments have been carried out (Munir et al., 2009; Jeguirim et al., 2010; Sung and Seo, 2009; Yu et al., 2009; Ross et al., 2008; Haykiri-Acma and Yaman, 2008; Leroy et al., 2006; Garcia-Ibanez et al., 2006; Basso et al., 2005; Collura et al., 2005; Meszaros et al., 2004; Safi et al., 2004). However, there has been relatively little information on thermal behaviour of giant sensitive plants (Wongsiriamnuay and Tippayawong, 2010). Studies concerning the thermal degradation characteristics and kinetics of the weed under oxidizing environment were even less. In this study, thermal oxidative degradation characteristics of Mimosa were investigated. Thermal degradation rate in different steps was examined. Kinetic parameters were extracted. Change of kinetic behaviour with conversion was also analyzed. The kinetics of this thermal degradation is more closely related to combustion process. The work will therefore contribute to the development of efficient combustion applications for the giant sensitive plant.

\* Corresponding author. Tel.: +66 5394 5146; fax: +66 5394 4145.

E-mail address: [n.tippayawong@yahoo.com](mailto:n.tippayawong@yahoo.com) (N. Tippayawong).

## 2. Methods

### 2.1. Samples

The samples of Mimosa were collected from an agricultural zone in Chiang Mai, Thailand. The preparation and analysis methods of the Mimosa samples can be found in the previous study (Wongsiriamnuay and Tippayawong, 2010). Contents of the major constituents of the weed from proximate and ultimate analyses for the samples, as well as the heating value of the Mimosa are shown in Table 1, in comparison to other biomass materials. The proximate chemical compositions of Mimosa stems were found to be similar to hard woods, with higher ash content than woods but lower ash content than other agro-residues. Ultimate analysis showed that raw Mimosa consisted of moderately high carbon content (43.9%) and low amounts of hydrogen (6.0%) and nitrogen (1.4%).

### 2.2. Thermogravimetric apparatus

Thermal decomposition of the biomass materials were analyzed using a TGA/SDTA 851e Thermogravimetric Analyser (sensitive microbalance, 1 µg resolution, 1300 °C maximum temperature at atmospheric pressure, 50 bar maximum at 1000 °C). This high performance TG analyser has high sensitivity, vibration resistance and structure that permit rapid replacement of samples. The system is logged to a personal computer for data handling and analysis. Prior to TGA, temperature, weight, and sample platform calibrations were carried out. Each sample was placed in the platinum pan securely and in such a way that it was confined within the pan sides and not in contact with the sides of the oven. All handling of samples were done using brass tweezers to avoid contamination. Non-isothermal experiment runs were carried out at 10, 30, and 50 °C/min under atmospheric pressure, with an initial weight sample of 5 mg and a purge gas flow of 50 cm<sup>3</sup>/min. The purge gases used were high purity nitrogen, air or oxygen. The sample was initially preheated to and equilibrated at 40 °C in air under a flow rate of 50 cm<sup>3</sup>/min for 10 min. The sample was then heated to 1000 °C at a constant heating rate. The continuous records of weight loss and temperatures were obtained. At least three runs were performed for each condition.

### 2.3. Reaction kinetics

Kinetics of non-thermal thermogravimetric behaviour were analyzed to determine apparent activation energy and pre-exponential factor for the Mimosa thermal degradation.

Thermal decomposition behaviours of Mimosa under flowing air were obtained. The results of thermogravimetric experiments were expressed as conversion  $\alpha$ , defined as:

$$\alpha = \frac{W_i - W_t}{W_i - W_f} \quad (1)$$

where  $W_i$ ,  $W_t$  and  $W_f$  are the initial mass of the sample, the mass of oxidized sample, and the final residual mass, respectively. The kinetic parameters for the global thermal degradation process of Mimosa can be calculated using similar procedure adopted by Wongsiriamnuay and Tippayawong (2010). The general non-isothermal, decomposition reaction rate is:

$$\frac{d\alpha}{dt} = k(1 - \alpha)^n \quad (2)$$

where

$$k = A \exp(-E/RT) \quad (3)$$

$T$  is the temperature,  $A$  is the pre-exponential or frequency factor,  $t$  is the time,  $E$  is the activation energy,  $R$  is the universal gas constant,  $n$  is the order of reaction. The logarithmic form for Eq. (2) is:

$$\ln \left( \frac{d\alpha}{dt} \right) = \ln A + n \ln \alpha - \frac{E}{RT} \quad (4)$$

Activation energy can be determined from the relationship between  $\ln(d\alpha/dt)$  and  $1/T$ .

When the apparent order of reaction is assumed to be 0th, 1st or 2nd, the pre-exponential or frequency factor can be obtained from the following equation:

$$\ln(A\alpha^n) = \ln A + n \ln \alpha \quad (5)$$

## 3. Results and discussion

TGA in air represents burning profiles and indicates a complex degradation route for the giant sensitive plant. The degree of conversion versus temperature at different heating rates of 10, 30 and 50 °C/min for Mimosa is shown in Fig. 1. The differential rates of instantaneous conversion,  $d\alpha/dt$ , were obtained from TG analysis at different heating rates, shown in Fig. 2. During thermal degradation in air, weight loss occurred continuously until the weight became almost constant. It can be seen that an initial weight loss of the samples was due to a loss of moisture starting at around 30 °C and continuing up to about 140 °C. The giant sensitive plant samples started to decompose and release volatiles at around 200 °C. The TG curves of the giant sensitive trees clearly showed changes

**Table 1**  
Properties of Mimosa and other biomass materials.

Reference	Biomass	Proximate analysis (% w/w)				Ultimate analysis (%)				Heating value (MJ/kg)
		Moisture	Volatile	Fixed carbon	Ash	C	H	N	O	
This work	Mimosa	1.6	71.1	23.6	3.7	43.9	6.0	1.4	48.7	17.5 (HHV)
Haykiri-Acma and Yaman (2008)	Rapeseed	8.4	70	15.8	5.8	41.1	6.0	5.1	47.8	19.4 (HHV)
Kumar et al. (2008)	Corn stove	–	8.2	17.0	74.9	47.4	5.01	0.8	38.1	18.4 (HHV)
Munir et al. (2009)	Cotton stalk	–	76.1	18.8	5.1	47.1	4.6	42.1	1.2	17.4 (HHV)
	Sugar cane Bagasse	–	81.5	13.3	5.2	43.8	6.0	43.4	1.7	17.7 (HHV)
	Shea meal	–	66.3	28.7	5.0	48.6	5.9	37.7	2.9	19.8 (HHV)
Jeguirim et al. (2010)	Arundo donax	8.2	68.4	18.4	5.0	42.7	7.5	8.0	48.7	17.2 (HHV)
	Miscanthus	10.0	78.8	9.5	2.7	43.7	5.7	1.1	44.8	17.8 (HHV)
Shen et al. (2009)	Pine	12.9	71.5	15.3	0.3	41.9	4.5	0.2	40.2	16.8 (LHV)
	Aspens	8.2	80.4	11.0	0.4	45.8	5.2	0.4	39.9	18.8 (LHV)
	Birch	11.4	74.4	13.5	0.8	44.4	3.5	0.3	36.7	15.5 (LHV)
	Oak	8.8	76.8	14.2	0.2	45.4	5.0	0.3	41.3	18.9 (LHV)
Sun et al. (2010)	Cotton stalk	15	63.1	19.2	2.7	40.4	5.1	0.2	36.5	13.5 (LHV)
Otero et al. (2010)	Sewage sludge	6.8	59.2	8.4	32.4	55.3	7.8	9.7	25.6	16.5 (HHV)
	Animal manure	6.9	70.3	16.0	13.7	49.9	6.4	3.5	38.8	17.8 (HHV)
Safi et al. (2004)	Pine needle	–	74.2	24.1	1.7	45.8	5.4	1.0	46.1	18.5 (LHV)

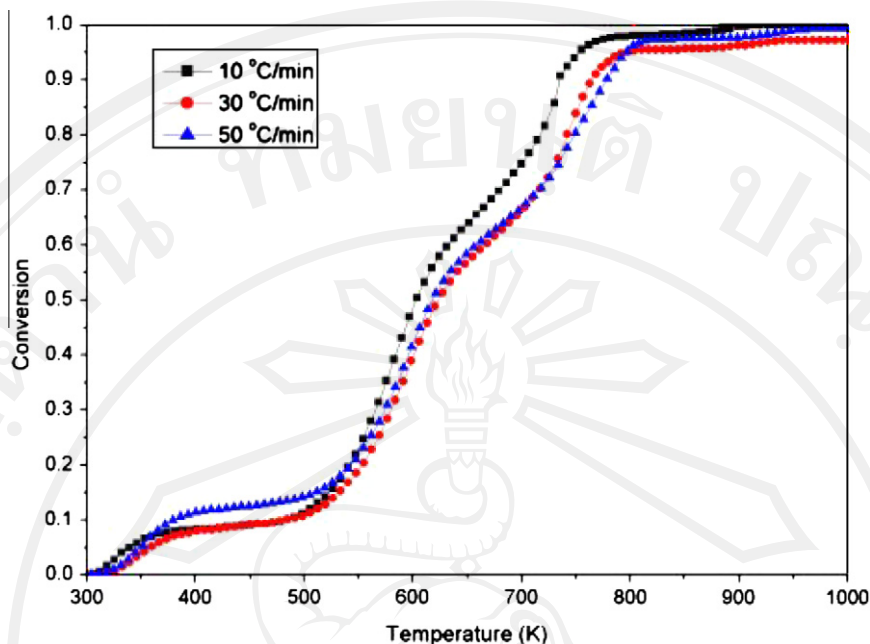


Fig. 1. Conversion as a function of temperature in the thermal degradation of Mimosa under air atmosphere at different heating rates.

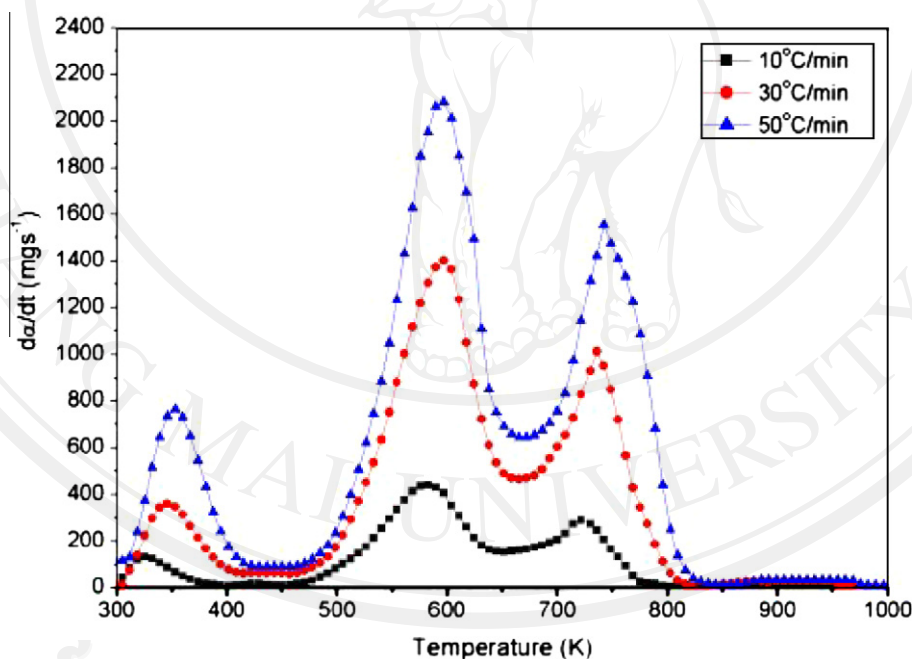


Fig. 2. DTG curves of thermal decomposition of Mimosa under air at different heating rates.

in the slope of the curve. The conversions at different heating rates exhibited similar patterns. It was observed at temperatures above 250 °C that the TG curve shifted slightly to the right with increasing heating rate. It was clear that the DTG curve of each heating rate exhibited two extensive peaks, occurred between 200 and 400 °C, and between 400 and 550 °C. From the TG curves, these two zones accounted for about 40% and 45% of total weight loss, respectively. The first stage was due to oxidative degradation and release of volatiles, while the second stage was due to char combustion. An overlapping between these regions was also apparent. The interpretation of TG results was along the similar line to Bilbao et al. (1997) and Fang et al. (2006) in which the first stage may be

attributed to the devolatilisation of cellulose, hemicellulose, and lignin while the second stage may be due to the combustion of remaining char formed after the first stage. Safi et al. (2004) gave similar explanations that the first stage was caused by the total decomposition of cellulose and hemicellulose and partial decomposition of lignin while the second stage was due to the decomposition of remaining lignin and the combustion of char. Jeguirim et al. (2010) suggested that the second stage of mass loss was attributed to the fast combustion of readily combustibles and the slow oxidation of the not readily combustible part. The results observed here were in similar agreement with Shen et al. (2009). The TG results obtained under oxidative conditions were different from



the pyrolysis of Mimosa (Wongsiriamnuay and Tippayawong, 2010), showing higher reaction rates. For a fixed heating rate, the weight loss stage due to oxidative pyrolysis was at higher rate than that observed from the pyrolysis of Mimosa in nitrogen atmosphere. Average rate of weight loss was so fast so that it reached maximum value at a lower temperature than that in an inert atmosphere. The presence of oxygen appeared to enhance decomposition of Mimosa at low temperature and promote the combustion of char residue. Higher heating rate was found to shift the DTG curve to a slightly greater range of temperature. This was attributed to the fact that increase in heating rate resulted in a reduction of the retention time, hence accelerating the evolution of volatiles. At higher heating rates, more reactions may be triggered simultaneously, leading to a rise in reaction rates and unstable radicals or intermediates. The DTG curves also showed consistently higher peaks with higher heating rates, shown in Table 2. The first and second peaks of the DTG curves occurred at 329, 460, 360, 480 and 374, 502 °C for heating rates of 10, 30 and 50 °C/min, respectively. It may be explained that thermal decomposition under high heating rate was affected by the rate of heat transfer inside the biomass materials as a result of the steep temperature gradient be-

tween the biomass particles and the surrounding. The maximum rate of decomposition tended to increase at higher heating rate because it provided higher thermal energy to facilitate better heat transfer between the surrounding and inside the samples. These results were in similar trends with previous reports (Kumar et al., 2008). This led the process of thermal decomposition to be delayed and the peaks of the DTG curves shifted towards higher temperatures. These behaviours were similar to those reported by Jeguirim et al. (2010). Also shown in Table 2 is the comparison of degradation characteristics in terms of maximum mass loss rate ( $dx/dT_{\text{peak}}$ ) and its corresponding temperature ( $T_{\text{peak}}$ ) between Mimosa and other biomass sources. Degradation of Mimosa was at similar peak temperatures (~310 and 450 °C) for the first and second stages to wood species at the same heating rate of 10 °C/min (Shen et al., 2009), but higher than energy plants and agro-residues (Jeguirim et al., 2010; Munir et al., 2009; Safi et al., 2004). At higher heating rate, peak temperatures for thermal decomposition of Mimosa were found to be higher than woods, energy plants and agro-residues. It was also apparent that the maximum mass loss rates for the thermal degradation of Mimosa under air atmosphere were generally lower than other plant samples, both during devolatilisa-

**Table 2**  
Comparison of degradation characteristic of various biomass materials.

Reference	Biomass	$T_1$ (°C)	$dx_1/dT$ (%/C)	$T_2$ (°C)	$dx_2/dT$ (%/C)	Heating rate (°C/min)
This work	Mimosa	310	0.26	448	0.19	10
		326	0.28	469	0.19	30
		326	0.25	469	0.20	50
Jeguirim et al. (2010)	Arundo donax	250	–	337	–	5
	Miscanthus	289	–	401	–	5
Munir et al. (2009)	Cotton stalk	285	0.28	373	0.12	20
	Bagasse	306	0.19	378	0.11	20
	Shea meal	279	0.21	442	0.14	20
Shen et al. (2009)	Pine	329	1.13	443	0.55	10
	Aspens	321	1.23	415	0.79	10
	Birch	323	1.29	428	0.85	10
	Oak	325	1.29	450	0.44	10
Safi et al. (2004)	Pine needles	290	0.71	390	–	15
		310	0.845	370	–	30

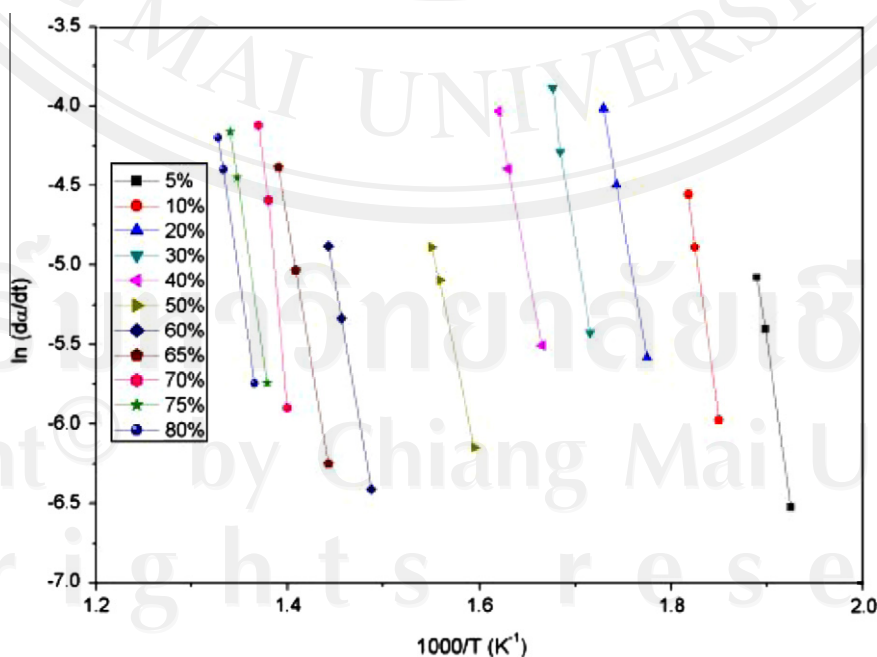


**Fig. 3.** Relationships between the rate of conversion with temperature for conversions of 5–80%.



**Table 3**  
Calculated combustion kinetic parameters for Mimosa at each conversion.

References	Biomass	$n$	Conversion (%)	5	10	20	30	40	50	60	70	80	85
This work	Mimosa	0th	$E$ (kJ/mol)	344.24	366.98	285.95	319.27	268.80	235.23	284.21	497.53	341.54	399.34
				$6.09 \times 10^{31}$	$7.47 \times 10^{32}$	$1.23 \times 10^{24}$	$1.79 \times 10^{26}$	$9.79 \times 10^{20}$	$8.55 \times 10^{16}$	$1.99 \times 10^{19}$	$6.76 \times 10^{33}$	$7.42 \times 10^{21}$	$2.70 \times 10^{25}$
				$1.22 \times 10^{31}$	$7.47 \times 10^{31}$	$6.13 \times 10^{22}$	$5.98 \times 10^{24}$	$2.45 \times 10^{19}$	$1.71 \times 10^{15}$	$3.32 \times 10^{17}$	$9.66 \times 10^{31}$	$9.27 \times 10^{19}$	$3.18 \times 10^{23}$
		1st	$A$ ( $s^{-1}$ )	$2.44 \times 10^{30}$	$7.47 \times 10^{30}$	$3.06 \times 10^{21}$	$1.99 \times 10^{23}$	$6.12 \times 10^{17}$	$3.42 \times 10^{13}$	$5.54 \times 10^{15}$	$1.38 \times 10^{30}$	$1.16 \times 10^{18}$	$3.47 \times 10^{21}$
		2nd											

tion and char combustion. The findings obtained here may be due to the fact that different lignocellulosic materials contain a varying degree of cellulose, hemicellulose, and lignin. It is widely accepted that thermal decomposition behaviour of biomass is affected by its chemical composition. Several studies reported that hemicellulose started to degrade first, followed by cellulose, and lignin (Gronli et al., 2002; Orfao et al., 1999). The higher degradation temperatures observed for Mimosa can be explained by its relatively high lignin content (33.9%).

Fig. 3 shows the relationship between  $\ln(d\alpha/dt)$  and  $1/T$  at various conversions from 5% to 80%. Thus, a family of parallel straight lines with a slope of  $-E/R$  is obtained. From the slope of  $\ln(d\alpha/dt)$  against  $1/T$  at the conversion of 10%, the activation energy and the intercept ( $\ln(A\alpha^n)$ ) can be obtained at each conversion. The variation of activation energy and the calculated pre-exponential factors assuming the reaction order as zeroth, first or second as a function of the conversion level, calculated using Eq. (5) is presented in Table 3. The activation energy for the thermal degradation of Mimosa in air atmosphere ranged from 235 to 498 kJ/mol, with an average value of 334 kJ/mol. Main decomposition appeared to occur at the conversions of 5–10% and 70%, where the activation energies were high and the pre-exponential factors were in the range of  $10^{30}$ – $10^{33} s^{-1}$ . At other conversions, the pre-exponential factors were found to drop rapidly to  $10^{13}$ – $10^{26} s^{-1}$ . The increase in activation energy at higher conversion may be attributed to ignition and oxidation of char residues. Fernandes et al. (2006) showed that during thermal decomposition of overlapping regions between cellulose and hemicellulose, and between hemicellulose and lignin, the associated activation energies were observed to jump radically. Similar observation was evident here, but at smaller rise. It was generally accepted that thermal decomposition was favoured in oxygen-containing atmosphere. A change from inert to oxidative atmosphere should result in an increase in apparent activation energy. The values found here were as much as 35 kJ/mol higher than those obtained from the pyrolysis of Mimosa reported in Wongsiriamnuay and Tippayawong (2010), at conversion up to 30%. But at higher conversions, the difference appeared to diminish. The observed fluctuation of activation energy at high conversions, around region for thermal decomposition of lignin in air, was similar to that reported by Fernandes et al. (2006). Table 4 compares the average activation energy among various biomass materials, obtained at similar temperature range. The average activation energy values for Mimosa was higher than those obtained from woods (Shen et al., 2009), and much higher than those from rapeseed, agro-residues and biowastes (Haykiri-Acma and Yaman, 2008; Kumar et al., 2008; Munir et al., 2009; Sun et al., 2010; Safi et al., 2004; Otero et al., 2010). Shen et al. (2009) reported the activation energies for wood species to be 145–210 kJ/mol while Munir et al. (2009), Kumar et al. (2008) and Sun et al. (2010) reported the range of 57–139 kJ/mol for agro-residues. Corn stalk was reported to have similar magnitude of kinetic parameters (Tian and Fu, 2009) to Mimosa. Its activation energy for thermal degradation in air atmosphere was reported to be about 350 kJ/mol. It was not yet known why Mimosa exhibited high activation energy. It was suggested that combustion rate could not only depend on the composition but also on the mutual interaction between the individual components (Rhen et al., 2007). Attempt was therefore made to relate these unique kinetic parameters with their chemical composition, shown in Tables 1 and 5. It was apparent that the chemical composition in terms of CHNO between these biomass materials and Mimosa were similar. It did not appear to have any significant correlation. With respect to the lignocellulosic composition, Mimosa was found to have higher lignin content and lower holocellulose, sum of hemicellulose and cellulose, content than other agro-residues. However, based on thermal decomposition of lignin, the activation energy obtained was small, compared to other components.

**Table 4**

Comparison of average combustion kinetic parameters between Mimosa and other biomass materials.

Reference	Biomass	Atmosphere	Heating rate (°C/min)	Temperature range (°C)	E (kJ/mol)
This work	Mimosa	Air	10, 30, 50	200–500	334
Haykiri-Acma and Yaman (2008)	Rapeseed	Air	20	127–752	21
Kumar et al. (2008)	Corn stover	Air	10	250–560	57
			30	250–560	126
			50	250–560	139
Munir et al. (2009)	Cotton stalk	Air	20	200–500	113
	Bagasse				75
	Shea meal				108
Shen et al. (2009)	Pine	Air	10	200–370	119
	Aspens				114
	Birch				116
	Oak				117
Shen et al. (2009)	Pine	Air	10	370–490	145
	Aspens				205
	Birch				210
	Oak				150
Sun et al. (2010)	Cotton stalk	Air	20	200–360	108
				360–500	125
Otero et al. (2010)	Sewage sludge	Air	5, 10, 25, 50	200–480	129
	Animal manure				133
Safi et al. (2004)	Pine needle	Air	10	192–503	85
			30	181–575	87

**Table 5**

Lignocellulosic composition and average activation energy between Mimosa and other biomass materials.

Reference	Biomass	Hemicellulose	Cellulose	Lignin	Atmosphere	E (kJ/mol)
This work	Mimosa	58.2 as holocellulose		33.9	Air	334
Tian and Fu (2009)	Corn stalk	16.8–35.0	35.0–39.6	7.0–18.4	Air	302.6
Barneto et al. (2010)	Hemicellulose	100			N <sub>2</sub>	88.4
	Cellulose		100		N <sub>2</sub>	203
	Lignin			100	N <sub>2</sub>	75.1
Varhegyi and Antal (1989)	Hemicellulose	100			N <sub>2</sub>	187
	Cellulose		100		N <sub>2</sub>	213–234
Shen et al. (2009)	Pine	15.37	52.10	27.45	Air	119
	Aspens	19.06	60.70	14.80	Air	114
	Birch	24.79	56.47	12.17	Air	116
	Oak	28.97	53.95	9.43	Air	117

Furthermore, reported contents of lignocellulosic composition of these biomass materials showed variation (Garrote et al., 1999). Relation between chemical composition and activation energy was not conclusive. Other possible explanation may be associated with the presence and absence of mineral content in various biomass materials (Varhegyi and Antal, 1989). The resulting kinetic parameters were dependent on whether reaction mechanism of lignocellulosic decomposition was catalyzed or uncatalyzed. Biomass materials obtained from agriculture may have high mineral content from fertilization, compared to weeds like Mimosa. The effects of mineral content in biomass ash may be investigated further.

#### 4. Conclusion

Thermal degradation of Mimosa under air environment was investigated using TGA at different heating rates. Kinetic parameters in terms of apparent activation energy and pre-exponential factor were determined. Oxidative thermal degradation of Mimosa exhibited two major mass loss stages due to devolatilisation and combustion. DTG curves showed similar peak decomposition temperatures to woods, but at higher temperatures than energy plants, agro-residues and biowaste samples. Increasing heating rate resulted in increasing mass loss rates, but delayed thermal decomposition to higher temperatures. During combustion, the kinetic parameters changed with conversion between 5% and 80%. The average activation energy was about 334 kJ/mol.

#### Acknowledgements

This research is supported by the Thailand Research Fund (contract no. RSA5080010) and Faculty of Engineering, Chiang Mai University. The Royal Golden Jubilee PhD scholarship (PHD/0047/2550) awarded to T.W. is greatly appreciated. Support from the Energy Research and Development Institute, Chiang Mai University is also acknowledged.

#### Reference

- Barneto, A.G., Carmona, J.A., Ferrer, J.A.C., Blanco, M.J.D., 2010. Kinetic study on the thermal degradation of a biomass and its compost: composting effect on hydrogen production. *Fuel* 89, 462–473.
- Basso, M.V., Cerrella, E.G., Buonomo, E.L., Bonelli, P.R., Cukierman, A.L., 2005. Thermochemical conversion of *Arundo donax* into useful solid products. *Energy Sources* 27, 1429–1438.
- Berndes, G., Hoogwijk, M., van den Broek, R., 2003. The contribution of biomass in the future global energy supply: a review of 17 studies. *Biomass and Bioenergy* 25, 1–28.
- Bilbao, R., Mastral, J.F., Aldea, M.E., Ceamanos, J., 1997. Kinetic study for the thermal decomposition of cellulose and pine sawdust in an air atmosphere. *Journal of Analytical and Applied Pyrolysis* 39, 53–64.
- Collura, S., Azambre, B., Weber, J.V., 2005. Thermal behaviour of *Miscanthus* grasses, an alternative biological fuel. *Environmental Chemistry Letters* 3, 95–99.
- Di Blasi, C., 2008. Modeling chemical and physical processes of wood and biomass pyrolysis. *Progress in Energy and Combustion Science* 34, 47–90.
- Fang, M.X., Shen, D.K., Li, Y.X., Yu, C.J., Luo, Z.Y., Cen, K.F., 2006. Kinetic study on pyrolysis and combustion of wood under different oxygen concentrations by using TG-FTIR analysis. *Journal of Analytical and Applied Pyrolysis* 77, 22–27.

- Fernandes, D.M., Hechenleitner, A.A.W., Pineda, E.A.G., 2006. Kinetic study of the thermal decomposition of poly(vinyl) alcohol/kraft lignin derivative blends. *Thermochimica Acta* 441, 101–109.
- Garcia-Ibanez, P., Sanchez, M., Cabanillas, A., 2006. Thermogravimetric analysis of olive oil residue in air atmosphere. *Fuel Processing Technology* 87, 103–107.
- Garrote, G., Dominguez, H., Parajo, J.C., 1999. Hydrothermal processing of lignocellulosic materials. *European Journal of Wood and Wood Products* 57, 191–202.
- Gronli, M.G., Varhegyi, G., Di Blasi, C., 2002. Thermogravimetric analysis and devolatilization kinetics of wood. *Industrial and Engineering Chemistry Research* 41, 4201–4208.
- Haykiri-Acma, H., Yaman, S., 2008. Thermal reactivity of rapeseed (*Brassica napus* L.) under different gas atmospheres. *Bioresource Technology* 99, 237–242.
- Jeguirim, M., Dorge, S., Trouve, G., 2010. Thermogravimetric analysis and emission characteristics of two energy crops in air atmosphere: *Arundo donax* and *Miscanthus giganteus*. *Bioresource Technology* 101, 788–793.
- Kumar, A., Wang, L., Dzenis, Y.A., Jones, D.D., Hanna, M.A., 2008. Thermogravimetric characterization of corn stover as gasification and pyrolysis feedstock. *Biomass and Bioenergy* 32, 460–467.
- Leroy, V., Cancellieri, D., Leoni, E., 2006. Thermal degradation of ligno-cellulosic fuels: DSC and TGA studies. *Thermochimica Acta* 451, 131–138.
- Lewandowski, I., Scurlock, J.M.O., Lindvall, E., Christou, M., 2003. The development and current status of perennial rhizomatous grasses as energy crops in the US and Europe. *Biomass and Bioenergy* 25, 335–361.
- Meszaros, E., Varhegyi, G., Jakab, E., Marosvolgyi, B., 2004. Thermogravimetric and reaction kinetic analysis of biomass samples from an energy plantation. *Energy and Fuels* 18, 497–507.
- Munir, S., Daood, S.S., Nimmo, W., Cunliffe, A.M., Gibbs, B.M., 2009. Thermal analysis and devolatilization kinetics of cotton stalk, sugar cane bagasse, and shea meal under nitrogen and air atmospheres. *Bioresource Technology* 100, 1413–1418.
- Orfao, J.J.M., Antunes, F.J.A., Figueiredo, J.L., 1999. Pyrolysis kinetics of lignocellulosic materials – three independent reactions model. *Fuel* 78, 349–358.
- Otero, M., Sanchez, M.E., Gomez, X., Moran, A., 2010. Thermogravimetric analysis of biowastes during combustion. *Waste Management* 30, 1183–1187.
- Rhen, C., Ohman, M., Gref, R., Wasterlund, I., 2007. Effect of raw material composition in woody biomass pellets on combustion characteristics. *Biomass and Bioenergy* 31, 66–72.
- Ross, A.B., Jones, J.M., Kubacki, M.L., Bridgeman, T., 2008. Classification of macroalgae as fuel and its thermochemical behaviour. *Bioresource Technology* 99, 6494–6504.
- Safi, M.J., Mishra, I.M., Prasad, B., 2004. Global degradation kinetics of pine needles in air. *Thermochimica Acta* 412, 155–162.
- Shen, D.K., Gu, S., Luo, K.H., Bridgwater, A.V., Fang, M.X., 2009. Kinetic study on thermal decomposition of woods in oxidative environment. *Fuel* 88, 1024–1030.
- Sun, Z., Shen, J., Jin, B., Wei, L., 2010. Combustion characteristics of cotton stalk in FBC. *Biomass and Bioenergy* 34, 761–770.
- Sung, Y.J., Seo, Y.B., 2009. Thermogravimetric study on stem biomass of *Nicotiana glauca*. *Thermochimica Acta* 486, 1–4.
- Tian, S., Fu, X., 2009. Study on characteristics in combustion process of cornstalk and wheat straw. *Asia Pacific Power and Energy Engineering Conference*, 27–31 March, Wuhan, China.
- Varhegyi, G., Antal, M.J., 1989. Kinetics of the thermal decomposition of cellulose, hemicellulose, and sugar cane bagasse. *Energy and Fuels* 3, 329–335.
- Wongsiriamnuay, T., Tippayawong, N., 2010. Non-isothermal pyrolysis characteristics of giant sensitive plants using thermogravimetric analysis. *Bioresource Technology* 101, 5638–5644.
- Yu, Z., Ma, X., Liu, A., 2009. Thermogravimetric analysis of rice and wheat straw catalytic combustion in air- and oxygen-enriched atmospheres. *Energy Conversion and Management* 50, 561–566.

# Product Gas Distribution and Composition from Catalyzed Gasification of Mimosa

Thanasit Wongsiriamnuay\*, Nakorn Tippayawong\*

\*Department of Mechanical Engineering, Faculty of Engineering, Chiang Mai University, Chiang Mai, 50200, Thailand

†Corresponding Author; Thanasit Wongsiriamnuay, Department of Mechanical Engineering, Faculty of Engineering, Chiang Mai University, Chiang Mai, 50200, Thailand, +6653945146, w\_thanasit@hotmail.com, n.tippayawong@yahoo.com

Received: 04.04.2012 Accepted: 29.05.2012

**Abstract-** The aim of this study is to analyze the potential of giant sensitive plant or Mimosa for gaseous fuel production by means of gasification process. An experimental study was carried out in a bench scale, fixed bed gasifier with air at atmospheric pressure. Parametric investigation was performed to determine the effect of temperature (600-900°C), collection time (10-110 min) and catalyst to biomass ratio (0.5-2) on product gas yields and composition. Experimental results showed that high temperature favors hydrogen, carbon monoxide and carbon dioxide yield (11, 18 and 24 mol %), while methane was found to follow opposite trend. Production rates of hydrogen and carbon monoxide appeared to increase during volatile releasing step, but decrease during carbonization. With catalyst to biomass ratio of 1, high hydrogen and carbon monoxide concentrations in the product gas (27 and 29 mol%, respectively) were achieved.

**Keywords-** Biomass; Dolomite; Fixed Bed; Giant Sensitive Plant; Thermo-chemical Conversion; Renewable Energy.

## 1. Introduction

Biomass plays an important role in the world's energy resources, now representing around 10-14% share after coal and crude oil [1]. It is a renewable source, which can be diversified and has continuous supply of energy, compared to fossil fuels. It is also carbon neutral in its life cycle. Biomass resources include agricultural and forestry products and their derivatives, woods, woody plants and weeds, municipal solid wastes, animal wastes, wastes from food processing, and aquatic plants and algae. Biomass can be converted into useful forms of energy by means of a number of different processes to meet a variety of energy needs, including heat, electricity, transportation fuels and chemicals. Thermochemical conversion is well known process for biomass conversion from which includes direct combustion, pyrolysis, liquefaction, and gasification.

Gasification is a process used to convert biomass into a combustible gas. Gasification of biomass with air, oxygen, steam or a mixture of these gasification medium is a well established technology. The process produces a gaseous mixture of hydrogen, carbon monoxide, carbon dioxide, methane, and light hydrocarbons with organic and inorganic compounds from following reactions [2, 3].

It is well documented that important parameters affecting gas yields, gas compositions and tar content include biomass composition, temperature, heating rate, residence time, equivalence ratio (ER) and type of medium. Typically, increases in temperature, heating rate and residence time lead to increased gas product yields from gasification [4]. With increasing ER, the gas yields such as hydrogen and carbon dioxide were increased, while carbon monoxide, tar and low heating value of gas product was decreased [5, 6]. Low temperatures have some disadvantages such as low heating value of product gas and high tar content [7]. In order to obtain high gas yields, high temperatures were employed or catalytic substances were used to obtain high yields of fuel gas and reduce its tar content. Some attentions were paid in using dolomite as a catalyst in biomass gasification because it is inexpensive and abundant. But dolomite is known to be significantly active only above 800°C such that tar can be reduced by over 90% [8]. Dolomite was also reported to be effective as an in-bed additive for upgrading the product gas from air gasification process [5, 9].

One type of biomass sources that is often overlooked is weeds. Mimosa, known in Thai as a giant sensitive plant (*Mimosa pigra* L.) is one of the worst weeds because of its invasiveness, potential for spread, and economic and environmental impacts [10]. Mimosa forms dense stands that



replace all native plant. Its invasion threatens crop production. The inedible and thorny mimosa smothers and replaces grasslands, blocks access to stock watering points and hinders mustering, reduces the biodiversity of plant and animal life on the floodplains by outcompeting native plants and reducing available habitat for animals. The habitats of Mimosa are wet land places in the humid and sub-humid tropics. It grows along roadsides, watercourses and seasonally inundated wetlands. It is found on a wide variety of soils and is tolerant of flooding. Mimosa is native to tropical America but is now a serious weed in Africa, Australia [10], India, South-East Asia, Taiwan [11], Northern part of Thailand and some Pacific islands [12]. It was purposely introduced to Thailand as a green manure and cover crop in tobacco plantation. It has been utilized for its ornamental value, medicinal use, and erosion control. Mimosa has also been used for animal feed, timber, temporary fences, and firewood. However, the use is still limited in small scale applications. Utilization as energy source may be useful options and a good mean for the weed management.

From the existing literature, reports on utilization of the weed as bioenergy material were quite scarce. Studies on thermal decomposition of Mimosa in inert and air atmospheres were carried out [13, 14]. Preliminary investigation on gasification of Mimosa in a laboratory scale [15, 16] and a pilot plant [17] showed promising results. But work on the effects of temperature and catalyst to biomass ratio on gasification of Mimosa is non-existent. Attempt was therefore made to fill this gap. In this study, influences of reactor temperature and catalyst to biomass ratio were experimentally studied. Effects of difference air flow rates and collection times on product gas yields and composition were also investigated.

## 2. Materials and Methods

### 2.1. Raw Biomass Material

Mimosa was used as biomass material in this study. The stalk of Mimosa were cut, milled, sieve and classified to fraction of particle size of 0.1-0.7 mm. Proximate and ultimate analyses as well as analysis for the heating value and composition of Mimosa were carried out [15]. Results of this biomass samples are presented in Table 1. It was shown that Mimosa has high volatile content (71.1 %). Carbon and oxygen account for 43.9 and 48.7% w/w, respectively, with calorific value of 17.5 MJ/kg. These values are similar to those of hard woods. The weed appears to be a promising candidate for bioenergy material.

### 2.2. Experimental Setup and Procedure

The experimental setup employed in this work was similar to our previous study [16]. The laboratory scale, test rig used in this study is a fixed bed reactor, schematically shown in Fig 1. The cylindrical reactor has an inside diameter of 40 mm and is 0.5 m high. It was equipped with a 5 kW heating coil and surrounded by thick insulating wool.

The heating coil and the reactor were electrically separated by small ceramic spacers. There was a fixed grate between the middle and the bottom. The outlet of the gasifier is connected to gas coolers and traps where tarry components are removed, and to a sampling bag. Air is supplied from a compressed tank, serving as a purge gas and protective gas to avoid coking occurred on the surface of the reactor before and after operation and is measured with a calibrated flow meter. Reaction temperature is measured by a thermocouple inserted thru its cover and can be automatically controlled by means of a data logger. Prior to the test, the empty reactor was heated externally by an electrical heater for about 30 min.

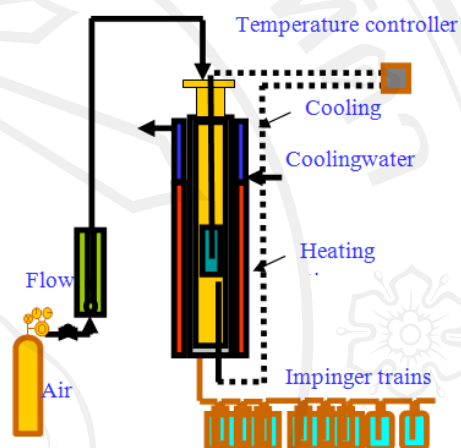


Fig. 1. A fixed bed reactor

Pre-weighed batches (10 g) of biomass materials were then introduced into the reactor. Air was supplied and regulated such that oxidation zone inside the gasifier can be established and gaseous products produced from the biomass is combustible. The reaction was initiated by moving the basket downward into a heating section where the reaction temperature was kept at the pre-determined values. After about 110 min, the biomass sample was taken out of the heating section immediately into a cooling section to terminate the reaction. In this study, reactor temperature was obtained from thermocouple readings inside the reactor and represented as gasification temperature. The gaseous products were collected at the exit of the dry filter in a 0.40 dm<sup>3</sup> sampling bag. The volatiles were immediately sent for composition analysis. A Shimadzu Gas Chromatography model GC-8A was used to analyze CO, CO<sub>2</sub>, H<sub>2</sub>, CH<sub>4</sub>, O<sub>2</sub> and N<sub>2</sub>. The high purity standard gases were used to calibrate the instrument. The duration of operation for certain condition is determined by ensuring that no combustible gas is released and gas yield is dropped to more than 10% of its steady value. At the end of every experiment, the solid and liquid residues are weighed to determine mass balance. The gas yield is computed directly, based on its measured volume. Experiments were performed for air gasification at 100 cm<sup>3</sup>min<sup>-1</sup> with Eq.(1) varying temperatures between 600 - 900°C, Eq.(2) with varying gas collection times, and Eq.(3) catalytic gasification with natural dolomite at varying catalyst and biomass ratios at 900°C. It should be noted that the residence time of the volatile phase is varied during the experimental runs depending on the air flow rates. All experiments were carried out isothermally.

### 3. Results and Discussion

#### 3.1. Effect of Reaction Temperature

The effect of temperature on product distributions from gasification of Mimosa is shown in Fig. 2. A clear increase in gas yields with increasing reaction temperature was observed, similar to that reported in [4, 18]. At higher temperatures, higher gas production may be attributed to the pyrolysis step [19] with endothermic (reactions Eq.(1, 3-5, 8), cracking reactions of the tar (reaction Eq.(2)) and gasification reactions of the char (reactions Eq(3, 5, 7, 8). These reactions are favorable at elevated temperatures, from 600 to 900°C. It was found that when the temperature was increased from 600 to 900°C, the gas yields increased from 59.5% to 81.1%, while the tar and char decreased from 20.5% to 11.9% and 20.0% to 7.0%, respectively. Reduction of the char yields with increasing temperature was due to higher degree of carbonization reaction with air [7]. Fig. 3 shows the effect of temperature on the gas composition. It was found that concentrations of H<sub>2</sub>, CO and CO<sub>2</sub> were increased and whereas CH<sub>4</sub> were decreased at elevated temperatures, in similar trends with those reported in [4, 6, 19-22]. A product gas with H<sub>2</sub>, CO, CO<sub>2</sub> and CH<sub>4</sub>, concentrations of 10.8, 17.9, 24.5, 12.6 and 5.1 mol% was generated at 900°C.

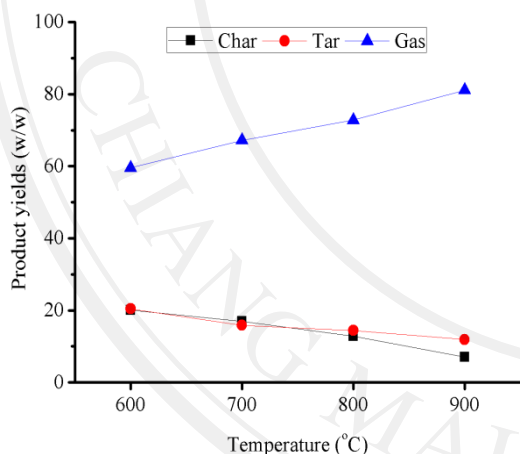


Fig. 2. Effect of temperature on product yields

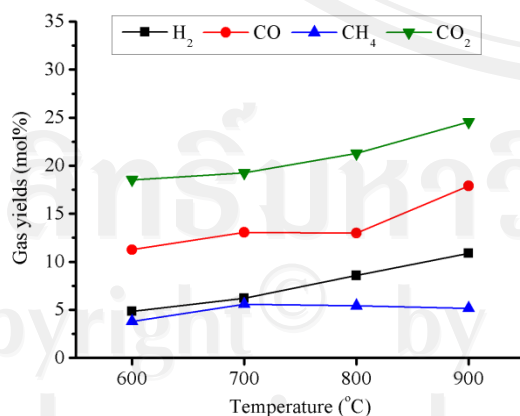


Fig. 3. Effect of temperature on product gas composition

From Fig. 4, increasing temperature resulted in an increase in the H<sub>2</sub>/CO and CO/CO<sub>2</sub> at molar ratios from 0.4

to 0.6 and 0.6 to 0.7. Increase in temperature appeared to strengthen the endothermic reactions, such as reactions Eq.(3-5) and Eq.(8), leading to increased H<sub>2</sub> and CH<sub>4</sub> contents and decreased CO<sub>2</sub> contents.

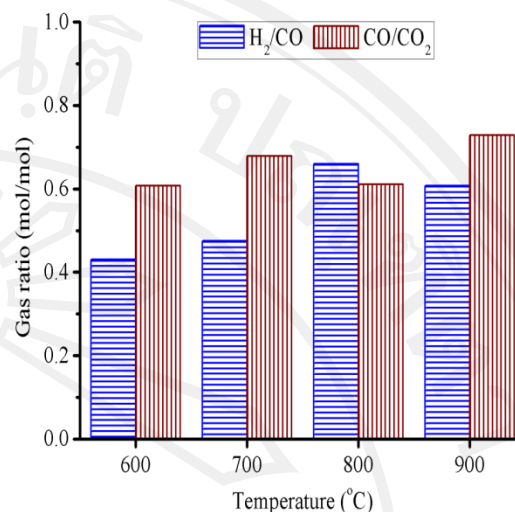
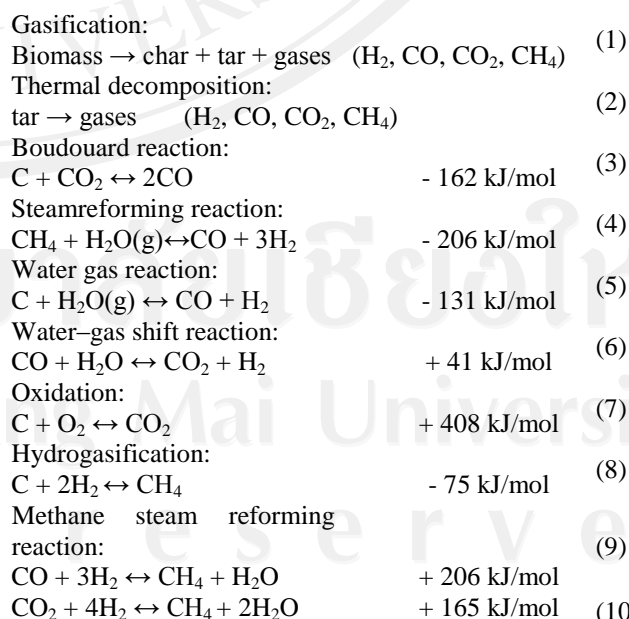


Fig. 4. Effect of temperature on product gas ratio

High concentrations of H<sub>2</sub> may come from thermal decomposition of heavy hydrocarbons and tars into lighter hydrocarbons (reaction Eq.(2)) [21, 24]. It was found to increase due to endothermic reactions Eq.(4-5) at low temperatures and exothermic reaction Eq.(6) at high temperatures. The increase in gas yields was also observed from 600 to 900°C. It might be attributed to the fact that reactions Eq.(3) and Eq. (5) were favored at high temperature [18], and reforming of tar and char were accelerated. From 600 to 900°C, the H<sub>2</sub> content was found to increase greatly. This observation could be a result of exothermic behaviors of reactions Eq.(8-10) [20, 21]. High CO<sub>2</sub> was produced from decomposition of carboxyl groups and from the exothermic reactions Eq(6-7). When temperature was increased, the CO<sub>2</sub> concentration was found to decline. The product gas from wood that has high content in lignin have high yields of CO<sub>2</sub> [22], similar to our observation here.



### 3.2. Effect of Collection Time

Fig. 5 shows the effect of collection time at 800°C on gas yield. It was found that H<sub>2</sub> and CO increased from 7% and 18% to 14% and 29% after 20 min, and subsequently decreased to 5% and 10% after 110 min. Meanwhile, CO<sub>2</sub> was found to increase with time from 5% to 33%. Changes in H<sub>2</sub> and CO were similar to those reported by Encinar et al. [23]. The first 10 min was volatile releasing process. High volatile matter content biomass material will have long devolatilization time which can delay the subsequent char gasification and carbonization processes [24]. An increase in residence time of the volatile phase resulted in increasing gas yield. There were many highly competitive reactions in these processes. Formation of H<sub>2</sub> and CO appeared to be more rapid than other gases. Within reaction time of 60 min, the yields of CO and CO<sub>2</sub> were parity, but after that, CO<sub>2</sub> was found to be more competitive [24]. High concentration of CO<sub>2</sub> seemed to suppress CO yield, in line with those reported by Mitsuoka et al. [25].

### 3.3. Effect of catalyst

In this work, dolomite was used as catalyst for gasification. The effect of catalyst was studied for the temperature at 900°C. Fig. 6 shows the gas, tar and char yields between the non-catalytic and catalytic processes. It can be seen that the gas yields were higher when catalyst was used, while tar and char yields were lower for the uncatalyzed process. This observation was in line with [22, 26].

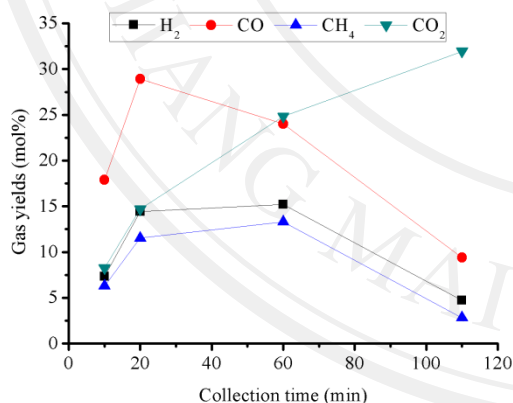


**Fig. 5.** Effect of collection time on product gas composition at 800 °C

Catalyst was found to have positive effect on tar elimination causing change in the gas composition and heating value [27].

The evolution of the concentrations of the gas produced (%mol) as a function of catalyst to biomass ratio at 900°C was shown in Fig. 7. It can be seen that the presence of dolomite clearly encouraged the production of H<sub>2</sub>. At the catalyst to biomass ratio equal to 1, H<sub>2</sub> content was amounted to 27.6 mol% and CO was about 29 mol%. The quantity of CO<sub>2</sub> was found to be higher than that obtained from the uncatalyzed case [22, 28]. As far as the product gas ratio was concerned (Fig. 8), H<sub>2</sub>/CO was found to increase with

increasing catalyst to biomass ratio while The light hydrocarbon appeared to decrease. H<sub>2</sub>/CO and CO/CO<sub>2</sub> exhibited similar trend that they reached maximum at the catalyst to biomass ratio of 1. At 900°C, the presence of catalyst did not appear to improve H<sub>2</sub> production.

In comparison with temperature, the presence of the catalyst was found to affect the product gas compositions more. For non-catalyzed experiments, water-gas reaction seemed to be promoted at high temperatures. This was consistent with the tendencies found from 600 to 900°C where CO and CO<sub>2</sub> were decreased. The catalyst used appeared to cause higher CO<sub>2</sub> content in the product gas [7, 29].

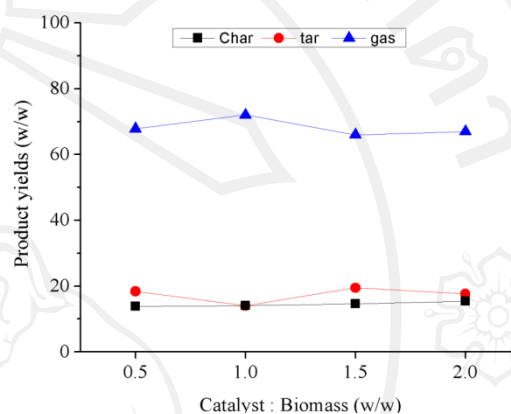


**Fig. 6.** Effect of catalyst biomass ratio on the product yields

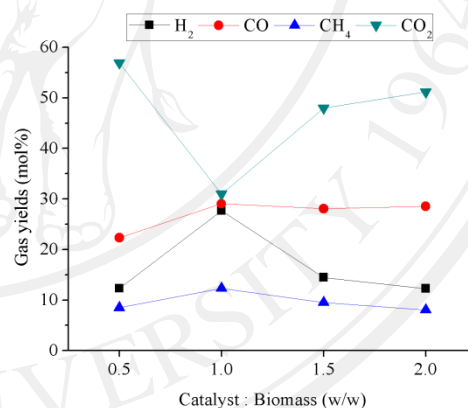


**Fig. 7.** Effect of catalyst to biomass ratio on product gas composition

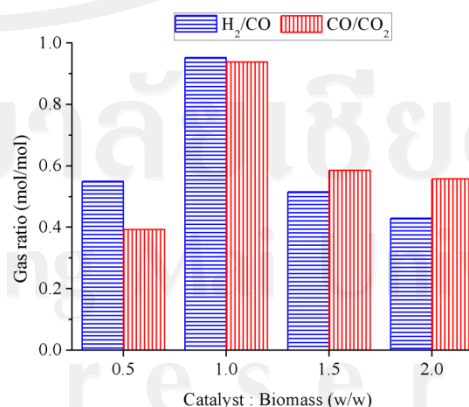


**Fig. 8.** Effect of catalyst to biomass ratio on gas ratio



#### 4. Conclusion

Study on air gasification of Mimosa has been presented. Effect of reaction temperature and catalyst to biomass ratio on the product distribution has been experimentally investigated. The results showed that increasing temperature have positive effect on the production of H<sub>2</sub>, CO and CO<sub>2</sub> and reduction of CH<sub>4</sub> content in the product gas. Maximum H<sub>2</sub> concentration of 11 mol% was achieved at 900°C.

The collection time appeared to have positive effect on H<sub>2</sub> and CO yields during devolatilization and char oxidation process. The presence of catalyst in gasification process was generally believed to improve the product distribution. However, within the range considered in this work, yields of H<sub>2</sub> appeared to peak at the catalyst to biomass ratio of 1. Increasing the amount of catalyst did not offer higher H<sub>2</sub> content.

#### Acknowledgements

This research is financially supported by the Thailand Research Fund (no.RSA5080010) and Faculty of Engineering, Chiang Mai University. The Royal Golden Jubilee PhD

scholarship (no. PHD/0047/2550) awarded to TW is greatly appreciated. Supports from the Energy Research and Development Institute, Chiang Mai University are also acknowledged.

#### References

- [1] R. C. Saxena, D. K. Adhikari, and H. B. Goyal, "Biomass-based energy fuel through biochemical routes: A review," *Renewable and Sustainable Energy Reviews*, vol. 13, pp. 167-178, 2009.
- [2] I. De Bari, D. Barisano, M. Cardinale, D. Matera, F. Nanna, and D. Viggiano, "Air Gasification of Biomass in a Downdraft Fixed Bed: A Comparative Study of the Inorganic and Organic Products Distribution," *Energy & Fuels*, vol. 14, pp. 889-898, July 2000.
- [3] R. J. B. Smith, M. Loganathan, and S. Shantha Murthy, "A Review of the Water Gas Shift Reaction Kinetics," in *International Journal of Chemical Reactor Engineering* vol. 8, ed, 2010, p. 1.
- [4] G. Chen, J. Andries, Z. Luo, and H. Spliethoff, "Biomass pyrolysis/gasification for product gas production: the overall investigation of parametric effects," *Energy Conversion and Management*, vol. 44, pp. 1875-1884, 2003.
- [5] I. Narváez, A. Orío, M. P. Aznar, and J. Corella, "Biomass Gasification with Air in an Atmospheric Bubbling Fluidized Bed. Effect of Six Operational Variables on the Quality of the Produced Raw Gas," *Industrial & Engineering Chemistry Research*, vol. 35, pp. 2110-2120, January 1996.
- [6] P. Plis and R. K. Wilk, "Theoretical and experimental investigation of biomass gasification process in a fixed bed gasifier," *Energy*, vol. 36, pp. 3838-3845, 2011.
- [7] J. F. González, S. Román, D. Bragado, and M. Calderón, "Investigation on the reactions influencing biomass air and air/steam gasification for hydrogen production," *Fuel Processing Technology*, vol. 89, pp. 764-772, 2008.
- [8] S. Thiha, N. Tippayawong, T. Wongsiriamnuay, and C. Chaichana, "Catalytic destruction of biomass tar by dolomite in a dual packed bed reactor," *International conference on green and sustainable innovation 2009 (ICGSI)*, Chiang Rai, Thailand, pp., 2009.
- [9] J. Gil, J. Corella, M. a. P. Aznar, and M. A. Caballero, "Biomass gasification in atmospheric and bubbling fluidized bed: Effect of the type of gasifying agent on the product distribution," *Biomass and Bioenergy*, vol. 17, pp. 389-403, 1999.
- [10] J. Firn and Y. M. Buckley, "Impacts of Invasive Plants on Australian Rangelands," *Rangelands*, vol. 32, pp. 48-51, February 2010.
- [11] W.-M. Chen, E. K. James, J.-H. Chou, S.-Y. Sheu, S.-Z. Yang, and J. I. Sprent, "β-Rhizobia from *Mimosa pigra*, a newly discovered invasive plant in Taiwan," *New Phytologist*, vol. 168, pp. 661-675, 2005.
- [12] W. M. Lonsdale, "Rates of Spread of an Invading Species--*Mimosa Pigra* in Northern Australia," *Journal of Ecology*, vol. 81, pp. 513-521, 1993.
- [13] T. Wongsiriamnuay and N. Tippayawong, "Non-isothermal pyrolysis characteristics of giant sensitive plants using thermogravimetric analysis," *Bioresource Technology*, vol. 101, pp. 5638-5644, 2010.
- [14] T. Wongsiriamnuay and N. Tippayawong, "Thermogravimetric analysis of giant sensitive plants under air atmosphere," *Bioresource Technology*, vol. 101, pp. 9314-9320, 2010.
- [15] T. Wongsiriamnuay, T. Phengpom, P. Panthong, and N. Tippayawong, "Renewable Energy from Thermal Gasification of a Giant Sensitive Plant (*Mimosa pigra* L.)", 5th International Conference on Combustion, Incineration/Pyrolysis and Emission Control, Chiang Mai, Thailand pp., 16-19 December 2008.
- [16] T. Wongsiriamnuay and N. Tippayawong, "Gasification of Giant Sensitive Plants in a Fixed Bed Reactor," 23rd International Conference on Efficiency, Cost, Optimization, Simulation and Environmental Impact of Energy Systems, Lausanne, Switzerland, pp., 14-17 June 2010.
- [17] K. Presnell, "The potential use of mimosa as fuel for power generation.," 3rd International Symposium on the Management of *Mimosa pigra*, Darwin, Australia, pp. 68-72 22-25 September 2002.
- [18] L. Wang, C. L. Weller, D. D. Jones, and M. A. Hanna, "Contemporary issues in thermal gasification of biomass and its application to electricity and fuel

- production," *Biomass and Bioenergy*, vol. 32, pp. 573-581, 2008.
- [19] K. Raveendran, A. Ganesh, and K. C. Khilar, "Pyrolysis characteristics of biomass and biomass components," *Fuel*, vol. 75, pp. 987-998, 1996.
- [20] M. Lapuerta, J. J. Hernández, A. Pazo, and J. López, "Gasification and co-gasification of biomass wastes: Effect of the biomass origin and the gasifier operating conditions," *Fuel Processing Technology*, vol. 89, pp. 828-837, 2008.
- [21] M. Pohořelý, M. Vosecký, P. Hejdová, M. Punčochář, S. Skoblja, M. Staf, J. Vošta, B. Koutský, and K. Svoboda, "Gasification of coal and PET in fluidized bed reactor," *Fuel*, vol. 85, pp. 2458-2468, 2006.
- [22] T. Hanaoka, S. Inoue, S. Uno, T. Ogi, and T. Minowa, "Effect of woody biomass components on air-steam gasification," *Biomass and Bioenergy*, vol. 28, pp. 69-76, 2005.
- [23] J. M. Encinar, F. J. Beltrán, A. Ramiro, and J. F. González, "Pyrolysis/gasification of agricultural residues by carbon dioxide in the presence of different additives: influence of variables," *Fuel Processing Technology*, vol. 55, pp. 219-233, 1998.
- [24] I. Ahmed and A. K. Gupta, "Evolution of syngas from cardboard gasification," *Applied Energy*, vol. 86, pp. 1732-1740, 2009.
- [25] K. Mitsuoka, S. Hayashi, H. Amano, K. Kayahara, E. Sasaoaka, and M. A. Uddin, "Gasification of woody biomass char with CO<sub>2</sub>: The catalytic effects of K and Ca species on char gasification reactivity," *Fuel Processing Technology*, vol. 92, pp. 26-31, 2011.
- [26] A. Olivares, M. P. Aznar, M. A. Caballero, J. Gil, E. Francés, and J. Corella, "Biomass Gasification: Produced Gas Upgrading by In-Bed Use of Dolomite," *Industrial & Engineering Chemistry Research*, vol. 36, pp. 5220-5226, December 1997.
- [27] J. Gil, M. A. Caballero, J. A. Martín, M.-P. Aznar, and J. Corella, "Biomass Gasification with Air in a Fluidized Bed: Effect of the In-Bed Use of Dolomite under Different Operation Conditions," *Industrial & Engineering Chemistry Research*, vol. 38, pp. 4226-4235, November 1999.
- [28] M. Asadullah, S.-i. Ito, K. Kunimori, M. Yamada, and K. Tomishige, "Biomass Gasification to Hydrogen and Syngas at Low Temperature: Novel Catalytic System Using Fluidized-Bed Reactor," *Journal of Catalysis*, vol. 208, pp. 255-259, 2002.
- [29] J. S. Dennis and A. N. Hayhurst, "the effect of CO<sub>2</sub> on the kinetics and extent of calcination of limestone and dolomite particles in fluidised beds," *Chemical Engineering Science*, vol. 42, pp. 2361-2372, 1987.

## Renewable Energy from Thermal Gasification of a Giant Sensitive Plant (*Mimosa pigra* L.)

T. Wongsiriamnuay\*, T. Phengpom, P. Panthong and N. Tippayawong

Department of Mechanical Engineering, Faculty of Engineering, Chiang Mai University, Chiang Mai 50200, Thailand

\*Corresponding author: w\_thanasit@hotmail.com

**Abstract:** A giant sensitive plant or *Mimosa pigra* L. is a fast growing weed that poses a major problem in agricultural areas. In this study, the stalks of *Mimosa* sample were collected, and air dried. They were subsequently milled, sieved and classified into fractions of uniform particle size. Proximate, ultimate and elemental analyses of the weed were performed. Composition and weight fractions of carbon, hydrogen, nitrogen, and oxygen were determined. Holocellulose and lignin, the main constituents of biomass were also determined. Heating values of the weed was calculated, based on their composition and components, and compared with experimental results, following ASTM standards. Thermogravimetric analysis and gasification of *Mimosa* was carried out at atmospheric pressure in a laboratory-scale fixed-bed reactor to investigate mass loss rate, gas yields and product gas composition. Product gas was analyzed by gas chromatography for CO, CO<sub>2</sub>, H<sub>2</sub>, and CH<sub>4</sub>. From the results obtained, *Mimosa* was found to be potentially suitable as biofuel. It contains high proportion of holocellulose, and is rich in carbon and volatile matter, and low in ash content. Its heating value, in comparison with other biomass, is higher than most agricultural residues. The product gas from gasification contains high CO and H<sub>2</sub>, resulting in a useful lower heating value gaseous fuel. It was clear that the weed can be utilized as a useful renewable fuel source.

**Keywords:** Biomass, Gasification, *Mimosa*, Renewable energy, Thermogravimetric analysis

### 1. INTRODUCTION

Biomass for energy application has gained increasing interests in Thailand, with a stiff competition with traditional food applications. Presently, interests in perennial rhizomatous grasses such as miscanthus (*Miscanthus*), switchgrass (*Panicum virgatum*), reed canary grass (*Phalaris arundinacea*) and giant reed (*Arundo donax*) as alternative biomass resources are growing because of their high yield potential, appropriate biomass characteristics, low input demand and positive environmental impact [1, 2]. Others include bamboo [3] and rapeseed straw [4]. Non-plantation biomass resources have been assessed for their energy potential in Thailand context and found to be promising [5]. In this investigation, weed such as a giant sensitive plant (*Mimosa pigra*) is viewed to have potential as a useful energy plant. So far, there have been relatively few literatures reporting on utilization of *Mimosa* as feedstock for bioenergy [6].

Energy may be recovered from biomass via various conversions [7, 8]. Choice of conversion process depends on the type and quantity of biomass feedstock, end use requirement, emission standards, economic conditions and project specific factors. In this work, attention has been paid to gasification since the process can yield a gaseous product that can be readily used in a burner or an internal combustion engine.

### 2. MATERIALS AND METHODS

#### 2.1 Fuel composition analyses

*Mimosa* samples collected in agricultural zone in Chiang Mai, Thailand were used. The collected stalks were cleaned and air dried naturally in a dry store room at ambient condition. The dried samples were later ground in a high speed rotary mill, screen sieved and used for further analysis. Preparation of samples prior to analyses was conducted in accordance with TAPPI T 257 and T 264 standards. Contents of the major biopolymer constituents of the weed, holocellulose, lignin and solvent extractive components were evaluated using TAPPI standard methods. The solubilities of extractives in ethanol and benzene mixture as well as quantity of soluble substances in sodium hydroxide and in water were established. ASTM standard methods were followed to carry out proximate analysis for the samples. The carbon, hydrogen and nitrogen contents were determined using a CHN Elemental Analyzer. The oxygen content was calculated by difference. The heating value of the dried *Mimosa* stalk was determined in compliance with ASTM standard using a Parr bomb calorimeter. It is reported as a gross heat of combustion at constant volume.

#### 2.2 Thermal gravimetry

The biomass materials were also analyzed by thermogravimetric analysis (TGA) method, using a TGA/SDTA 851e Thermogravimetric Analyzer. This high performance TGA analyzer has high sensitivity, vibration resistance and structure that permit rapid replacement of samples. Large number of samples can be analyzed in a short time and in succession. The system was logged to a personal computer for data handling and analysis. Prior to TGA, temperature, weight and sample platform calibrations were carried out. Each sample was placed in the platinum pan securely and in such a way that it was confined within the pan sides and not in contact with the sides of the oven. All handling of samples were done using brass tweezers to avoid contamination. The prepared samples were hanged down in the reaction tube in which the atmosphere can be controlled, and weighed by a sensitive microbalance with resolution of 0.1 µg. The sample was initially preheated to and equilibrated at 40°C in nitrogen under a flow rate of 90 mL/min for 10 minutes. The sample was then heated to 1200 °C at a constant heating rate of 30 °C/min. The purge gas can be switched to oxygen or air.



### 2.3 Gasification

Limited experimental runs on gasification of the biomass material were performed in a batch fixed bed gasifier setup, as shown in Figure 1. The samples were in size range of 3 – 6 mm. The reactor was cylindrical shaped with 0.5 m high and inside diameter of 40 mm. It was made of 5 mm thick stainless steel, surrounded on the outside by heating coil and thick insulating wool (Figure 2). The heating coil and the reactor were electrically separated by small ceramic spacers. There was a fixed grate between the middle and the bottom. The outlet of the gasifier is connected to gas coolers and traps where tarry components are removed, and to a sampling bag. Air is supplied from a compressed tank, serving as a purge gas and protective gas to avoid coking occurred on the surface of the reactor before and after operation and is measured with a calibrated flow meter. Reaction temperature is measured by a thermocouple inserted thru its cover and can be automatically controlled by means of a data logger. Prior to the test, the empty reactor was heated externally by an electrical heater for about 30 min. Pre-weighed batches of biomass materials were then introduced into the reactor. Air was supplied and regulated such that oxidation zone inside the gasifier can be established and gaseous products produced from the biomass is combustible. In this study, reactor temperature was obtained from thermocouple readings inside the reactor and represented as gasification temperature. The gaseous products were collected at the exit of the dry filter in a 0.10 dm<sup>3</sup> sampling bag. The volatiles were immediately sent for composition analysis. A Shimadzu Gas Chromatography model GC-8A was used to analyze CO, CO<sub>2</sub>, H<sub>2</sub>, CH<sub>4</sub>, and N<sub>2</sub>. The high purity standard gases were used to calibrate the instrument. The duration of operation for certain condition is determined by ensuring that no combustible gas is released and gas yield is dropped to more than 10% of its steady value. It should be noted that the residence time of the volatile phase is varied during the experimental run depending on the air flow rates. At the end of every experiment, the solid and liquid residues are weighed to determine mass balance. The gas yield is computed directly, based on its measured volume.

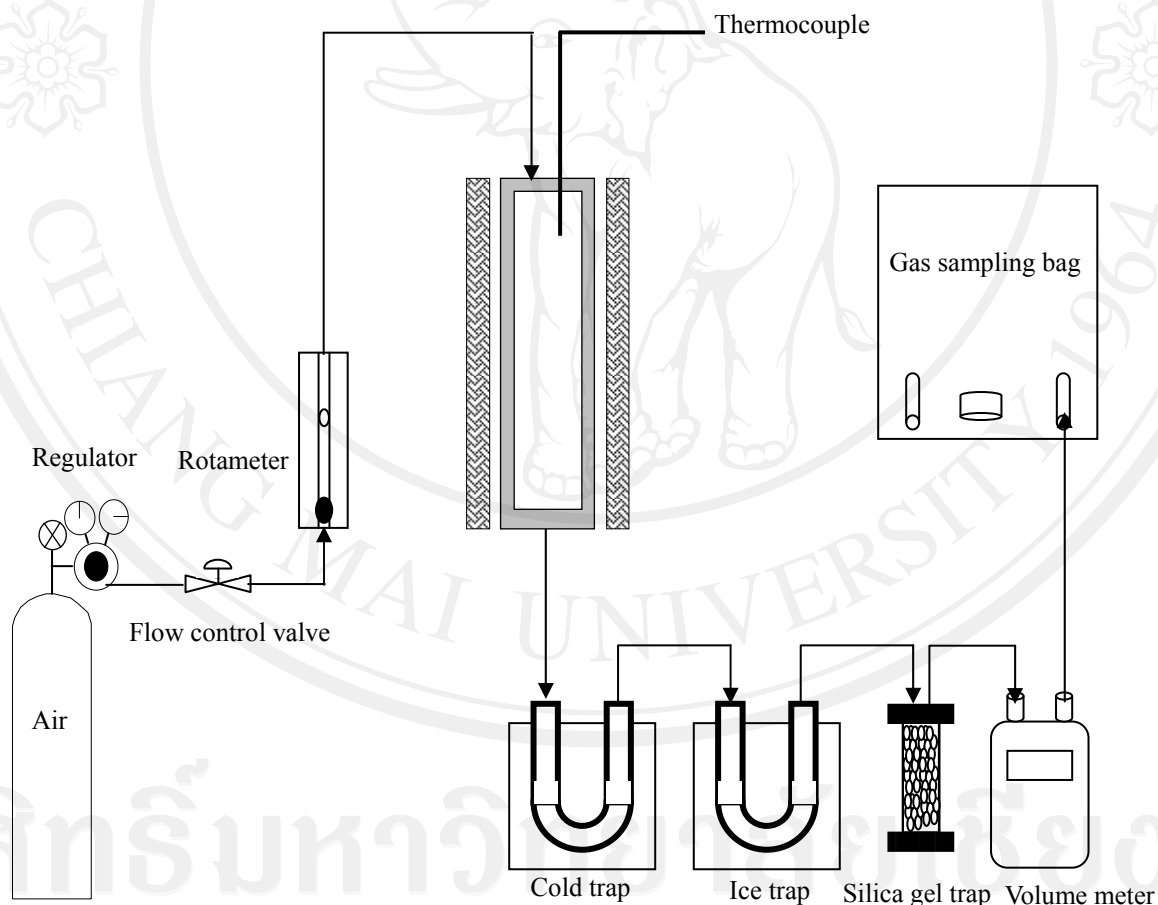


Fig. 1 Gasification experimental setup.

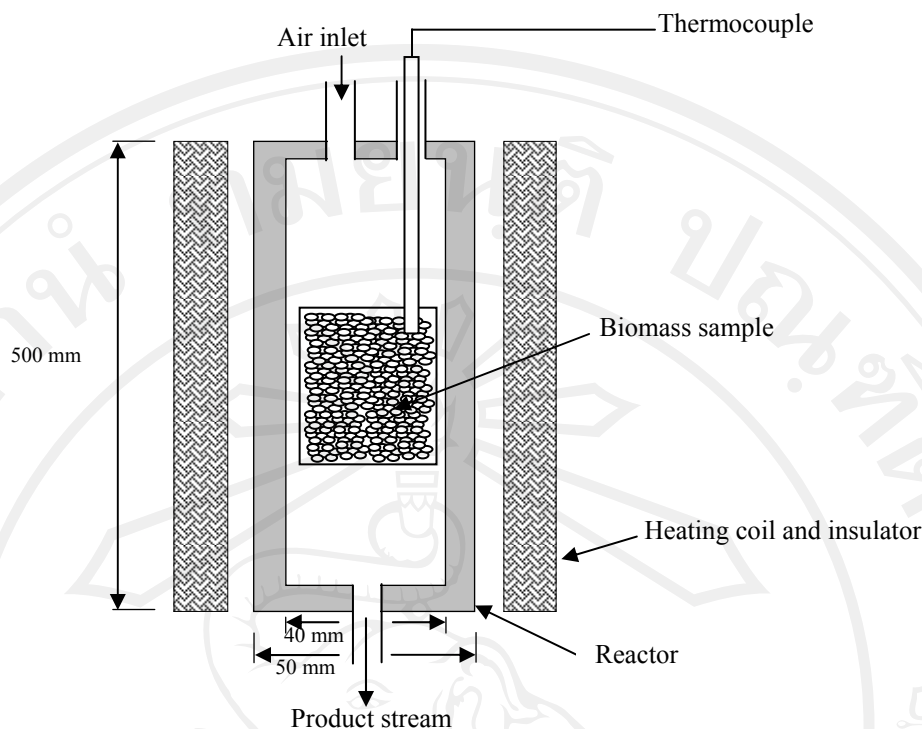


Fig. 2 Configuration of the fixed bed gasifier.

### 3. RESULTS AND DISCUSSION

#### 3.1 Biomass composition

The heating value, proximate and ultimate analyses of the plant samples are listed in Table 1. Moisture content of the air dried samples ranged from 1.5 to 2.4% with average value of 1.6%. The ash contents of all Mimosa samples were 4.5% or less with an average ash content of 3.75%. This was quite low, and therefore the ash could be removed less frequently and continuously from a gasifier or combustor, without interfering with continuous thermo-chemical conversion. Compared to other major biomass feedstocks [9], this ash content is comparable to those found in woody biomass materials. Grasses and straws have higher ash contents. The volatile content was 71% and the remainder was fixed carbon at about 24%. High volatile matter in biomass generally increases tar content in the product gas and must be removed before it fed to an internal combustion engine. All samples showed similar gross heating values, averaging at 17.5 MJ/kg. This value is in similar magnitude to, but slightly lower than woody biomass and higher than most grasses and straws.

Table 1 Properties of the air dried Mimosa stalk

Property	Method	Quantity
Proximate analysis (% w/w)		
Moisture	ASTM D 3173	1.6
Volatile	ASTM D 3175	71.1
Fixed carbon	ASTM D 3172	23.6
Ash	ASTM D 3177	3.7
Ultimate analysis (%)		
Carbon	ASTM D 3174	43.9
Hydrogen		6.0
Nitrogen		1.4
Oxygen		48.7
H/C molar ratio	calculation	1.64
O/C molar ratio	calculation	0.83
Empirical formula	calculation	$\text{CH}_{1.64}\text{O}_{0.83}\text{N}_{0.03}$
Higher heating value (MJ/kg)	ASTM 5865	17.5

The carbon and hydrogen contents of the samples were at about 44%C and 6%H, respectively. The nitrogen content of the Mimosa samples was quite high, about 1.4%, when compared with other biomass feedstocks. But, this is considered to be low N content from combustion perspective. It would be beneficial in terms of minimal fuel bound N-to-NO<sub>x</sub> conversion if the weed was used as fuel. Empirical formula of the weed, derived from the ultimate analysis, was obtained and can be represented as CH<sub>1.64</sub>O<sub>0.83</sub>N<sub>0.03</sub>. It is interesting to note that there have been attempts to correlate proximate analysis results with elemental composition [10] and higher heating value [11] using results based on the proximate analysis of biomass materials. The correlations developed were applied to the Mimosa results. It was found to give the predicted heating value of 18.3 MJ/kg and predicted C and H contents of 47.7% and 5.6%, respectively, which were in agreement with experimental determinations. Their relative differences were within 7.5%.

Table 2 shows lignocellulosic characteristics of the plant. Holocellulose was found to be about 58%. Cellulose content in this range makes Mimosa a useful feedstock for conversion to fuels, chemicals, and other bio-based materials. The lignin level of 34% puts the weed at the high end of a range of 24-37% reported for softwoods and was greater than 11-27% found in non woody biomass [3]. Its high lignin content contributes to a relatively high heating value and structural rigidity, similar to softwoods. Meanwhile, the extractive substances were low. With regards to its solubility, it was observed that high proportion of the plant samples were soluble in dilute base solution. This was considerably higher than its solubilities in water, and ethanol-benzene mixture, respectively. Comparison of selected properties with other solid biofuels is presented in Table 3. The fuel characteristics of the weed appeared to be among the main solid fuels used.

**Table 2** Lignocellulosic properties and solubility of the air dried Mimosa stalk.

Property	Method	Quantity (% w/w)
Holocellulose	Wise method	58.2
Lignin	TAPPI T 222	33.9
Extractives, soluble in ethanol and benzene	TAPPI T 204	1.7
Solubility in hot water	TAPPI T 207	10.5
Solubility in cold water	TAPPI T 207	7.4
Solubility in 1% NaOH solution	TAPPI T 212	36.2
Solubility in ethanol and benzene	TAPPI T 204	5.2

**Table 3** Comparison of selected characteristics between the air dried Mimosa and other solid fuels.

Fuel property	Mimosa	Wood	Corn cob	Rice husk	Lignite
Gross heating value (MJ/kg)	17.5	19.0	16.3	15.4	24.5
Moisture content (%)	1.62	1.5	10.0	8.2	4.5
Ash content (%)	3.75	2.5	3.4	13.2	7.2

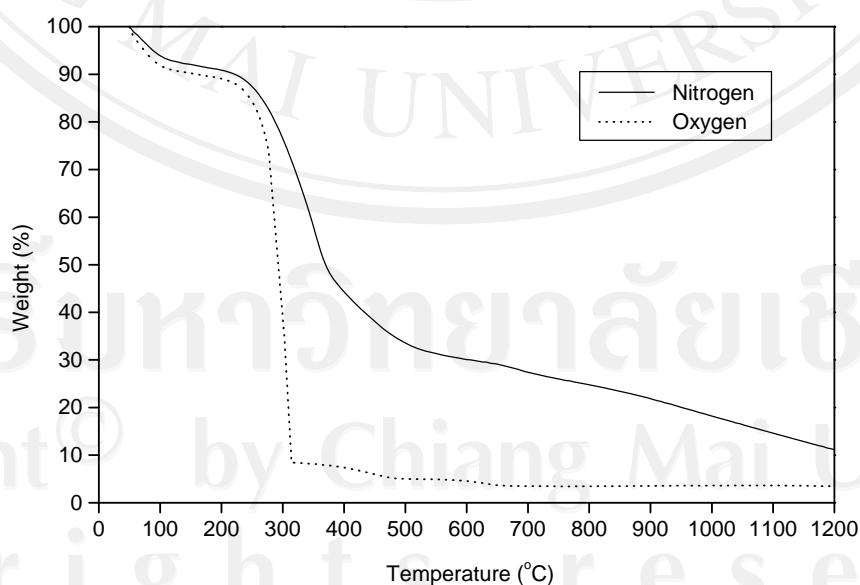


**Fig. 3** TGA thermogram for the air dried Mimosa sample.

### 3.2 Thermal degradation characteristics

TGA was used to determine the thermal degradation of the biomass material. Figure 3 shows the TGA thermogram of weight change for Mimosa at heating rate of 30 K/min under N<sub>2</sub> and O<sub>2</sub> atmospheres. From the TGA data under N<sub>2</sub> environment, it can be seen that there was an initial weight loss of volatile component from the samples at approximately 250°C. The main devolatilization proceeded to about 600°C with total weight of 60%. Further thermal decomposition continued gradually at slower loss rate towards 1200°C. Under O<sub>2</sub> environment, similar thermal degradation character under N<sub>2</sub> environment was observed up to about 250°C. However, a major weight loss was evident between 280°C, and completed by about 300°C due primarily to oxidation. There was essentially no loss observed afterwards. The residual char and ash amounted to about 5%.

### 3.3 Gaseous fuel evolution

Preliminary results of the gasification experiments are shown in Table 4. For the given operating condition, the gas yield was found to be about 1.0 Nm<sup>3</sup>/kg biomass. CO, CO<sub>2</sub> and H<sub>2</sub> were found to be 17.3%, 16.0% and 19.0%, respectively. This resulted in an average lower heating value of the producer gas of approximately 4.7 MJ/Nm<sup>3</sup>.

**Table 4** Results of the air dried Mimosa gasification

Property	Unit	Quantity
Test condition		
Equivalence ratio	(%)	0.25
Temperature	(°C)	900
Biomass feed	(g/hr)	10.0
Air flow rate	(dm <sup>3</sup> /hr)	11.0
Average gas composition		
CO	(% v/v)	17.3
CO <sub>2</sub>	(% v/v)	16.0
H <sub>2</sub>	(% v/v)	19.0
CH <sub>4</sub>	(% v/v)	3
O <sub>2</sub>	(% v/v)	3.2
Nitrogen	(% v/v)	balance
Gas yield	(Nm <sup>3</sup> /kg)	1.0
Lower heating value	(MJ/kg)	4.7
Cold gas efficiency	(%)	27
Carbon conversion	(%)	46
Product distribution		
Gas	% w/w	52
Liquid	% w/w	22
Solid	% w/w	26
Total	% w/w	100

## 4. CONCLUSIONS

Potential use of Mimosa as fuel was considered in this study. Physico-chemical characterization of the plant was conducted and gasification trials in a fixed bed reactor were investigated. It was found that Mimosa contains 59% holocellulose, 34% lignin and small amounts of extractive matter. It is rich in carbon and has considerable amount of volatile matter with relatively high heating value. It shares a number of desirable fuel characteristics with certain other biomass feedstocks. It appeared to present no obstacles in utilizing it as solid fuel with thermal conversion process. Present analyses indicated that Mimosa is potentially suited as useful solid biofuels and may be utilized through gasification at relatively moderate conditions. Its potential use as fuel is an important option for management of this weed. Further research may be required to develop cost effective management, harvesting and treatment prior to use in a power plant.

## 5. ACKNOWLEDGEMENTS

Supports from the Thailand Research Fund for this project and a Royal Golden Jubilee PhD scholarship awarded to TW are acknowledged. Chiang Mai University Graduate College is thanked for a grant awarded to PP.



## 6. REFERENCES

- [1] Basso, M. V., Cerrella, E. G., Buonomo, E. L., Bonelli, P. R. and Cukierman, A. L. (2005) Thermochemical conversion of *Arundo donax* into useful solid products, *Energy Sources*, **27**, pp. 1429-1438.
- [2] Lewandowski, I., Scurlock, J. M. O., Lindvall, E. and Christou, M. (2003) The development and current status of perennial rhizomatous grasses as energy crops in the US and Europe, *Biomass and Bioenergy*, **25**, pp. 335-361.
- [3] Scurlock, J. M. O., Dayton, D. C. and Hames, B. (2000) Bamboo: an overlooked biomass resource?, *Biomass and Bioenergy*, **19**, pp. 229-244.
- [4] Karaosmanoglu, F., Tetik, E., Gurboy, B. and Sanli, I. (1999) Characterization of the straw stalk of the rapeseed plant as a biomass energy source, *Energy Sources*, **21**, pp. 801-810.
- [5] Sujjakulnukit, B., Yingyuad, R., Maneekhao, V., Pongnarintasut, V., Bhattacharya, S. C. and Abdul Salam, P. (2005) Assessment of sustainable energy potential of non-plantation biomass resources in Thailand, *Biomass and Bioenergy*, **29**, pp. 214-224.
- [6] Presnell, K. (2004) The potential use of mimosa as fuel for power generation, In *Research and Management of Mimosa pigra*, edited by M. Julien, G. Flanagan, T. Heard, B. Hennecke, Q. Paynter, and C. Wilson, Canberra, Australia: CSIRO Entomology.
- [7] Bridgewater, A. V. (2003) Renewable fuels and chemicals by thermal processing, *Chemical Engineering Journal*, **91**, pp. 87-102.
- [8] Demirbas, A. (2007) Progress and recent trends in biofuels, *Progress in Energy and Combustion Science*, **33**, pp. 1-18.
- [9] Nordin, A. (1994) Chemical and elemental characteristics of biomass fuels, *Biomass and Bioenergy*, **6**, pp. 339-347.
- [10] Parikh, J., Channiwala, S. A. and Ghosal, G. K. (2007) A correlation for calculating elemental composition from proximate analysis of biomass materials, *Fuel*, **86**, pp. 1710-1719.
- [11] Demirbas, A. (1997) Calculation of higher heating value of biomass fuels, *Fuel*, **76**, pp. 431-434.

## Catalytic Destruction of Biomass Tar by Dolomite in a Dual Packed Bed Reactor

Soe Thiha\*, Nakorn Tippayawong, Thanasit Wongsiriamnuay, and Chatchawan Chaichana

Department of Mechanical Engineering, Faculty of Engineering, Chiang Mai University, Chiang Mai, 50200, Thailand

\*Corresponding Author: soethiha9@gmail.com, +66-8-4482-7735

### Abstract

Biomass gasification contributes to bio-energy production without generating greenhouse gases into the environment. Commercialization of the technology is limited by tar contained in the product gas. Catalytic treatment of the gas can destroy the tar almost completely. In this study, a fixed bed catalytic reactor was designed, built and tested. A downdraft gasifier was used to generate a producer gas for tar cracking tests. This paper presents catalytic treatment of the producer gas in dual packed bed in a tar cracker using dolomite, calcined dolomite and char as catalysts. Experiments were carried out for a temperature range between 650 – 850°C. High tar conversions over 90% were obtained for all the catalysts used. It was evident that catalytic tar destruction in the dual catalyst bed could be a promising option for significant tar removal to be employed in a gasification system.

**Keywords:** Biomass gasification, Catalytic cracking, Dolomite, Tar removal

### 1. Introduction

With the depletion of fossil fuel sources as well as the global warming issues, utilization of biomass is getting increased attention as a potential source of renewable energy. Biomass fuels and residues can be converted to energy via thermal, biological and physical processes [1]. Biomass gasification is a complex thermochemical process including pyrolysis, partial oxidation of lignocellulosic materials. Product gas is composed of  $H_2$ ,  $CO$ ,  $CO_2$ ,  $H_2O$ ,  $CH_4$  and various light hydrocarbons along with undesirable dust (ash and char), tar,  $NH_3$ , alkali (mostly potassium) and some other trace contaminants [2]. The continual build-up of

condensable organic compounds (often referred to as tars) present in the product gas can cause blockages and corrosion, leading to a reduction in overall efficiency [3]. The producer gas can be used in engine and turbine for energy generation, fuel cells and methanol synthesis. Therefore, contaminants especially tars must be removed to meet the specific applications of the gas.

Commercial gasifiers use conventional filters and wet cleaning methods to remove the gas, discharging tar dissolved waste water that requires treatment before disposal. Thermal and catalytic treatment of the gas can ultimately destroy tar. Catalytic tar removal can operate at

lower temperatures than thermal processes and result in high tar removal efficiency. Extensive reviews on the use of several catalysts for tar destruction can be found in the literatures [3-5]. Dolomite is usually employed due to its low cost. It is calcium magnesium ore with the general formula  $\text{CaMg}(\text{CO}_3)_2$  that contains ~ 20%  $\text{MgO}$ , ~ 30%  $\text{CaO}$ , and ~ 45%  $\text{CO}_2$  on a weight basis, with other minor mineral impurities. Calcination decomposes  $\text{CO}_2$  to form  $\text{CaO} \cdot \text{MgO}$  [5]. The use of dolomite inside gasifier and downstream reactor has been studied extensively. In this paper, investigation of the catalytic cracking of tar from biomass gasification in a dual packed bed reactor was presented.

## 2. Experimental Method

### 2.1 Equipments

Experimental setup includes a throat type, downdraft gasifier for producing the gas required for catalytic tar cracking tests. A laboratory scale catalytic tar cracker was built using stainless steel pipe with ID of 14mm and 70cm in length. It was heated by an insulated external electrical heating chamber, power rating of 3 kW. A dual

packed bed was housed inside the tar cracker. Internal temperatures along the cracker were measured by type K thermocouples. The outlet of the cracker was connected to a tar sampling impinger trains. Gas flow rate was regulated by means of a pump and flow meters. The impinger train consists of six impinger bottles in which iso-propanol was used as solvent. The sketch of the experimental set up is shown in Fig. 1.

### 2.2 Catalytic cracking

Catalytic cracking of biomass tar experiments were performed using dolomite, calcined dolomite and charcoal as catalysts. The particle sizes of the catalysts ranged from 2.12 mm to 4.75 mm, having average particle diameter of 3.41 mm. The bulk densities of the dolomite, calcined dolomite and charcoal were 1.23, 0.68, and 0.37  $\text{g/cm}^3$ , respectively. Calcination of the dolomite was performed at 900°C for 2 hours in an oven. It was found that dolomite became softer after calcination, reducing its mechanical strength. The length of each catalyst bed inside the cracker was set at 270 mm.

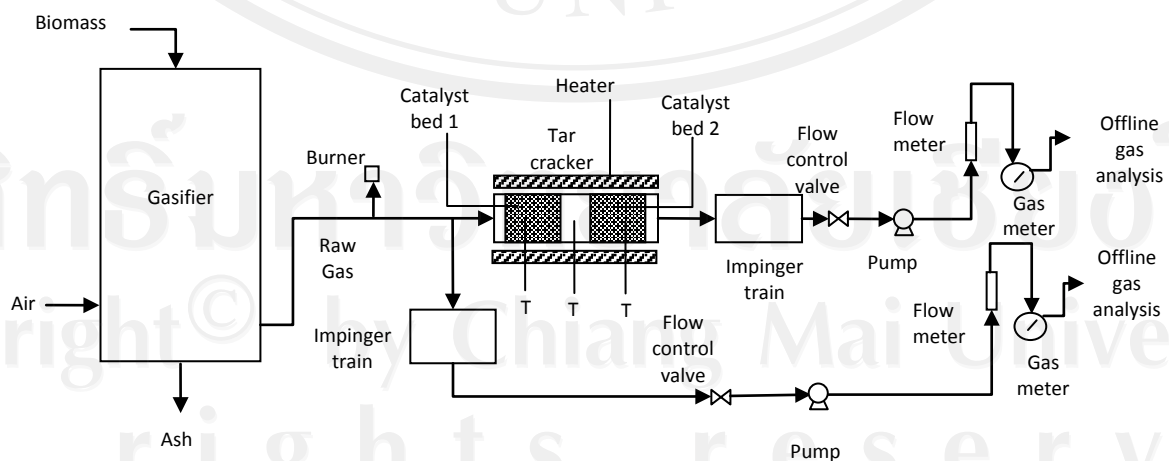


Fig.1 Experimental setup of a catalytic tar cracking system

## 2.3 Procedure

Cashew nut shells were used as biomass feedstock. Its moisture content was about 10.8% (as-received basis). The heating value and elemental composition of the cashew nut shells were taken from the works of Singh et al. [7], Das and Ganesh [8], shown in Table 1. At the start of each experiment, the gasifier was loaded with cashew nut shells and ignited at the bottom. The tar cracker was also simultaneously heated to reach the desired set point temperature, at a temperature range between 650 – 850°C. When the producer gas generated from the gasifier became combustible and operated in a stable manner, the cracking tests were started. The controlled parameters of the tar destruction test were temperature and residence time inside the dual packed bed. Each operation was performed for 15 – 20 minutes and repeated in triplicate for one controlled temperature. Tar containing gases upstream and downstream of the cracker were sampled separately. Measurement of tar content in the producer gas was carried out gravimetrically, following the method shown in tar sampling and analysis protocol [6]. Weight measurements after evaporation were carried out using Metler digital analytical balance. Sample gases from the gasifier and the cracker after cleaning were collected in Tedlar gas bag and analysed offline by Shimadzu GC-8A/TCD using helium as carrier gas. Tar conversion,  $X$ , [10] was calculated by;

$$X = \frac{c_{in} - c_{out}}{c_{in}} \times 100 \quad (1)$$

where  $c_{in}$  and  $c_{out}$  are inlet and outlet tar concentrations ( $\text{g/Nm}^3$ ), respectively.

Table 1 Properties of cashew nut shells

property	value
C	48.7 %
H	7.0 %
O	43.9 %
N	0.4 %
Heating value	17.6 MJ/kg

Table 2 Composition of the producer gas

component	%
CO	17.07
H <sub>2</sub>	5.04
CH <sub>4</sub>	3.15
CO <sub>2</sub>	19.72
N <sub>2</sub>	balance

## 3. Results and Discussion

### 3.1 Gasifier operation

The gasifier was able to start within 15 min and attain steady state operation from cold start in about 30-60 min. Although feeding was done intermittently, gasification seemed to operate well. Oxidation and reduction reactions appeared to proceed continuously. The system was able to run rather smoothly without any sign of significant deterioration. Fuel flow did not show any problem during the test runs. Nonetheless, poking at regular interval (1 h) was done to ensure trouble-free operation. Exit gas temperature of the gasifier was about 170°C. Producer gas was combustible, with bright orange flame. The composition of the gas was determined and shown in Table 2. The lower heating value of the producer gas was estimated to be about 3.51 MJ/m<sup>3</sup>.

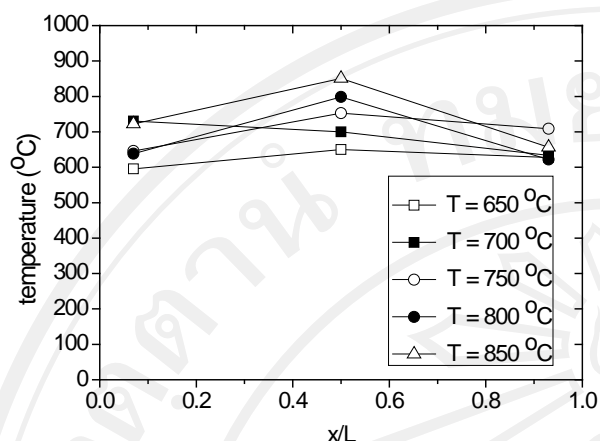


Fig. 2 Axial temperature distributions along the reactor length at different set point temperatures

### 3.2 Cracker operation

Prior to tar cracking tests, heater of the cracker was switched on to the set point temperatures. Fig. 2 shows axial temperature profiles along the cracker length for each set point. At axial distance  $x = 0$  represents the inlet and  $x = L$  is at the exit of the tar cracker.

### 3.3 Tar conversion

Temperature profiles inside the cracker are depicted in Fig. 2. Tar conversion results are shown in Fig. 3. These conversions were average values of triplicate experiments. Tar conversions with dolomite, calcined dolomite, and charcoal were found to be very high inside two catalyst beds reactor. The highest conversion obtained at 750 and 700°C for dolomite and calcined dolomite, respectively. Tar conversions above 90% were obtained with the charcoal as catalyst. The highest tar conversion of 99.5% was found at 800°C. Fig. 4 shows tar concentration in the producer gas after treated with catalytic cracker. The final tar content was observed to be well below 35 mg/Nm<sup>3</sup> for all tested catalyst types and temperatures.

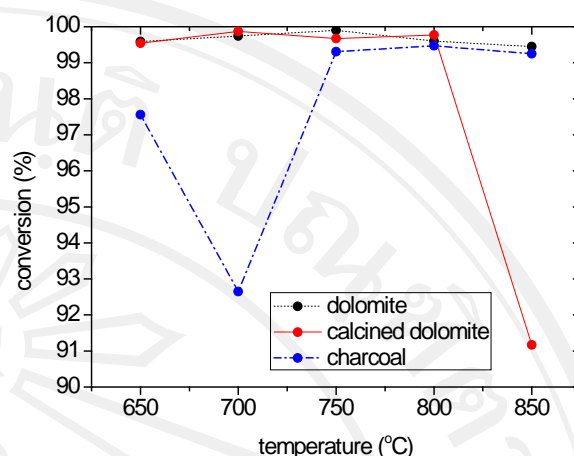


Fig. 3 Tar conversion for different catalysts

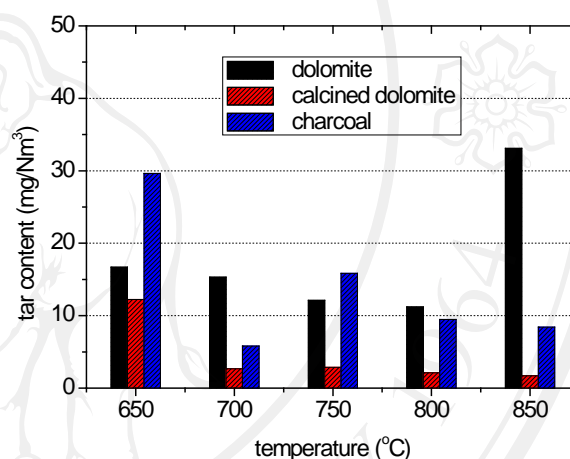


Fig. 4 Final tar contents in the treated producer gas after treatment with different catalysts

The observed fluctuation in conversion may be due to varying tar content in the producer gas with time and operating conditions.

Reduction in tar conversion due to catalyst deactivation has not been observed for all the three catalysts. However, coke formation was observed with dolomite catalysts, as shown in Fig. 5. It was found that the catalyst removed from first catalyst bed served as a guard and coke formation was severe. The second catalyst bed appeared to be less affected. Coke formation for calcined dolomite and charcoal was not clearly evident and difficult to identify.



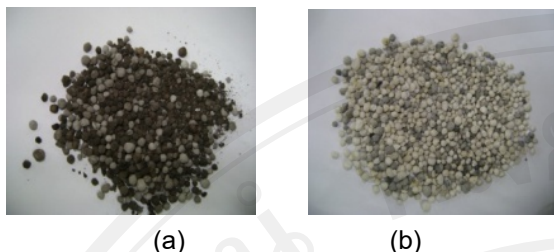


Fig. 5 Appearances of spent dolomite (a) first bed discharge and (b) second bed discharge

#### 4. Conclusion

In this work, a catalytic tar cracker was designed and tested. Low cost catalysts were used. The use of dolomite, calcined dolomite and charcoal in a dual bed catalytic reactor showed over 90% tar reduction.

Catalytic hot gas conditioning of the producer gas to reduce the tar content doesn't produce waste water. Since the low cost and abundance the catalysts used in this study, it might be more economical than using expensive metal and noble synthesized catalysts. It can cut the excess equipment costs since the first bed serves as a guard for the second bed. Moreover, it could be combined with metal catalyst in second catalyst bed with the first guard bed so that high quality syngas could be generated.

#### 5. Acknowledgement

Supports from the Energy Research and Development Institute, and the Graduate School, Chiang Mai University to SH are gratefully acknowledged. Supports from the Thailand Research Fund (contract no. RSA5080010) and a Royal Golden Jubilee PhD scholarship awarded to TW are acknowledged.

#### 6. References

[1] Li, C. and Suzuki, K. (2009). Tar property, analysis, reforming mechanism and model for

biomass gasification - an overview, *Renewable and Sustainable Energy Reviews*, vol. 13, pp. 594–604.

[2] Zhang, R., Brown, R. C., Suby, A. and Cummer, K. (2004). Catalytic destruction of tar in biomass derived producer gas, *Energy Conservation and Management*. vol. 45, pp. 995-1014.

[3] Sutton D., Kelleher, B. and Ross, J. R. H. (2001). Review of literature on catalysts for biomass gasification, *Fuel Processing Technology*, vol. 73, pp. 155-173.

[4] Milne, T.A., Evans, R. J. and Abatzoglou, N. (1998). Biomass gasifier "tars": their nature, formation, and conversion, *NREL/TP-570-25257*, National Renewable Energy Laboratory, Colorado, USA.

[5] Dayton. D. (2002). A review of the literature on catalytic biomass tar destruction. *NREL/TP-510-32815*, National Renewable Energy Laboratory, Colorado, USA.

[6] Simell, P., Stålberg, P., Kurkella, E., Albrecht, J., Deutsch, S. and Sjöström, K (2000). Provisional protocol for sampling and analysis of tar and particulates from large-scale biomass gasifiers, *Biomass and Bioenergy*, vol 18, pp. 19-38.

[7] Singh, R. N., Jena, U., Patel, J. B. and Sharma, A. M. (2006). Feasibility study of cashew nut shells as an open core gasifier feedstocks, *Renewable Energy*. Vol. 31, pp. 481-487.

[8] Das, P. and Ganesh. A. (2003). Bio-oil from pyrolysis of cashew nut shell - a near fuel, *Biomass and Bioenergy*, vol. 25, pp. 113-117.



## Gasification of Giant Sensitive Plants in a Fixed Bed Reactor

*Thanasit Wongsiriamnuay and Nakorn Tippayawong*

*Department of Mechanical Engineering, Faculty of Engineering, Chiang Mai University, Chiang Mai, Thailand*

**Abstract:** A giant sensitive plant (*Mimosa pigra* L.) is a fast growing and spreadable weed. It infests strongly along the rivers, surrounding large reservoirs, wetland reserves and agricultural fields. Its invasion threatens the production and preservation values of wetlands, and poses a major problem in agricultural areas. To avoid food-fuel dilemma, the weed may be utilized as a biorenewable energy source. In this study, it was used as feedstock for generation of producer gas. Mimosa sample were collected, and air dried. They were subsequently milled, sieved and classified into fractions of uniform particle size between 0.3 and 0.6 mm. Fuel characterization was performed using proximate and ultimate analyses. Gasification of giant sensitive plants was carried out at atmospheric pressure in a laboratory-scale fixed bed reactor to investigate the effect of reactor temperature and catalyst biomass ratio on gas yields and product gas composition. The product gas from thermochemical process was found to contain high CO and H<sub>2</sub> which was a useful low heating value gaseous fuel. With an increase in temperature, gas yield was found to increase while char and tar were found to decrease. Increasing catalyst to biomass ratio was found to result in an increase in hydrogen, and a decrease in carbon monoxide. It appeared that the weed can be utilized as a useful renewable fuel.

**Keywords:** Biomass, Gasification, Mimosa, Renewable energy, Fixed bed.

### 1. Introduction

Mimosa, known in Thai as a giant sensitive plant, is a native plant of Central and South America. It was purposely introduced to Thailand in the late 1940s as a green manure and cover crop in tobacco plantations [1]. It is a leguminous thorny shrub that can grow to a height of six meters. Mimosa is able to form mono-specific stands, replacing the native wet vegetation and thereby reducing the available habitats of native flora and fauna. It is considered to be one of the worst environmental weeds of wetland in Thailand. When faced with an extensive weed infestation, it is natural to find ways to utilize it. Mimosa has been utilized for its ornamental value, medicinal use, green manure and erosion control. It has also been used as animal feed, timber and biomass material [1]. In Thailand, it has been used for firewood, temporary fences, and tested for fiberboard. However, the use is still limited in rather small scale applications. Alternative energy utilization method may offer different options and a mean for the weed management.

Thermochemical processing is recognized as the most important available technology for biomass

conversion. Gasification is viewed to be a suitable conversion technology that offers high thermal efficiency and environmental acceptability. Gasification process is favourable for producing low to medium calorific value gas. If the weed is gasified efficiently, it may generate a high yield of clean product gas. Thermal decomposition of mimosa has been investigated [2, 3]. It was viewed to have potential as a bioenergy source via gasification. However, tar can potentially impair the product gas quality. Using of catalysts in the gasification process has been proved to be an effective method to reduce tar and improve gasification efficiency. Dolomite is among the cheapest and most available catalysts used to control tar. Natural dolomite has been shown to reduce tar content in producer gas [4, 5].

In this work, giant sensitive plants were used as a biomass feedstock for the generation of producer gas. A laboratory scale, fixed bed reactor was developed. The thermochemical conversion of mimosa was performed in the fixed bed reactor. The influence of different operation conditions, including reactor temperature and catalyst to biomass ratio on product yields (gas, char, and tar) and the composition of fuel gas in terms of H<sub>2</sub> and

H<sub>2</sub>/CO was investigated. Air was used as gasification medium. Natural dolomite was used as an *in situ* catalytic gas conditioning agent.

## 2. Experimental setup

### 2.1. Sample characterization

Mimosa samples collected in agricultural zone in Chiang Mai, Thailand were used. The collected stalks were cleaned and air dried naturally in a dry store room at ambient condition. The dried samples were later ground in a high speed rotary mill, screen sieved and used for further analysis. The proximate analysis of the weed was carried out according to standard norms. The determination of moisture, volatile matter and ashes was performed following the standards; ASTM D 3173, ASTM D 3175, ASTM D 1372, ASTM 3177, respectively. The fixed carbon was calculated by difference to 100%. The determination of the ultimate analysis was made using a CHN-932 elemental analyzer (ASTM F 3174). The higher heating value of the weed waste was determined with a Parr calorimeter bomb (ASTM 5865). These parameters are displayed in Table 1. One can see that the weed has a high content of volatile matter and low content of ash, which is very interesting with respect to its applications in gasification and pyrolysis processes. The low N content ensures that thermal NO<sub>x</sub> formation during the gasification process is negligible.

### 2.2. Test apparatus and procedures

Gasification experiments were performed at an atmospheric pressure using air as gasification medium. The experimental setup is shown schematically in Fig. 1. The fixed bed reactor was equipped with electric heaters around its perimeter which was covered with a thick insulation layer.

Table 1. Properties of the air dried mimosa stalk.

Property	Quantity
Proximate analysis (% w/w)	
Moisture	1.6
Volatile	71.1
Fixed carbon	23.6
Ash	3.7
Ultimate analysis (% w/w)	
Carbon	43.9
Hydrogen	6.0
Nitrogen	1.4
Oxygen	48.7
Higher heating value (MJ/kg)	17.5

Its setup consists of the fixed bed reactor, an air compressor and an feed air heater. The reactor was made of 1Cr18Ni9Ti stainless steel tube. The effective height of the reactor was 900 mm, with an internal diameter of 60 mm. Two type K thermocouples were used to measure and control the temperatures in the middle of the gasifier and the biomass in a basket.

A collection module was used as cooling unit for fuel gas cooling and tar capture. It consists of two series of impinger bottles containing a solvent for tar absorption, placed separately in two cold baths. The first three impinger bottles were immersed in a temperature below 5 °C, whereas, the next three impinger bottles were cooled at a temperature under -20 °C which tar and moisture will be completely collected. The tar aerosols were collected by both condensation and absorption in the solvent. Each impinger bottle was filled with approximately 100 ml of isopropanol, which was considered to be the most suitable solvent for tar absorption [5]. The gas flow rate was measured with a volume meter. The cool, dry, clean gas was sampled using gas bags and analyzed on a Shimadzu Model GC-8A gas chromatograph fitted with a ShinCarbon ST Micropacked column and a thermal conductivity detector, for measuring volumetric concentration of H<sub>2</sub>, O<sub>2</sub>, N<sub>2</sub>, CH<sub>4</sub>, CO,

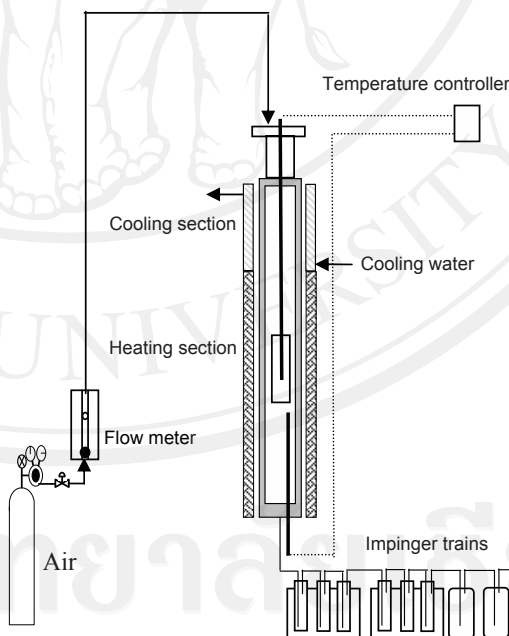


Fig. 1. Gasification experimental setup.

Corresponding Author: Thanasit Wongsiriamnuay, Email: w\_thanasit@hotmail.com

CO<sub>2</sub>. Standard gas mixtures were used for quantitative calibration.

Initially, the electric heater was switched on to heat the reactor. Once the set point temperature was achieved in the gasification reactor, the biomass was displaced from the cooling section to the heating section. Air was fed from the top of the gasification reactor. When stabilization was reached with respect to the temperatures, gas sampling and analysis were carried out. It was normally completed in about 20 min. Experiments were performed for (i) air gasification at 500 cm<sup>3</sup>min<sup>-1</sup> with varying temperature between 600 – 900°C and (ii) catalytic gasification with natural dolomite at varying proportions (% w/w referred to catalyst and biomass ratio) at 900°C with the same air flow condition. All experiments were carried out isothermally and initial mimosa mass of 10 g was used.

### 3. Results and discussion

#### 3.1. Product yields

Fig. 2 shows effect of reaction temperature on the product yields from gasification of mimosa without presence of catalyst. The gas yields were found to increase from about 51% to 64% as the reaction temperature was raised from 600°C to 900°C. The char and tar fractions appeared to decrease with increasing temperature. Changes from 700°C to 800°C showed only marginal effect on the yields. Fig. 3 shows the product yields from gasification of mimosa at different catalyst to biomass ratios between 0.5 – 2.0 at a fixed temperature of 900°C. It was observed that while the char yield stayed relatively constant, the gas yield appeared to go through a maximum of 72% at a catalyst to biomass ratio of 1.0.

#### 3.2. H<sub>2</sub> and H<sub>2</sub>/CO yields

Figs. 4 and 5 show effects of reaction temperature on the H<sub>2</sub> and H<sub>2</sub>/CO yields from non-catalytic gasification. It can be seen from the experimental results that both the hydrogen yields and hydrogen to carbon monoxide ratios were primarily influenced by the operating temperature. Changing the temperature from 600 to 900°C resulted in an increase in the H<sub>2</sub> yields [6, 7], while H<sub>2</sub>/CO yields were found to decrease slightly from 0.72 to below 0.60. The increases of the hydrogen fraction with

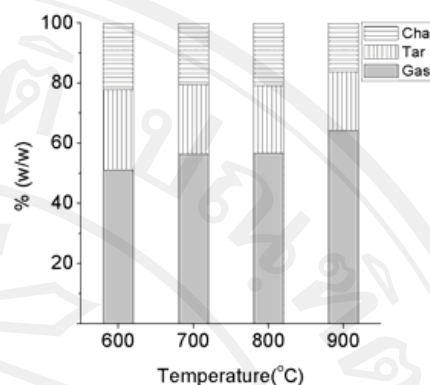


Fig. 2. Effect of reaction temperature on yields of gasification products

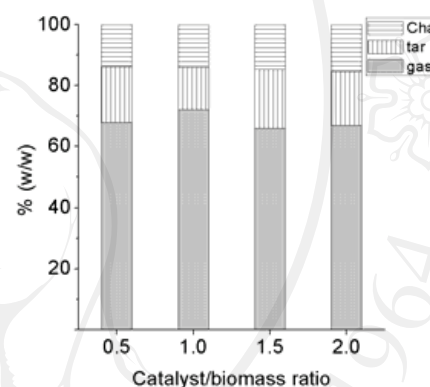


Fig. 3. Effect of catalyst/biomass ratio on yields of gasification products

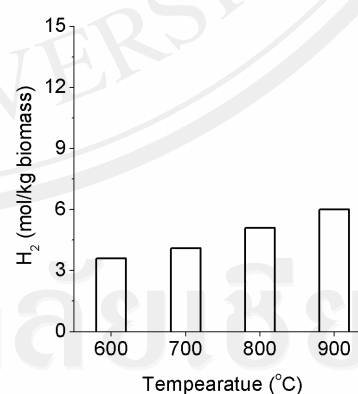


Fig. 4. Effect of reaction temperature on H<sub>2</sub> yields.

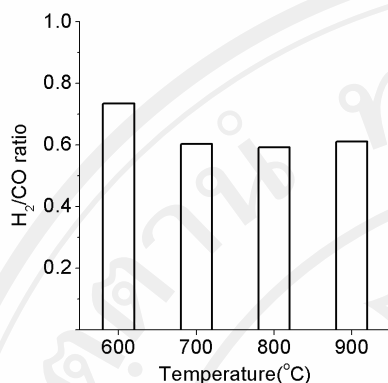


Fig. 5. Effect of reaction temperature on  $H_2/CO$  ratio.

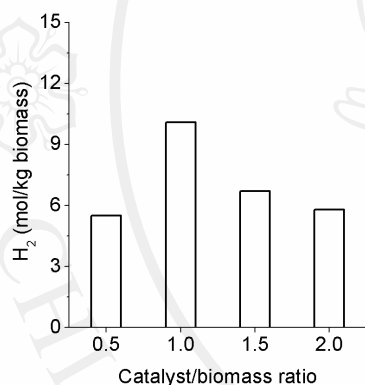


Fig. 6. Effect of catalyst/ biomass ratio on  $H_2$  yields.

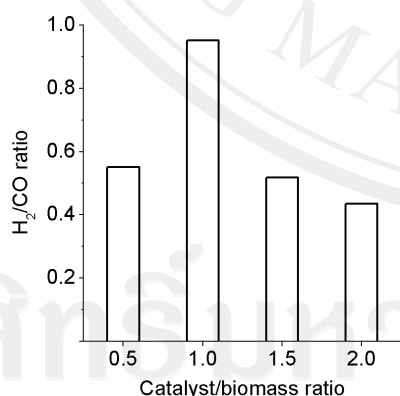


Fig. 7. Effect of catalyst/biomass ratio on  $H_2/CO$  ratio.

Table 2. Comparison of  $H_2$  yields for different types of biomass without catalyst.

Reference	Biomass	Temp (°C)	$H_2$ yield (%)
This work	Mimosa	900	17
[6]	Sawdust	900	38
[9]	Saw dust	810	10
[9]	Wood	550	8
[10]	Rice straw	800	10
[10]	Rice straw	900	23

Table 3. Comparison of  $H_2$  yields for different types of biomass with dolomite catalyst.

Reference	Biomass	Temp (°C)	$H_2$ yield (%)
This work	Mimosa	900	26
[10]	Rice straw	900	37
[11]	Sawdust	800	11
[12]	Pine sawdust	850	52
[13]	Pine sawdust	750	51

temperature were due to the greater production of gas in the initial pyrolysis (faster at higher temperatures), and the endothermic reactions of gasification of the char, which increases with temperature. It was clear that temperature has integrated effects on these results.

The effects of catalyst to biomass ratio on  $H_2$  and  $H_2/CO$  yields when the reactor temperature was kept constant at 900°C are shown in Figs. 6 and 7. Generally, the  $H_2$  yields were observed to increase with the presence of catalyst. The peak value of  $H_2$  yield appeared at the catalyst to biomass ratio of 1.0 was twice as much as that at similar condition without the catalyst. This may be attributed to an increase in surface reaction area on the dolomite, greater the contact area between the biomass and the dolomite, leading to higher chemical reaction rates and gasification reactions [8]. However, increasing catalyst/biomass ratio did not prove to increase the hydrogen yield further. With respect to  $H_2/CO$  ratios, similar pattern to  $H_2$  yields was observed that a maximum ratio of 0.95 was obtained at catalyst to biomass ratio of 1.0. However, at other catalyst to biomass ratios, the  $H_2/CO$  yields appeared to be slightly lower than the value at similar condition without the catalyst.

### 3.3. Comparison with literature

$H_2$  yields obtained from gasification of mimosa in this study were compared against those obtained from other types of biomass at similar thermal conditions. Results (in % by volume) are shown in Tables 2 and 3 for the cases with and without



catalyst, respectively. It was found that H<sub>2</sub> yields were comparable to other biomass considered.

#### 4. Conclusions

In this work, air gasification of giant sensitive plants under atmospheric pressure in a fixed bed reactor has been carried out with and without dolomite as a catalyst. Effects of reaction temperature and catalyst to biomass ratio have been investigated. Gas yields were found to increase with increasing temperatures. With catalysts, over 60% gas yields were obtained. Increase in temperature resulted in an increase in H<sub>2</sub> yields. The H<sub>2</sub> yields were found to increase further with presence of catalyst. A peak of H<sub>2</sub> yield was observed at catalyst to biomass ratio of 1.0. Producer gas yields and composition obtained from gasification of mimosa were in similar magnitude and comparable to other types of biomass. Mimosa appeared to have potential as a biofuel candidate.

#### References

- [1] Miller, I. L., 2004, Uses for *Mimosa pigra*, In: *Research and Management of Mimosa pigra*, eds Julien, M., Flanagan, G., Heard, T., Hennecke, B., Paynter, Q. and Wilson, C., pp 63-67, CSIRO Entomology, Canberra, Australia.
- [2] Wongsiriamnuay, T., et al., 2008, Renewable Energy from Thermal Gasification of a Giant Sensitive Plant (*Mimosa pigra* L.), 5<sup>th</sup> International Conference on Combustion, Incineration/ Pyrolysis and Emission Control, Chiang Mai, Thailand.
- [3] Wongsiriamnuay, T., and Tippayawong, N., 2010, Non-isothermal Pyrolysis Characteristics of Giant Sensitive Plants Using Thermogravimetric Analysis, *Bioresource Technology*, in press.
- [4] Sutton, D., et al, 2001, Review of Literature on Catalysts for Biomass Gasification, *Fuel Processing Technology*, 73(2), pp. 155-173.
- [5] Li, C., and Suzuki, K., 2009, Tar Property, Analysis, Reforming Mechanism and Model for Biomass Gasification - An Overview, *Renewable and Sustainable Energy Reviews*, 13(3), pp. 594-604.
- [6] Turn, S., et al., 1998, An Experimental Investigation of Hydrogen Production from Biomass Gasification, *International Journal of Hydrogen Energy*, 23(8), pp. 641-648.
- [7] Lv, P.M., et al., 2004, An Experimental Study on Biomass Air-steam Gasification in a Fluidized Bed. *Bioresource Technology*, 95(1), pp. 95-101.
- [8] Rapagna, S., and Latif, A., 1997, Steam Gasification of Almond Shells in a Fluidised Bed Reactor: the Influence of Temperature and Particle Size on Product Yield and Distribution. *Biomass and Bioenergy*, 12(4), pp. 281-288.
- [9] Ni, M., et al., 2006, An Overview of Hydrogen Production from Biomass. *Fuel Processing Technology*, 87(5), pp. 461-472.
- [10] Xie, Y. R., et al., 2009, Influences of Additives on Steam Gasification of Biomass: 1 Pyrolysis Procedure, *Energy and Fuels*, 23(10), pp. 5199-5205.
- [11] Hanping, C., et al., 2008, Experimental Investigation of Biomass Gasification in a Fluidized Bed Reactor, *Energy and Fuels*, 22(5), pp. 3493-3498.
- [12] Lv, P., et al., 2007, Bio-syngas Production from Biomass Catalytic Gasification, *Energy Conversion and Management*, 48(4), pp. 1132-1139.
- [13] Delgado, J., et al, 1996, Calcined Dolomite, Magnesite, and Calcite for Cleaning Hot Gas from a Fluidized Bed Biomass Gasifier with Steam: Life and Usefulness, *Industrial and Engineering Chemistry Research*, 35(10), pp. 3637-3643.

**Acknowledgements:** This research is financially supported by the Thailand Research Fund (no. RSA5080010) and Faculty of Engineering, Chiang Mai University. The Royal Golden Jubilee PhD scholarship (no. PHD/0047/2550) awarded to TW is greatly appreciated. Supports from the Energy Research and Development Institute, Chiang Mai University are also acknowledged.



## Fuel Gas Production from Low Temperature Gasification of Bamboo in Fluidized Bed Reactor

Nattakarn Kannang\*, Thanasit Wongsiriamnuay and Nakorn Tippayawong

Department of Mechanical Engineering Faculty of Engineering, Chiang Mai University, Chiang Mai, Thailand, 50200

\*Corresponding author: Nattakarn\_K@gmail.com, 0867283166

### Abstract

Fuel gas production from gasification of bamboo in a fluidized bed reactor was investigated in this work. Experiments were performed to determine the effects of reactor temperature (700, 800, 900 K), biomass to catalyst ratio (1:0, 1:1) on product gas, composition,  $H_2/CO$  ratio and heating value. From the results obtained, in the case of no catalyst, the optimum condition was at temperature of 700 K, air flow rate of 20 lpm, obtaining maximum hydrogen content of 9.77 %vol,  $H_2/CO$  ratio of 0.63 and lower heating value (LHV) of 5.26 MJ/Nm<sup>3</sup>. With catalyst, the optimum condition was at temperature of 900 K, air flow rate of 20 lpm and biomass to catalyst ratio of 1:1. Hydrogen content of 11.49 %vol,  $H_2/CO$  ratio of 0.65 and LHV of 5.85 MJ/Nm<sup>3</sup> were obtained.

**Keywords:** Bamboo, Biomass, Fluidized bed, Renewable energy

### 1. Introduction

At present, there are concerns about the depletion of fossil fuel reserves and pollution caused by continuously increasing energy demands [1]. These problems lead many researchers to search for new energy sources in replacement of fossil fuels. As an alternative to fossil fuels in the future, biomass is renewable fuel, and has significant environmental benefits: near zero CO<sub>2</sub> emissions to reduce global warming [2,3].

Thailand is an agriculture-based country. There are plenty of biomass in Thailand. Bamboo is one of the interesting biomass because it is easy to cultivate, is one of the fastest-growing plant, and it could be harvested in 1-3 years [4].

Biomass energy conversion can be achieved through several thermochemical processes namely 1) combustion 2) pyrolysis and 3) gasification. Among them, gasification process for hydrogen production is one of the promising methods [2,5,6]. It is well known that biomass gasification offers a great potential to produce fuel gas that can be used for synthesis gas applications. But, producer gas from this process usually contains unacceptable levels of tar. Tar can cause operational problems by blocking gas cooler and filter elements. Most producer gas applications also require removal of dust and tar before the gas can be used [7]. Tar can be effectively minimized in raw producer gas by catalytic cracking [8].



Therefore, addition of catalyst in gasification process should be made to remove tar and obtain higher  $H_2$  content. Many researchers have been extensively studied and proved that calcined dolomite was useful and effective in decreasing tar, improving gas quality in the process of biomass gasification [1, 7].

In this study, a fluidized bed reactor was utilized to investigate fuel gas production from gasification of bamboo in a fluidized bed reactor with air and calcined dolomite in the reactor. The purpose of this study is to evaluate the hydrogen production from low temperature gasification of bamboo, as well as to explore the effects of some operating parameters such as reactor temperature, and biomass to catalyst ratio on the product gas composition,  $H_2/CO$  ratio and heating value of fuel gas.

## 2. Experiments

### 2.1 Feed materials and catalysts

Bamboo obtained locally, was used as feedstock for experimental runs. The particle size of this bamboo was between 0.1-0.25 mm. The properties of the bamboo are given in Table 1.

For pyrolysis and low temperature gasification, alumina sand was used as inert bed material in the fluidized bed gasifier, while calcined dolomite were used as catalyst. The dolomite was first crushed and sieved to obtain a fraction with a particle size of 0.1-0.25 mm, and then calcined in air at  $900^\circ C$ .

### 2.2 Experimental apparatus and procedure

Fig. 1 shows a schematic of the fluidized bed gasification system used in this study. Its main components are following: a fluidized bed reactor, a biomass feeder, a steam generator, an air preheater, gas metering cleaning and gas sampling.

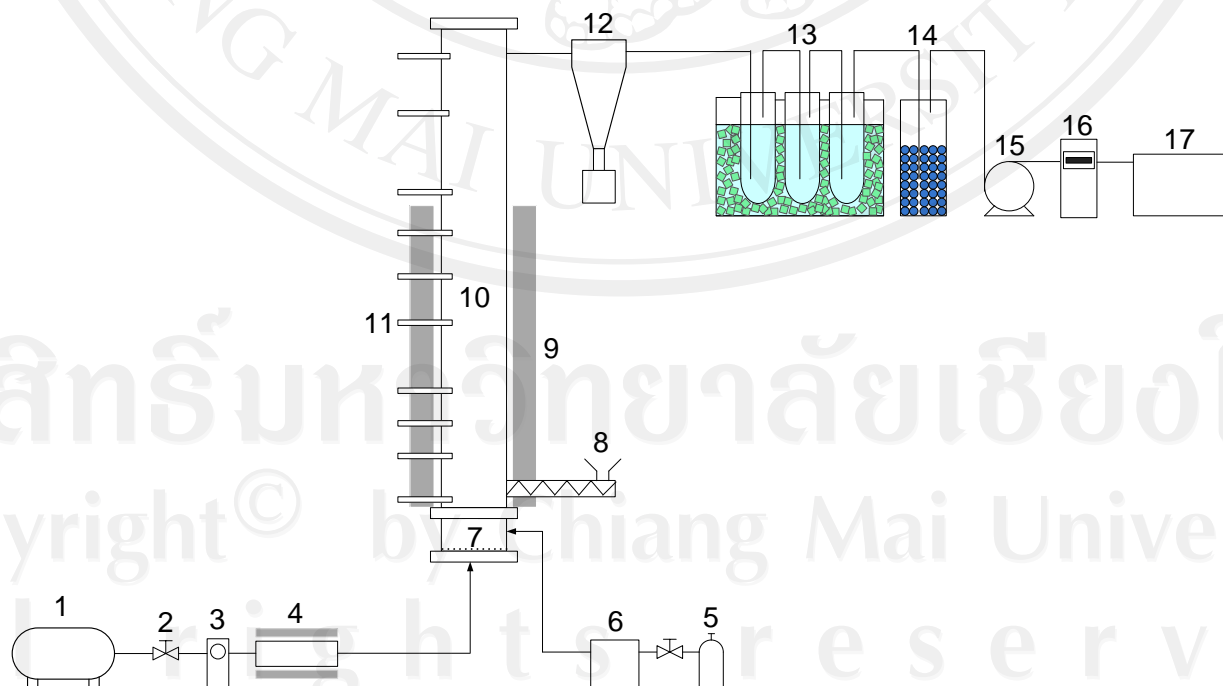


Fig. 1 Schematic diagram of low temperature gasification reactor:(1) air pump, (2) valve, (3) flow meter



- (4) preheater, (5) LPG tank, (6) burner, (7) distributor, (8) biomass feed hopper, (9) insulator, (10) gasifier, (11) thermocouple, (12) cyclone, (13) tar remover section, (14) silica gel, (15) pump, (16) gas flow meter, and (17) gas bag.

Table. 1 Main characteristics of the bamboo

Characteristics	value
Proximate analysis, (% w/w dry basis)	
Moisture	5.73
Volatile	74.68
Fixed Carbon	14.04
Ash	5.55
Ultimate analysis, (% w/w dry basis)	
C	45.66
H	4.32
O	49.72
N	0.24
S	0.06
LHV(MJ/kg)	17.8

The fluidized bed reactor was made from stainless steel cylinder and was externally covered by insulator. The total height of the reactor was 2 m, 50 mm in diameter. The reactor was installed with thermocouples along the length in order to measure the temperature distribution inside the reactor while fluidizing. Below the reactor, an air distributor is installed for better air distribution. The biomass was fed into the reactor through a screw feeder driven by a variable speed metering motor with the rate of 250-300 mg/h. Air was used as the fluidizing agent from the air compressor with maximum flow of 20 lpm. Before the air entered into the reactor, it was preheated to 300-500°C. The produced gas flow exits the reactor through a cyclone, into gas sampling system.

Each run was started by filling of the bed of alumina or silica sand mixed with dolomite up to the desired height. The propane burner was start-up. The propane shut-off valve was then opened and the burner was turned on. The start-up period was necessary to preheat the bed up to the desired temperature before commencement of the fuel feeding.

The burner was turned on to preheat alumina or silica sand for about 40 min. After the bed temperature reached the desired level and steady, the air compressor was turned on to force the air through the preheater, air distributor, and into the reactor. When the bed temperature remained steady, biomass was fed into the reactor by the screw feeder from the hopper at the bottom of the reactor, continuously carried out at constant flow rate. The feeding of biomass was at 10 g/min. The air and biomass flow rates were varied to give the desired equivalence ratio. After the bed temperature was stabilized, the char carried by the producer gas was separated in the cyclone, the produced gas was passed through an ice trap for cleaning. Then, the dry and clean gas was sampled using gas bags and analyzed by gas chromatography. The GC (model GC-8A of Shimadzu) was fitted with a Shin-carbon column, TCD detector. The gas chromatograph was calibrated using standard gases. Helium was used as carrier gas, to detect H<sub>2</sub>, O<sub>2</sub>, N<sub>2</sub>, CH<sub>4</sub>, CO and CO<sub>2</sub>. Each condition was repeated at least three times.

### 3. Results and Discussion

#### 3.1. Effect of reactor temperature

In order to study the effect of the temperature on product gas composition in fluidized bed reactor, the experiments were performed under three temperatures, 700, 800, and 900 K, respectively. Air flow rate was 20 lpm. Biomass feed rate was 10 g/min.

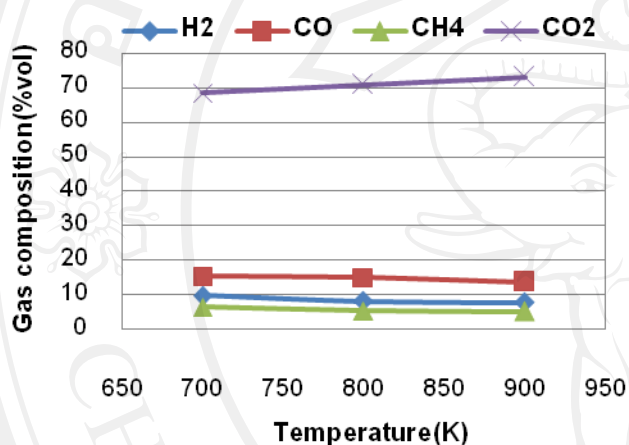
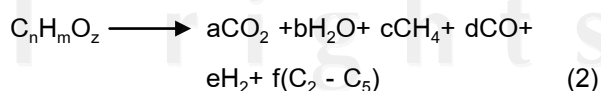
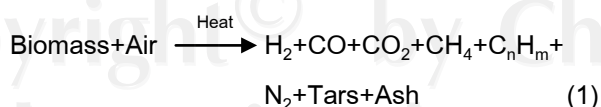


Fig. 1 Effect of temperature on gas composition

Fig. 1 shows the effect of temperature on gas compositions. It can be found that the content of H<sub>2</sub> and CO in the fuel gas decreased with increasing temperature, while the content of CO<sub>2</sub> increased. The content of CH<sub>4</sub> was found to slightly decrease. This may be due to low temperature. The content of hydrogen can be obtained from dehydrogenation of hemicelluloses, cellulose, and lignin, or secondary decomposition of their pyrolyzed products (Eq. 1 or 2) [9].



At higher temperatures, the content of hydrogen was decreased due to high reactivity of the char with air. The reaction tended to complete oxidation (Eq. 3) and partial oxidation (Eq. 4) [10].

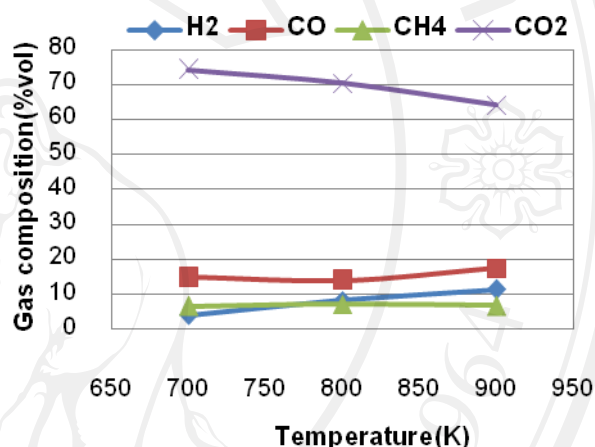
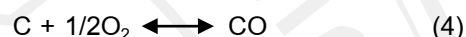
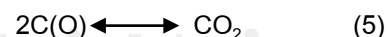


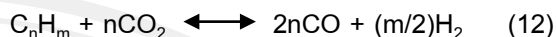
Fig. 2 Effect of catalyst on gas composition

Total combustion may occur to release more CO<sub>2</sub>. Combustion reactions hardly produce H<sub>2</sub> [9].

According to Skolou [10], at low temperature, the desorption process (Eq. 5) and Eq. 6) will be a controlling step. At high temperature, the controlling step is adsorption process (Eq. 7).



where C(O) represents the carbon-oxygen complex



### 3.2. Effect of catalyst

The experiments were performed under three temperatures; 700, 800, and 900 K, respectively. Air flow rate was 20 lpm, biomass feed rate 10 g/min, and catalyst ratio 1:1.

The effect of catalyst on gas compositions are indicated in Fig. 2. It can be seen that the content of  $H_2$  and CO in fuel gas increased with increasing temperature, whereas the trends were opposite for  $CO_2$ . The content of

Reduction of  $CO_2$  content and increase in CO content with increasing temperature were due to Eqs. 13 and 14 at high temperature. It was found that  $CO_2$  reacts with excess carbon in the solid particles, producing CO (Eq. 13) [9,11,15].  $CO_2$  might be reacted with tar, (Eq. 14) producing CO and  $H_2O$  [9].

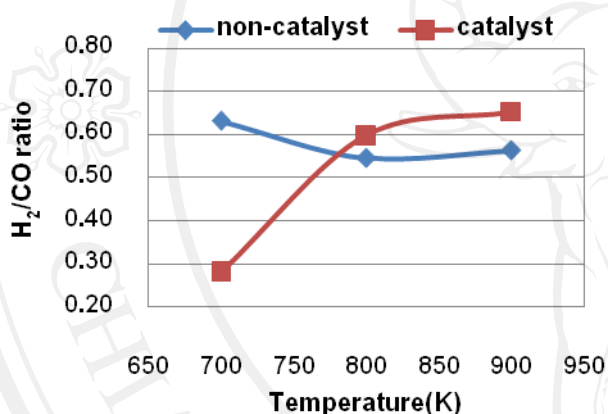
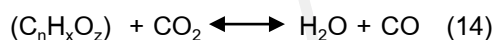


Fig. 3 Effect of temperature on the ratio of  $H_2/CO$

$CH_4$  showed a slight change. The content of  $H_2$  increased with increasing temperature due to the catalyst capture with carbon to produce more  $H_2$ , according to Eqs. 8 and 9 [11].



Furthermore, tar cracking and tar reforming reactions resulted in increased content of  $H_2$  at higher temperature, according to following reactions (Eqs. 10 - 12) [12,13,14].

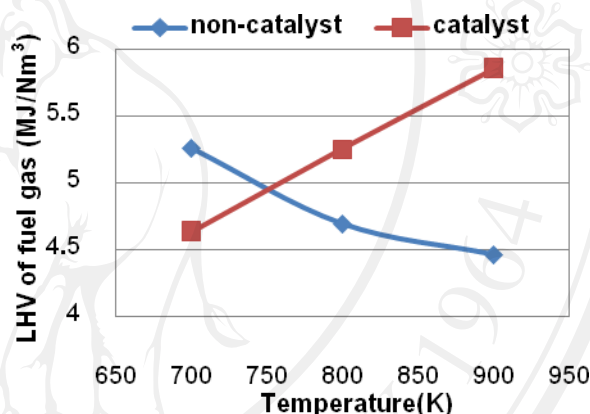
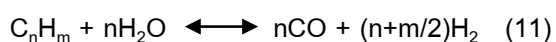
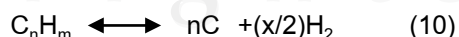


Fig. 4 Effect of temperature and catalyst on LHV of the fuel gas

However, the reactions in gasification are very complex and can occur simultaneously. The product gas depends on the influence from many factors such as temperature, catalyst etc.

### 3.3 $H_2/CO$ ratio

Fig. 3 showed influence of temperature on the ratio of  $H_2/CO$ . It can be seen that, when the temperature increases, the ratio of  $H_2/CO$  was higher, with catalyst. It showed that the catalyst was an important factor for controlling  $H_2/CO$  ratio.





$H_2/CO$  ratio in the gasification product gas was an important parameter in synthesis of the reactant gases into desired products such as gasoline, Fischer Tropsch synthesis, and methanol. For example, gasoline may need the  $H_2/CO$  ratio to be 0.5 to 1.0. Fischer Tropsch synthesis need  $H_2/CO$  ratio to be 0.5 to 2.0, and methanol may need it to be about 2.0.

Fig. 3 showed that at  $H_2/CO$  ratio = 0.65 at 900 K. At this condition, It may be useful for gasoline and Fischer Tropsch synthesis. However, in a commercial gasifier the  $H_2/CO$  ratio of the product gas is typically less than 1.0 [14].

Table. 2 Comparison with literature

Ref.	Material	Catalyst	Reactor	Temp (K)	ER	Gas composition (%Vol)			$H_2/CO$	LHV <sub>Gas</sub> (MJ/Nm <sup>3</sup> )
						H <sub>2</sub>	CO	CH <sub>4</sub>		
This work	bamboo	-	Bubbling fluidized bed	700	0.40	9.8	15.4	6.5	0.6	5.3
		Dolomite		900		11.5	17.6	6.8	0.7	5.9
[10]	olive kernel	-	Bubbling fluidized bed	1,023	0.20	24.0	14.3	3.8	1.7	6.5
[13]	woody waste	-	Fluidized bed	1,073	0.20	13.2	38.5	8.1	0.3	10.3
[15]	sewage sludge	-	Bubbling fluidized bed	1,123	0.30	12.1	10.1	3.3	1.2	3.9
		Dolomite				13.9	12.7	2.8	1.1	4.2
[16]	sawdust	-	Entrained flow	1,073	0.28	7.6	26.0	3.3	0.3	6.0
[17]	rice husk	-	Fluidized bed	938-	0.25-	4.0-	19.9-	2.9-	0.2-	3.1-5.0
				1,103	0.35	3.3	12.3	1.8	0.3	

### 3.4 Heating value of fuel gas

Temperature and catalyst were found to affect the heating value of fuel gas. It was shown in Fig. 4. When the temperature increased, the heating value of the fuel gas was reduced. This was because the content of H<sub>2</sub>, CO and CH<sub>4</sub> in the fuel gas decreased with increasing temperature. With catalyst, the heating value of fuel gas increased with increasing temperature, due to increase in contents of H<sub>2</sub>, CO and CH<sub>4</sub> in the fuel gas from catalytic effect.

### 3.5 Comparison with literature

Table 2 shows that comparison of gas composition and heating value of fuel gas obtained from this work at optimum condition with different biomass materials, and different reactors configuration with air gasification. Generally, H<sub>2</sub> and CO obtained from this work were in slightly lower than those from literature. This may be contributed to lower temperature and higher ER used.

## 4. Conclusions

In this study, effects of temperature and catalyst on gas composition,  $H_2/CO$  ratio and LHV of fuel gas from low temperature gasification of





bamboo in fluidized bed reactor with air were investigated.

Results showed that the effect of temperature on gas compositions, the content of  $H_2$  and CO in the fuel gas decreased with increasing temperature, while the content of  $CO_2$  increased. The content of  $CH_4$  was found to slightly decrease. For  $H_2/CO$  ratio and LHV of fuel gas, it was found that both decreased with increasing temperature. The presence was found to increase content of  $H_2$  and CO in fuel gas at higher temperature, whereas the trends were opposite for  $CO_2$ .

### 5. Acknowledgements

The authors would like to thank the National Research Council of Thailand (NRCT), the Department of Industrial Chemistry, and the Department of Chemistry, Faculty of Science, the Department of Environmental Engineering, Faculty of Engineering, Chiang Mai University for supports of this work.

### References

- [1] Lv, P., Chang, J., Wang, T., Fu, Y. and Chen, Y. (2004). Hydrogen-rich gas production from biomass catalytic gasification, *Energy & Fuel*, vol. 18, May 2004, pp. 228-233.
- [2] Wei, L., Xu, S., Zhang, L., Liu, C., Zhu, H. and Lin, S. (2007). Steam gasification of biomass for hydrogen-rich gas in a free-fall reactor, *International Journal of Hydrogen Energy*, vol. 32, July 2007, pp. 24-31.
- [3] Panigrahi, S., Dalai, A.K., Chaudhari, S.T. and Bakhshi, N.N. (2003). Synthesis gas production from steam gasification of biomass-derived oil, *Energy & Fuel*, vol. 17, March 2003, pp. 637-642.
- [4] Xiao, G., X., Ni, M.J., Huang, H., Chi, Y., Xiao, R., Zhong, Z.P. and Cen, K.F. (2007). Fluidized-bed pyrolysis of waste bamboo, *Journal of Zhejiang University*, vol. 9, March 2007, pp. 1495-1499.
- [5] Acharya, B., Dutta, A. and Basu, P. (2010). An investigation into steam gasification of biomass for hydrogen enriched gas production in presence of CaO, *International Journal of Hydrogen Energy*, vol. 35, December 2010, pp. 1582-1589.
- [6] Li, J., Yin, Y., Zhang, X., Liu, J. and Yan, R. (2009). Hydrogen-rich gas production by steam gasification of palm oil wastes over supported trimetallic catalyst, *International Journal of Hydrogen Energy*, vol. 34, October 2009, pp. 9108-9115.
- [7] Li, C. and Suzuki, K. (2008). Tar property, analysis, reforming mechanism and model for biomass gasification-an overview, *Renewable and Sustainable Energy Reviews*, vol. 13, January 2008, pp. 594-604.
- [8] Yu, Q.-Z., Brage, C., Nordgreen, T. and Sjoström, K. (2009). Effects of chinese dolomites on tar cracking in gasification of birch, *Fuel*, vol. 88, May 2009, pp. 1922-1926.
- [9] Zhang, Y., Kajitani, S., Ashizawa, M. and Oki, Y. (2010). Tar destruction and coke formation during rapid pyrolysis and gasification of biomass in a drop-tube furnace, *Fuel*, vol. 89, September 2010, pp. 302-309.
- [10] Skoulou, V., Koufodimos, G., Samaras, Z. and Zabaniotou, A. (2008). Low temperature gasification of olive kernels in a 5-kW fluidized bed reactor for  $H_2$ -rich producer gas, *International*



*Journal of Hydrogen Energy*, vol. 33, October 2008, pp. 6515-6524.

[11] Meesuk, S. (2009). Hydrogen gas production from sawdust by steam catalytic gasification, MSc Thesis (Industrial Chemistry), Chiang Mai University, Thailand.

[12] Narvaez, I., Orio, A., Aznar, M.P. and Corella, J. (1996). Biomass gasification with air in an atmospheric bubbling fluidized bed. effect of six operational variables on the quality of the produced raw gas, *Industrial & Engineering Chemistry Research*, vol. 35, April 1996, pp. 2110-2120.

[13] Mun, T.Y., Seon, P.G. and Kim, J.S. (2010). Production of a producer gas from woody waste via air gasification using activated carbon and a two-stage gasifier and characterization of Tar, *Fuel*, vol. 89, June 2010, pp. 3226-3234.

[14] Basu, P. (2010). Biomass gasification and pyrolysis: practical design and theory, Elsevier, USA.

[15] Andres, J.M., Narros, A. and Rodriguez, M.E. (2011). Behaviour of dolomite, olivine and alumina as primary catalysts in air-steam gasification of sawage sludge, *Fuel*, vol. 90, October 2011, pp. 521-527.

[16] Zhao, Y., Sun, S., Zhou, H., Sun, R., Tian, H., Luan, J. and Juan Qian (2010). Experimental study on sawdust air gasification in an entrained-flow reactor, *Fuel Processing Technology*, vol. 91, January 2010, pp. 910–914.

[17] Mansaray, K.G., Ghaly, A.E., Al-Taweel, A.M., Hamdullahpur, F. and Ugursal, V.I. (1999). Air gasification of rice husk in a dual distributor type fluidized bed gasifier, *Biomass and Bioenergy*, vol. 17, April 1999, pp. 315-332.

## **CURRICULUM VITAE**

**Name** Mr.Thanasit Wongsiriamnuay

**Date of Birth** February 5, 1977

**Education** B. Eng. (Mechanical Engineering), Chiang Mai University, 1998.  
M. Eng. (Mechanical Engineering), Chiang Mai University, 2001.

### **Papers in International Journal**

1. Wongsiriamnuay, T. and Tippayawong, N. (2010). "Non-isothermal pyrolysis characteristics of giant sensitive plants using thermogravimetric analysis." Bioresource Technology **101**(14): 5638-5644.
2. Wongsiriamnuay, T. and Tippayawong, N. (2010). "Thermogravimetric analysis of giant sensitive plants under air atmosphere." Bioresource Technology **101**(23): 9314-9320.
3. Wongsiriamnuay, T. and Tippayawong, N. (2012). "Product gas distribution and composition from catalyzed gasification of mimosa." International Journal of Renewable Energy Research **2**(3): 363-368.

### **Papers in International Conferences**

1. Wongsiriamnuay, T., Phengpom, T., Panthong, P., et al. (2008). "Renewable Energy from Thermal Gasification of a Giant Sensitive Plant (Mimosa pigra L.)." 5th International Conference on Combustion, Incineration/Pyrolysis and Emission Control. Chiang Mai, Thailand

2. Thiha, S., Tippayawong, N., Wongsiriamnuay, T., et al. (2009). "Catalytic destruction of biomass tar by dolomite in a dual packed bed reactor." International conference on green and sustainable innovation 2009 (ICGSI). Chiang Rai, Thailand.
3. Wongsiriamnuay, T. and Tippayawong, N. (2010). "Gasification of Giant Sensitive Plants in a Fixed Bed Reactor." 23rd International Conference on Efficiency, Cost, Optimization, Simulation and Environmental Impact of Energy Systems. Lausanne, Switzerland.
4. Kannang, N., Wongsiriamnuay, T. and Tippayawong, N. (2012). "Fuel Gas Production from Low Temperature Gasification of Bamboo in Fluidized Bed Reactor." The International conference of the Thai Society of Agricultural Engineering 2012. Chiangmai, Thailand.